M-PM-Min1 NMR RELAXATION AND PROTEIN DYNAMICS: THEORY, EXPERIMENT, AND COMPUTER SIMULATIONS. R.M. LEVY, DEPARTMENT OF CHEMISTRY, RUTGERS UNIVERSITY, NEW BRUNSWICK, NEW JERSEY 08903.

Since the motions of molecules with many internal degrees of freedom (e.g., nucleic acids and proteins) are complicated, the interpretation of experimental measurements in terms of molecular dynamics is not unique. While it is often possible to fit the experimental results using empirical rules or analytical models, the data generally are not sufficient to determine whether a model gives the correct description of the dynamics. A powerful method that can be used to interpret the experimental data and to develop and test appropriate analytical models is provided by computer simulations of the molecular dynamics. Applications of the method for interpretation of experimental NMR relaxation, and fluorescence depolarization experiments on proteins will be presented. The use of specific motional models and of an approach to the analysis of relaxation based on the extraction of an order parameter which describes the spatial restriction of the probe will be discussed.

We will also discuss the results of a recent molecular dynamics study of the rotational motion of methyl groups attached to aliphatic residues in myoglobin. We have evaluated the effective potentials within which the methyls move in different regions of the protein. The results demonstrate that the activation energy for methyl rotation depends on the local atomic packing around the group and this raises the possibility that methyls may be used as "reporter groups" to follow protein conformational changes.

M-PM-Min2 SOLID STATE NMR STUDIES OF INTERNAL MOTIONS IN PROTEINS. Dennis A. Torchia. National Institute of Dental Research. National Institutes of Health, Bethesda, MD 20205

Information about internal protein dynamics is obtained more directly in solids than in solution because complicating factors arising from overall motion of the macromolecules are absent in the solid state. Using recently developed NMR techniques, internal dynamics can be studied at specific sites if isotopes such as deuterium, carbon-13 or nitrogen-15 are incorporated into the protein. I will begin my talk with a brief discussion of the NMR methods that have been used to derive information about dynamics in solids. I will then review models of protein internal dynamics that have been obtained from a variety of recent solid state NMR studies. The talk will conclude with a discussion of the problem of deriving a unique dynamic model from NMR experiments.

M-PM-Min3 NMR STUDIES OF LIPID MOTIONS IN BILAYER MEMBRANES, J.H. Prestegard, Chemistry Department Yale University, New Haven, CT.

A biological membrane is far from a static structure. Membrane proteins must move and reorient. Solutes must be translocated. Membranes must rupture and rejoin in exocytotic and endocytotic processes. The internal dynamics of the lipids on which bilayer membranes are based have therefore attracted a great deal of attention over the past decade. Nuclear magnetic resonance (nmr) has contributed a great deal to a dynamic characterization of membrane lipids. The level of characterization has become increasingly complex as the number and variety of experimental observations have increased. It will be shown that a number of recent treatments based on ^{2}H, ^{1}H and ^{13}C spin relaxation studies of lipids lead to reasonable agreement on motional timescales. There is less agreement on assignment of timescales to specific motions largely because lack of sufficient data has made assignments model dependent.

While it is possible to introduce model independent treatments of existing data, it is also possible to introduce new spin relaxation experiments which display a different sensitivity to geometry of motion. One type of experiment, spin relaxation of ^{1}H coupled ^{13}C spectra, has been applied to analysis of hydrocarbon chain and glycerol backbone motion in dimyristoylphosphotidylcholine bilayer membranes and will be discussed in detail. Analysis in terms of crosscorrelation and autocorrelation spectral densities allows distinction among commonly proposed motional models.

M-PM-Min4 OPTICAL PROBES OF THE DEFORMATIONAL DYNAMICS OF LINEAR AND SUPERCOILED DNAs, J. Michael Schurr, John H. Shibata, Jess P. Wilcoxon, and John C. Thomas, Department of Chemistry, University of Washington, Seattle, WA 98195.

Spontaneous Brownian twisting deformations of DNAs in solution dominate the rotational dynamics from 1-100 ns and provide novel information about the magnitude of the twisting rigidity and its uniformity along the filament. Recent studies from several laboratories of both the transient fluorescence polarization anisotropy (FPA) of intercalated ethidium dye, and the transient photoinduced dichroism (TPD) of intercalated methylene blue monitor both twisting and tumbling dynamics from $\sim$1 nsec to $\sim$20 μsec. The correct geometrical relation between the measured optical anisotropy and the twisting and tumbling correlation functions is now available, as is the theory of the twisting correlation function for discrete and continuum filaments of arbitrary length. An empirical tumbling correlation function from electric birefringence measurements at long-times $t>2$ μs can be combined with FPA results at very short times $t\lesssim 100$ ns to give a predicted anisotropy curve in excellent agreement with the TPD data from 25 ns to 20 μs.

Reports of the effects of base-composition, helix-structure, and ionic strength are critically reviewed. In vitro and in vivo studies of DNA in the presence of nucleosomes are also discussed.

Multiple discrete metastable states of supercoiled M13 have recently been detected using FPA, dynamic light scattering, gel electrophoresis, and CD techniques. The prevalence of either of two distinct values of the twisting rigidity in all cases suggests the existence of two distinct secondary structures for supercoiled DNAs. A speculative hypothesis for the biological function of supercoiling and its relation to metastability is offered.

M-PM-Min5 DYNAMICS OF LIGAND BINDING TO HEMOGLOBIN AND MYOGLOBIN. James Hofrichter Laboratory of Chemical Physics, NIADDK, National Institutes of Health, Bethesda, MD 20205

The ability to probe rapid processes in proteins has been dramatically enhanced by improvements in pulsed laser technology over the past decade. Using pulsed sources to measure optical absorption and resonance Raman spectra of heme proteins after photolysis, kinetic data has been obtained on molecular species having lifetimes from 10^{-13} to 10^{-5} sec. The most important finding from these measurements is a 'geminate' rebinding of ligand before it escapes from the protein matrix. This process has been observed for NO, O_2 and CO in hemoglobin and myoglobin. The absence of complete rebinding requires that a rapid pathway exist for the ligand to leave the protein. Consequently, the geminate rebinding process can be used to probe both the rate of rebinding at the heme and the dynamics of the ligand moving inside the protein. In addition to ligand rebinding, transient absorption and Raman spectra can be used to probe changes in the protein structure. Both experiments suggest that the deoxy heme relaxes to at least a partially out-of-plane configuration within 30 ps. Protein conformational relaxations subsequent to photolysis have been observed for hemoglobin but not for myoglobin. Relaxation to the deoxy conformation is complex and only finally complete after the quaternary structural (R-T) change which requires about 20 us. By measuring the lifetimes of the observed kinetic intermediates, we obtain a detailed picture of the ligand dissociation process in Hb and Mb, which can be used to determine the source of kinetic cooperativity in the overall dissociation rates. These states further suggest several possibilities for the origin of cooperativity in the overall association rates.

M-PM-A1 HEMI-DEUTERATED LIPIDS AS PROBES OF CONFORMATIONAL ORDER IN SOAPS AND LIPID BILAYERS: A RAMAN SPECTROSCOPIC STUDY. J.P. Sheridan, B.P. Gaber, and R. Magni. Optical Probes Branch, Code 6510, Naval Research Laboratory, Washington, D.C. 20375.

The molecules (C_2 - C_8)D14 - palmitic acid, (C_9 - C_{16})D17 - palmitic acid and their corresponding sodium soaps have been characterized as sensitive probes of conformational order in lipid bilayers. Detailed Raman spectra have been recorded and analyzed in all spectral regions of interest between 50cm^{-1} and 3100cm^{-1}. In the case of the soaps (Lipid/H2O ~ 70:30 w/w), spectra were taken at various temperatures from the gel phase through the first-order phase transition into the L_α phase. Several conformationally sensitive bands originating from the protonated and deuterated parts of the lipids were monitored as markers of the phase transition process. It was found, from the temperature dependence of these bands, that the portion of the lipid chain closest to the terminal methyl group undergoes a much more dramatic change in intra- and inter-chain conformational characteristics than does the upper half of the chain nearest to the polar head group. In fact, it appears that only the lower half of the acyl chain in these soaps senses a first-order discontinuity at the phase transition, while the upper portion experiences a type of second-order monotonic decrease in order throughout the gel phase and into the L_α phase.

M-PM-A2 DIFFERENTIAL POLARIZED PHASE STUDIES OF THE EFFECTS OF HYDROSTATIC PRESSURE ON LIPID BILAYERS. Richard B. Thompson and Joseph R. Lakowicz, University of Maryland School of Medicine, Department of Biological Chemistry, Baltimore, Maryland 21201.

We have extended our studies of model membranes into the pressure domain in the range of 1-2000 bar. We measured the anisotropy, lifetime, and rotational rate and limiting anisotropy (r_∞) of diphenylhexatriene (DPH) in solvents and synthetic phospholipid bilayers as a function of pressure and temperature using steady state polarization, phase-modulation, and differential polarized phase fluorometry. The measured anisotropies and differential tangents were corrected for the pressure-induced birefringence of the bomb windows using the methods of Weber. We found that propylene glycol and mineral oil, which permit isotropic rotation of DPH at one atmosphere, appear to hinder the rotation of the fluorophore and to become more ordered with increasing pressure. Moreover, as the hindrance of the probe's rotation increases, its apparent rotation rate increases as well. We measured these same parameters for DPH in dipalmitoyl-, dimyristoyl-, and dioleolyl-phosphatidylcholine, and dimyristoyl phosphatidylcholine:cholesterol 7:1 unilamellar vesicles in Tris buffer @ pH 7.5. The pressure dependence of the phase transition, when observable, obeyed the Clausius-Clapeyron equation as has been seen by other investigators. We found that the order parameters of the acyl chain region of the phosphatidylcholines examined exhibited the same temperature-pressure equivalence. As for the viscous solvents, the apparent rotational rate of the probe increased with pressure as the acyl side chains became more highly ordered. Finally, we examined the behavior of trimethylammonium-DPH (TMA-DPH) in this system. This probe is positively charged and is therefore expected to localize at the lipid-water interface. The thermodynamics of the phase change as detected with this probe were closely comparable to the results from DPH.

M-PM-A3 FORMATION OF LIPID MULTILAYER ON ALKYLATED GLASS SURFACE. Leaf Huang. Dept. of Biochemistry, University of Tennessee, Knoxville, and Harden M. McConnell, Dept. of Chemistry, Stanford University.

Phosphatidylcholine (PC) could be deposited on the surface of an alkylated glass coverslip by dialysing the coverslip with a mixture of PC and deoxycholate. The amount of PC molecules on the coverslip was enough to form multiple lipid monolayers. The number of lipid layers depended on the composition of the lipids and the method of preparation. Increasing concentrations of cholesterol (0-50 mole %) brought about increasing numbers of lipid layers from approximately 6 to 15. Shortening of dialysis time reduced the number of lipid layers. Coverslips dipped in the lipid/deoxycholate solution and then washed extensively in detergent-free solutions contained only about 50-60% of lipids as compared to those dialysed for 2-3 days. Lateral diffusion of the phospholipid in multilayers was measured by photobleaching recovery of NBD-PE in the multilayers. The diffusion coefficient at room temperature was $8.2 \pm 6.7 \times 10^{-9}$ cm2/sec for multilayers composed of eggPC:chol (3:1); and was $< 1 \times 10^{-11}$ cm2/sec for those composed of dipalmitoyl PC. Palmitoyl IgG prepared by acylation of antibody (A. Huang, et al, BBA, 716 (1982) 140-150) could be incorporated into multilayers. We have used a monoclonal antibody to the mouse major histocompatability antigen ($H2K^k$). Mouse lymphoma cells of K haplotype, but not cells of other haplotypes, bound rapidly to multilayers containing palmitoyl anti-$H2K^k$. These results suggest that functional antibody molecules can be incorporated into multilayers. Supported by NIH grants.

M-AM-A4 GLYCEROL SUBSTITUTES FOR WATER IN LECITHIN BILAYERS. R.V.McDaniel*, T.J. McIntosh, and S.A. Simon, Departments of Anatomy and Physiology, Duke University Medical Center, Durham, N.C. 27710. *Present Address: Univ. of Connecticut Health Center, Division of Cardiology, Farmington, CT. 06032.

Multilamellar liposomes form in the absence of water when glycerol is added to lecithin. Moreover, glycerol substitutes for water in these liposomes in that the thickness of the liquid-crystalline phase bilayers, the thickness of the fluid space between bilayers, the apparent molar lipid heat capacity, and the gel to liquid-crystalline transition temperature and enthalpy are all similar for lecithin in pure water and in pure glycerol. One major difference is that the gel state of dipalmitoyl phosphatidylcholine (DPPC) in glycerol consists of a lamellar phase with fully interdigitated hydrocarbon chains. X-ray diffraction analysis shows that the interdigitated DPPC gel phase is also formed in ethylene glycol and methanol at low water content, and in fully hydrated DPPC containing certain small, bulky amphiphilic molecules, such as tetracaine, chlorpromazine, and benzyl alcohol.

M-PM-A5 BINDING OF DIVALENT CATIONS TO DIFFERENT PHASES OF PHOSPHATIDYLGLYCEROL. Joan M. Boggs, Research Inst., Biochemistry Dept., Hospital for Sick Children, Toronto, Ontario, Canada, M5G 1X8.

Divalent cations are known to induce metastable phase behavior in phosphatidylglycerol. The metastable phase undergoes a transition at a temperature approximately 20° above that of the Na^+-salt form to a more stable, dehydrated phase which subsequently melts at a much higher temperature and with a greater enthalpy than the pure lipid. This phase behavior has been investigated more extensively by differential scanning calorimetry and ESR spectroscopy. The cation to lipid ratio must be close to or greater than 0.5:1 in order to induce the stable phase, suggesting that the lipid head groups must be completely neutralized. However, the transition temperature of the metastable phase is not quite as high as that of the lipid in its protonated state, suggesting that the divalent cations do not completely neutralize the lipid in the metastable phase, even if sufficient cations are present. These observations suggest that divalent cations are released from the lipid when the stable phase melts and do not rebind in the gel phase. The rate of the exothermic transition from the metastable phase to the stable phase increased with increase in divalent cation concentration and decreased in the presence of Na^+. This suggested that the divalent cations rebind during the exothermic transition of the metastable phase, allowing more complete neutralization of the lipid head groups so that cross-linking of opposing bilayers into the stable dehydrated phase can occur. This was confirmed by quantitating the amount of bound and free Mn^{+2} above and below the phase transition and after conversion to the stable phase, from the ESR spectrum of Mn^{+2}.

(Supported by the Medical Research Council of Canada Grant MT-6506.)

M-PM-A6 THERMOTROPIC BEHAVIOR AND STRUCTURE OF HYDRATED 1,3-DIPALMITOYL-GLYCERO-2-PHOSPHOCHOLINE (β-DPPC) BILAYER MEMBRANES. E.N. Serrallach, G.H. de Haas and G.G. Shipley. Biophysics Inst.,Boston Univ. Schl. Med., Boston, Mass.;Biochemistry Lab.,State Univ. of Utrecht, Utrecht, The Netherlands.

The thermotropic properties and structure of hydrated β-DPPC were studied as a function of temperature and water content by means of differential scanning calorimetry (DSC) and x-ray diffraction. After prolonged storage at -3°C, DSC heating scans exhibit low and high temperature transitions (LTT and HTT) at 27 and 37°C with enthalpies of 9.1 and 10.5 Kcal/mol respectively. Upon cooling, the HTT is reversible with full enthalpy; in contrast, only ~2 Kcal/mol enthalpy are obtained for the LTT. Immediate reheating shows an exothermic transition prior to the endothermic LTT and HTT. Several hours incubation at 12°C (or several months at -3°C) are necessary to regain the full enthalpy of the LTT. X-ray diffraction studies indicate three different lamellar phases upon heating from -3°C: (a) below 18°C, a "crystalline" phase, Lc, with an ordered hydrocarbon chain packing mode and a bilayer periodicity d = 58Å; (b) between 30 and 35°C, a gel phase, Lβ, with hexagonal chain packing and d = 47Å; chain interdigitation is suggested by (i) the sharp reflection at 4.16Å, (ii) structure factor calculations using strip electron density models, (iii) a S/Σ ratio of ~ 4; and (c) above 37°C, a liquid crystalline phase, Lα, with d = 65Å. Comparison between the positional isomers α and β-DPPC suggests a different orientation of the glycerol backbone from perpendicular to parallel to the bilayer surface, and an increase in intramolecular acyl chain distance. These differences clearly influence the thermotropic behavior and molecular packing of hydrated DPPC.

M-PM-A7 MOLECULAR INTERACTION OF CHOLESTEROL IN N-PALMITOYLGALACTOSYLSPHINGOSINE (NPGS) (CEREBROSIDE) BILAYERS AND IN PHOSPHOLIPID (DPPC)-CEREBROSIDE LIPID BILAYERS. M.J. Ruocco*, E. Oldfield & G.G. Shipley, Biophysics Inst., Boston Univ. Sch. Med., Boston, MA & Sch. Chem. Sci., Urbana, IL

Scanning calorimetry and x-ray diffraction have been used to study hydrated NPGS:cholesterol (Chol) lipid mixtures over the 20 to 90°C range. At low Chol concentrations (<10 mol %) the NPGS crystal→liquid crystal transition (II) (T_m=82°C; ΔH=17.5 Kcal/mol NPGS) is reduced in enthalpy and temperature, while at $14 \leq c \leq 50$ mol % Chol, an additional, broad transition (I) is observed at 50-60 °C. X-ray diffraction experiments on mixtures containing 6 to 80.5 mole % Chol at 22°C, below transitions I and II, indicate NPGS and Chol crystal phases coexist. Between transitions I and II, at 66°C, diffraction patterns of mixtures containing <50 mol % Chol show that all Chol has been incorporated into NPGS liquid crystal (LC) bilayers. A second unmelted NPGS crystal phase persists until heating to $T>T_m$ (transition II) where the crystal melts into the pre-existing LC phase. At c >50 mol % Chol only a single transition I (ΔH_{max}=9 Kcal/mol NPGS) is observed at 56°C, above which NPGS:Chol LC bilayers and excess Chol coexist. Thus, at low temperatures the NPGS:Chol system exhibits solid phase immiscibility at all Chol concentrations. This behavior is proposed to result from strong, lateral molecular interaction (hydrogen bonding) between NPGS molecules. At high temperatures, NPGS-NPGS associations are disrupted, allowing the intercalation of Chol into the cerebroside bilayer.

Similar studies on NPGS:(DPPC:Chol) (1:1 mol ratio) mixtures show a miscibility limit of 20 mole % NPGS in DPPC:Chol bilayers. This is similar to the miscibility limit of NPGS in LC DPPC bilayers. Thus, the presence of Chol does not appear to influence the miscibility of NPGS in DPPC-containing bilayers.

M-PM-A8 STABILITY AND PHASE TRANSITIONS IN 18 CARBON FATTY ACID MONOLAYERS. Y. Hifeda and G.W. Rayfield. Physics Department, University of Oregon, Eugene, OR 97403.

π-A isotherms have been examined for 18 carbon fatty acids with varying numbers of trans double bonds. The position of the double bond in an alkene chain has a dramatic effect on the π-A curves. A phase transition (liquid expanded to liquid condensed) is indicated in 18:1 (6 trans) (figure) but not in 18:1 (11 trans). Stability of the monolayers as a function of surface pressure has also been examined. The phase transition in 18:1 (6 trans) appears to be between two quasi equilibrium states. Paranaric acid 18:4 (9, 11, 13, 15 all trans) shows several features in its π-A isotherms which indicate polymerization may occur at high surface pressures.

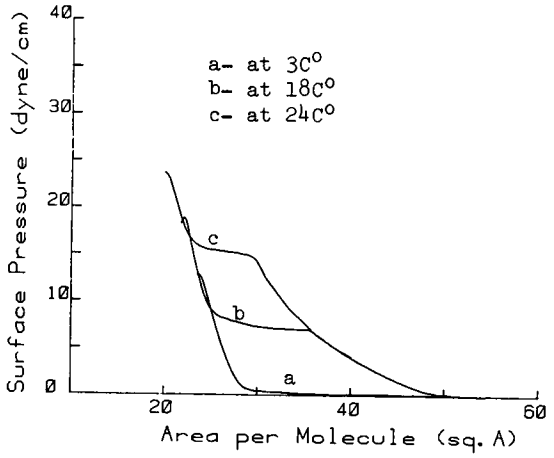

M-PM-A9 LIPID SOLUBILIZATION AND MICELLE FORMATION BY THE TRIHYDROXY β-MURICHOLIC BILE ACID. J.E. Staggers and M.A. Wells. Department of Biochemistry. University of Arizona. Tucson, AZ 85721.

In clinical practice the dihydroxy bile acids chenodeoxycholic (3α-7α-dihydroxy-5β-cholanic acid, CDC) and its 7β epimer ursodeoxycholic (UDC) are effective agents for the dissolution of cholesterol gallstones. However, physico-chemical studies by Carey et al. (Biochemistry 1981. 20, 3637) have demonstrated that, compared to CDC, micelles of UDC have a dramatically reduced ability to solubilize cholesterol, apparently related to the greater hydrophilicity of the UDC monomer. We have recently reported the abundance of β-muricholic bile acid (3α-6β-7β-trihydroxy-5β-cholanic acid, β-MC) in the neonatal rat (Staggers, J.E., Frost, S.C., and M.A. Wells. J.Lipid Research 1982. 23,1143). Our data suggest that the importance of β-MC in this animal model relates to the particular lipid-solubilizing ability imparted by its molecular configuration, which possibly can influence the observed secretory coupling of biliary lipids. To investigate this question we have undertaken a comparative analysis of the taurine conjugated salts ($\geq$ 95% of total neonatal rat bile salts) of β-MC, CDC, and UDC, as well as cholic (TC), the major bile acid of the rat. The critical micellar concentrations of these bile salts were determined by dye-binding with Rhodamine 6G in 0.15 M NaCl at 37° C and relative hydrophilicity was estimated by mobility on HPLC reversed-phase octadecylsilane columns. Cholesterol solubilization measurements were performed with solutions of the individual bile salts and a series of mixtures of β-MC and TC with and without the addition of phosphatidylcholine over a 10-fold range of the bile salt to phospholipid molar ratio (~6.3) that we have found to occur in the secreted bile. (This work was supported by NIH grant AM28337)

M-PM-A10 A NEW METHOD FOR MEASURING YIELD SHEAR RESULTANT AND PLASTIC VISCOSITY OF RED CELL MEMBRANE. Richard E. Waugh, Dept. of Rad. Biol. & Biophys., Univ. of Rochester Med. Ctr., Rochester, NY 14642.

The red cell membrane exhibits both solid and liquid properties. Under normal conditions the membrane behaves elastically, but if forces in the membrane become too large the elastic structure breaks down and the surface flows like a two-dimensional liquid. Measurement of the intensive force needed to produce this solid to liquid transition (the yield shear resultant) provides important information about the state of the molecules of the membrane skeleton which gives the membrane its shear elasticity.

A new technique has been developed to measure yield shear resultant and plastic viscosity coefficient. Swollen cells are aspirated into a micropipette with a pressure sufficient to make the outer portion spherical. The cell is attached to a large (50 μm) bead. A force is exerted on the bead by the suspending buffer which flows over the bead at a controlled rate. When the force is large enough the bead pulls away from the body of the cell forming a tether (strand of membrane) between the cell and the bead. The maximum force at which there is no tether growth provides a measure of the yield shear resultant, and the rate of tether growth at higher forces provides a measure of membrane viscosity. This technique has two advantages over previous techniques: (1) the force supported by the tether can be approximated by Stokes' drag on a sphere and is independent of cell geometry; (2) the radius of the tether can be determined from experimental observations. Analysis of the surface deformation has been completed, and preliminary data will be presented. (Supported by PHS Grant No. HL 26485.)

M-PM-A11 VISCOELASTIC PROPERTIES OF RED CELLS IN SICKLE CELL DISEASE. G.B.Nash and H.J.Meiselman Dept. of Physiology and Biophysics, U. So. California School of Medicine, Los Angeles, CA 90033.

Little data exist for the intrinsic membrane viscoelastic properties of irreversible or reversible sickle cells (ISC and RSC respectively). Nor is the process whereby ISC become less deformable well understood. We have used micropipette aspiration techniques to measure oxygenated ISC and RSC membrane shear elastic modulus (u), time constant for viscoelastic shape recovery (tc) and hence membrane surface viscosity (n=u.tc). ISC had relatively rigid membranes (u > 100% above normal AA controls) and tc close to normal values, so that their membrane viscosity was more than double control. Hypotonically swollen ISC (with internal hemoglobin concentration decreased to normal levels) retained their increased membrane stiffness but had markedly decreased tc, so that their n approached normal values. Thus ISC rigidity is not due solely to elevated hemoglobin concentration, although this does influence their tc and thus their effective membrane viscosity. Disc shaped RSC had u and tc close to control, but showed wider variation within samples and between sickle cell donors. Measurements on different fractions of density separated RSC showed that u was constant but that, on average, tc was longer for denser cells. Again, these differences varied between donors. We note that a small sub-population of discocytes were found to exist which had u and/or n close to ISC values. However, in general, as RSC become more dense (a process normally associated with in vivo ageing), they do not gradually approach ISC properties. Thus, ISC formation in vivo may not be a linear, time-dependent process but rather may involve a discontinuity in the normal ageing pattern.
Supported by NIH Grants HL15722 and HL15162 and by AHAGLAA Award 5371G6.

M-PM-A12 SHEARED PLANAR MEMBRANE MONOLAYERS: ANALYSIS OF BILAYER SPLITTING. Knute A. Fisher. Dept. Biochem. Biophys. and Cardiovasc. Res. Inst., Univ. of Calif., San Francisco, Calif. 94143.

I recently evaluated the effect of freeze-fracture on membrane polypeptides of chemically and enzymatically unmodified human erythrocytes, RBCs (Fisher, K. A., 1982, J. Cell Biol. 95, 250a). RBC or ghost monolayers were hydraulically sheared to produce planar membrane monolayers, one bilayer thick; the bilayers were split by freeze-fracture, and split portions analyzed by SDS-PAGE using silver staining to detect nanogram levels of polypeptides, including sialoglycopeptides. The results indicated that all RBC membrane polypeptides could be rapidly detected at high sensitivity and resolution, and led to the conclusion that the freeze-fracture process did not modify the covalent backbone of any membrane polypeptide. Experiments were designed to test the hypothesis that the single membrane monolayers split like intact cell monolayers. Intact RBCs were labeled with a lipid bilayer label (tritiated cholesterol) or a fluorescent surface label (FITC-Con A), attached to planar glasses, sheared, frozen, and fractured. Control and freeze-fractured samples were evaluated by light and electron microscopy, spectroscopy, fluorometry, and scintillation counting. Microscopy, cholesterol experiments, and FITC-Con A studies showed a significant enrichment of the extracellular "half" membrane on the glass side after fracturing. Amino group assay by fluorescamine and peptide analysis by silver-gels concomitantly revealed a significant fraction of cytoplasmic "half" partitioning to the opposite side. These data when taken together support the hypothesis that the single membrane bilayer does indeed split. Planar membrane splitting provides a useful tool for the analysis of hydrophobic interactions among membrane polypeptides in studies of their transmembrane functions. (Supported by NIH grant GM27049.)

M-PM-A13 INTERACTION OF DIVALENT CATIONS WITH PHOSPHATIDYLSERINE BILAYER MEMBRANES. H. Hauser and G.G. Shipley, Biophysics Institute, Boston Univ. Schl. Med., Boston, Mass.;Lab. für Biochemie, ETH-Zurich, Switzerland.

The interaction of divalent cations (M^{2+}) with an homologous series of 1,2-diacyl-phosphatidylserines has been studied by differential scanning calorimetry (DSC) and x-ray diffraction. Hydrated diC_{14}-PS (DMPS) exhibits a gel → liquid crystal bilayer transition at 39°C (ΔH = 7.2 Kcal/mol DMPS). With increasing molarity $MgCl_2$, progressive conversion to a high melting (92°C) high enthalpy ($\Delta H \simeq 11.0$ Kcal/mol DMPS) phase is observed. Similar behavior is observed for DMPS with increasing molarity $CaCl_2$. In this case, the high temperature transition of Ca^{2+}-DMPS occurs at ∿ 155°C and is immediately followed by an exothermic behavior probably associated with PS decomposition. For diC_{12}-, diC_{14}-, diC_{16}- (DPPS), and diC_{18}-PS the transition temperatures of the Ca^{2+}-PS complexes are in the range 151-155°C; only diC_{10}-PS exhibits a significantly lower value, 142°C. High melting complex formation has also been demonstrated for Sr^{2+}-DPPS and Ba^{2+}-DPPS, although the precise thermotropic behavior appears to be cation dependent. X-ray diffraction of Ca^{2+}-PS complexes at 20°C provides evidence of structural homology. All Ca^{2+}-PS complexes exhibit bilayer structures, the bilayer periodicity increasing linearly from 35.0Å for diC_{10}-PS to 52.5Å for diC_{18}-PS. Wide angle diffraction data indicate that hydrocarbon chain "crystallization" occurs on Ca^{2+} complex formation. Mg^{2+}-DPPS and Ca^{2+}-DPPS form similar ordered bilayer structures (periodicity d = 47-48Å), but the Sr^{2+}- and Ba^{2+}-DPPS complexes have an increased periodicity (d = 57-58Å) and different chain packing mode. Comparison with anhydrous/hydrated PS and M^{+}-PS complexes, allows the behavior of the different M^{2+}-PS complexes to be rationalized.

M-PM-B1 VARIABLE FLUORESCENCE IN PHOTOSYSTEM I PARTICLES. Gross, E. L. and Tripathy, B. C. Dept. of Biochemistry. The Ohio State University, Columbus, Ohio 43210.

Photosystem I particles (PSI) isolated according to the method of Bengis and Nelson (J. Biol. Chem. 250, 2783 (1975)) show variable fluorescence in response to changes in state of both P700 and X. Addition of DClPH$_2$ to PSI under aerobic conditions decrease fluorescence emission at both 689 and 730 nm by converting $P700^+X$ to P700X.

Under anaerobic conditions, both ferredoxin (Fd) and methyl viologen (MV) quench fluorescence by converting $P700X^-$ to P700X. Trypsin treatment of PSI which affects both the 70 and 20 KD polypeptides increases the K_m for both Fd and MV indicating that the binding site for the electron acceptors is affected. Chemical modification, pH and salts also affected the ability of electron donors and acceptors to interact with PSI as measured by variable fluorescence.

M-PM-B2 PROBING FLUORESCENCE INDUCTION IN CHLOROPLASTS ON A NANOSECOND TIME SCALE UTILIZING PICOSECOND PULSE PAIRS. N.E. Geacintov,* J. Breton, A. Dobeck and J. Deprez, Service de Biophysique, CEN-Sacley, 91191 Gif-sur-Yvette, France, and *Chemistry Department, New York University, New York, 10003.

The fluorescence properties of spinach chloroplasts at room temperature were probed utilizing two 30 ps wide laser pulses (530 nm) spaced Δt(s) apart in time (Δt = 5 $\longrightarrow$ 110 ns). The energy of the first pulse (P_1) was varied (10^{12} - 10^{16} photons cm^{-2} pulse^{-1}), while the energy of the second (probe) pulse (P_2) was held constant (5 x 10^{13} photons cm^{-2}). A gated (2 ns) optical multichannel analyzer-spectrograph system allowed for the detection of the fluorescence generated either by P_1 alone, or by P_2 alone (preceded by P_1). The dominant effect observed for the fluorescence yield generated by P_1 alone is the usual singlet-singlet exciton annihilation which gives rise to a decrease in the yield at high energies. However, when the fluorescence yield at dark-adapted chloroplasts is measured utilizing P_2 (preceded by pulse P_1) an increase in this yield is observed. The magnitude of this increase depends on Δt, and is characterized by a time constant of $\sim$ 25 ns. This rise in the fluorescence yield is attributed to a reduction of the oxidized (by P_1) reaction center $P680^+$ by a primary donor. At high pulse energies (P_1 > 4 x 10^{14} photons cm^{-2}) the magnitude of this fluorescence induction is diminished by another quenching effect which is attributed to triplet excited states generated by intense P_1 pulses.

This work was supported by a National Science Foundation Grant (PCM 8006109).

M-PM-B3 NANOSECOND TIME RESOLVED MAGNETIC RESONANCE OF THE PRIMARY RADICAL PAIR STATE P^F OF BACTERIAL PHOTOSYNTHESIS. M.R. Wasielewski, C.H. Bock, M.K. Bowman, J.H. Tang, and J.R. Norris Chemistry Division, Argonne National Laboratory, Argonne IL 60439

Photoexcitation of the reaction center protein from purple photosynthetic bacteria results in rapid (5 psec) formation of a radical pair, P^F composed of an oxidized bacteriochlorophyll a dimer, P^+ and a reduced bacteriopheophytin a molecule, I^-. If the endogenous quinone molecules in the protein are either removed or chemically reduced prior to excitation, P^F lives for about 15 nsec. During this time a fraction of the initially formed singlet population of P^F, $^1(P^+I^-)$ under the influence of local magnetic fields due to the nuclear hyperfine interactions in P^+ and I^- undergoes intersystem crossing to yield $^3(P^+I^-)$. $^1(P^+I^-)$ decays directly to the singlet ground state, while $^3(P^+I^-)$ back reacts to form ^3P which lives for microseconds before intersystem crossing back to ground state singlet P. Since the energy level of $^1(P^+I^-)$ is nearly degenerate with the three energy sublevels of $^3(P^+I^-)$ at zero magnetic field these states mix strongly. Similarly, upon application of a magnetic field the resultant T_0 level of $^3(P^+I^-)$ remains nearly degenerate with that of $^1(P^+I^-)$, so that either in the presence or absence of a magnetic field the mixed radical pair states are paramagnetic during most of the 15 nsec lifetime of P^F. The magnetic resonance parameters that describe the spin dynamics of P^F allow us to determine readical pair structure and mechanism of its formation. We will report fast direct detection of the time resolved magnetic resonance spectrum of P^F measured by observing microwave induced changes in the transient optical absorption of P^F. (Work funded by Div. of Chemical Sciences, Office of Basic Energy Sciences,USDOE

M-PM-B4 THE EFFECT OF TRANSMEMBRANE POTENTIALS ON ELECTRON TRANSFER IN REACTION CENTERS INCORPORATED IN PLANAR BILAYERS.* A. Gopher, Y. Blatt, M. Y. Okamura, G. Feher, & M. Montal, UCSD, La Jolla.

The effect of applied voltages (V_{ap}) on the rate of charge recombination (k_{obs}) between the reduced primary quinone Q_A and the oxidized donor D^+ (see insert) in oriented reaction centers from R. sphaeroides incorporated in planar lipid bilayers[1] was studied. When Q_A was the natural UQ-10, $k_{obs} \cong k_{AD}$ and was unaffected by V_{ap} up to $\pm$125 mV. However, when Q_A was anthraquinone (AQ) an e-fold change in k_{obs} was measured for V_{ap} = 175 mV (see Fig.). In this case, the recombination proceeds via I and k_{obs} is given by[2]:

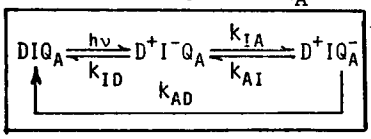

$$k_{obs} \cong k_{ID}/(k_{IA}/k_{AI}) = k_{ID} \exp[(-\Delta E_m \pm \Psi)/kT] = k_{obs(\Psi=0)} \exp(\pm\Psi/kT),$$

where ΔE_m is the redox energy difference and Ψ is the external potential difference between I and AQ. The equation predicts an e-fold change in k_{obs} for Ψ = 25 mV rather than the measured 175 mV, indicating that the effective potential difference between I and AQ is 1/7 of the applied potential.

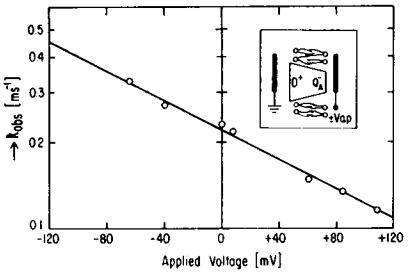

* Supported by grants from the NSF, NIH, and ONR.

[1] M. Montal, A. Darszon, and H. Schindler, Quart. Rev. Biophys. (1981) 14, 1.

[2] M. R. Gunner, Y. Liang, D. K. Nagus, R. M. Hochstrasser, and P. L. Dutton, Biophys. J. (1982) 37, 226a.

M-PM-B5 PHOTOVOLTAGES FROM REACTION CENTERS INCORPORATED IN INTERFACIAL LIPID LAYERS.* Y. Blatt, A. Gopher, M. Montal, and G. Feher, U.C.S.D., La Jolla, CA 92093.

The electrogenic and kinetic properties of light-induced electron transfer from the donor (D) to the quinone acceptors (Q_A,Q_B) in reaction centers (RCs) from R. sphaeroides were studied. Monolayers at the air-water interface, derived from lipid vesicles containing RCs, were adsorbed on a 12-μm thick teflon film separating two aqueous compartments.[1] Charge displacements in RCs with an effective orientation of ∿15% generated photovoltages consistent with D facing the solution and Q facing the teflon. The rise-time of the photovoltage was limited by the risetime of the laser and the response time of the electronics to 50 ns. The charge recombination time ($\tau_{1/e}$) was ∿100 ms when Q/RC ≤ 2 and 1 s when Q/RC reached 50. With terbutyrene, a blocker of Q_A to Q_B electron transfer, τ decreased from 1 s to 100 ms. Similar values of k_{AD}^{-1} and k_{BD}^{-1} were obtained optically for RCs in detergent solution. In the presence of reduced cytochrome c an additional component of the photovoltage buildup in the ms time range was observed. No voltage component, corresponding to the electron transfer from Q_A to Q_B, was observed (pH=8). Thus, the main electrogenic step is due to electron transfer from D to Q_A.[2] The Q_A to Q_B step is at least 30 times less electrogenic while the cytochrome c to D step is 0.4 as electrogenic as the D to Q_A step.

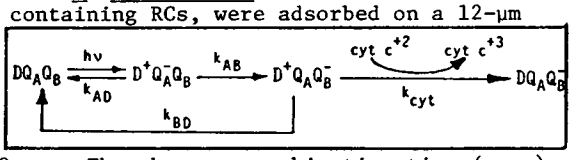

* Supported by grants from the NSF, NIH, and ONR.

[1] M. Montal, A. Darszon, and H. Schindler (1981) Quart. Rev. Biophys. 14, 1.

[2] N. K. Packham, P. L. Dutton, and P. Mueller (1982) Biophys. J. 37, 365.

M-PM-B6 FORMATION AND RECOMBINATION KINETICS OF THE STATES $D^+Q_AQ_B^-$ AND $D^+Q_A^-$ AT CRYOGENIC TEMPERATURE IN REACTION CENTERS FROM R. SPHAEROIDES.* D. Kleinfeld, M. Y. Okamura, & G. Feher, U.C.S.D., La Jolla, CA 92093.

Reaction centers (RCs) cooled to cryogenic temperature in the presence of strong illumination displayed kinetic behavior (i.e., recovery of the low temperature optical absorption change at 890 nm) which differed from that of RCs cooled in the dark. In RCs containing *two quinones*, the state $D^+Q_AQ_B^-$ was formed by illumination during rapid cooling in liquid nitrogen and decayed slowly in the dark. This decay, due to the charge recombination $D^+Q_AQ_B^- \rightarrow DQ_AQ_B$, followed approximately the power law $\Delta A_{890} \propto t^{-\gamma}$ with γ decreasing monotonically with temperature (see Fig.). Such a time dependence suggests a distribution of frozen-in conformations. After the charges recombined, $D^+Q_AQ_B^-$ could be regenerated at cryogenic temperatures. This contrasts with the situation in which the RCs were cooled in the dark; in this case no electron transfer to Q_B was observed upon illumination. When RCs with *one quinone* were cooled under illumination, the charge recombination time (1/e) due to $D^+Q_A^- \rightarrow DQ_A$ was 125 msec (T=77K), in contrast to 25 msec observed when the RCs were cooled in the dark. These results show that RCs frozen in the charge-separated state are different from those frozen in the dark. This difference may reflect either a conformational change or protonation during illumination at room temperature.

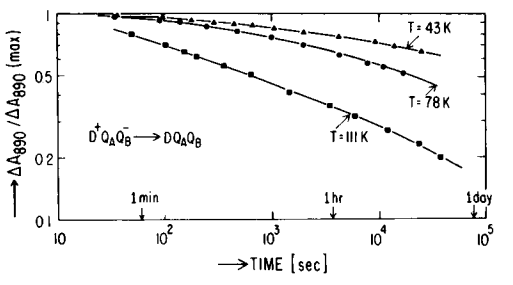

* Supported by grants from the NSF and the NIH.

M-PM-B7 SEQUENCING OF THE GENE ENCODING THE M SUBUNIT OF THE REACTION CENTER OF RHODOPSEUDOMONAS SPHAEROIDES.* JoAnn C. Williams, G. Feher, and M. I. Simon, U.C.S.D., La Jolla, CA 92093.

Molecular cloning and DNA sequencing are being used to determine the primary structure of the reaction center protein of Rhodopseudomonas sphaeroides. The amino terminal sequences (25 to 28 residues) of the three reaction center subunits, L, M, and H, had previously been determined by automated Edman degradation.[1] A mixture of oligonucleotides ($^{5'}AT^{A}_{G}TT^{T}_{C}TG^{A}_{G}TA^{T}_{C}CC^{3'}$), containing all possible coding sequences for a portion of the amino acid sequence of the M subunit, was synthesized[2] and used as a hybridization probe. A 13-kilobase pair (kb) BamHl restriction fragment of DNA from R. sphaeroides hybridized with this probe. This fragment was cloned in Escherichia coli using the plasmid pBR322. A 2.5-kb SalI fragment that hybridized with the probe was isolated from the BamHl fragment. Segments of the 2.5-kb fragment were cloned using the phage M13mp7 and sequenced by the dideoxy method.[3] The nucleotide sequence confirmed the amino terminal sequence of the M subunit. Approximately 80% of the 2.5-kb fragment has been sequenced to date.

* Supported by grants from the NIH and the NSF.

[1] M. R. Sutton, D. Rosen, G. Feher, and L. A. Steiner, Biochem. 16 (1982) 3842-3849.

[2] K. Miyoshi, T. Huang, and K. Itakura, Nucleic Acids Res. 8 (1980) 5491-5505.

[3] F. Sanger, A. R. Coulson, B. G. Barrell, A. J. H. Smith, and B. A. Roe, J. Mol. Biol. 143 (1980) 161-178.

M-PM-B8 LABELING THE CYTOCHROME c_2 BINDING SITE IN REACTION CENTERS FROM RHODOPSEUDOMONAS SPHAEROIDES.* M. Y. Okamura and G. Feher, U.C.S.D., La Jolla, CA 92093.

Treatment of reaction centers (RCs) with the reagent 1-ethyl-3[3-trimethylaminopropyl] carbodiimide (MEDC), 10 mM at pH 6.2, 1% octyglucoside, 25°C for 2 hr, results in loss of electron transfer activity between RCs and cyt c (horse) and an incorporation of 5-6 [^{14}C] MEDC molecules/RC. Most of this loss of activity is prevented if cyt c_2 (R. sphaeroides) 100 μM is present during the reaction. The difference in the labeling of the RC, with and without cyt c_2, assayed by SDS-PAGE (see Fig.), shows that cyt c_2 inhibits the binding of 1-2 MEDC molecules to the L and M subunits. The amount of MEDC bound to the H protein was not affected by cyt c_2. Since MEDC reacts specifically with carboxyl groups, these results indicate that carboxyl groups are important for cytochrome binding, as was shown by similar experiments performed on cytochrome oxidase,[1] and that the cytochrome binding site is on or near the L and M subunits, as previously proposed.[2]

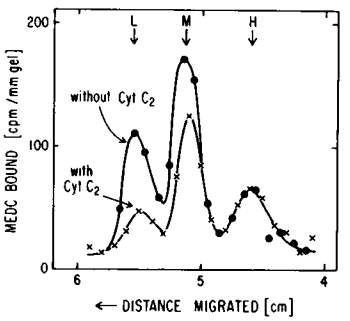

* Supported by grants from the NSF and the NIH.

[1] F. Millett, V. Darley-Usmar, and R. Capaldi, Biochem. (1982) 21, 3857.

[2] D. Rosen, M. Y. Okamura, E. C. Abresch, G. E. Valkirs, and G. Feher, Biochem. (1983), in press.

M-PM-B9 A MODEL FOR THE DAMPING OF OSCILLATIONS IN THE SEMIQUINONE ABSORPTION OF REACTION CENTERS AFTER SUCCESSIVE LIGHT FLASHES.* D. Kleinfeld, E. C. Abresch, M. Y. Okamura, and G. Feher, U.C.S.D., La Jolla, CA 92093.

The optical absorption changes due to semiquinone (λ = 450 nm) in bacterial reaction centers (RCs) exhibit a damped oscillatory behavior when RCs are excited with a series of short laser flashes in the presence of exogenous donors and quinone acceptors. The oscillations are explained by the formation of a stable semiquinone state, $Q_AQ_B^-$, formed after an odd number of flashes and an unstable state, $Q_AQ_B^=$, formed after an even number of flashes;[1,2] the latter state transfers both electrons to regenerate Q_AQ_B. A mechanism for the damping is the equilibration between the states $Q_AQ_B^-$ and $Q_A^-Q_B$, with $Q_A^-Q_B$ being photochemically inactive.[3] The predicted amplitudes are given by:

$$\frac{\Delta A_{450}(n^{th}\ flash)}{\Delta A_{450}(max)} = \frac{1}{2-\alpha}\left[1-(-1)^n(1-\alpha)^n\right]$$

with $\alpha = [Q_A^-Q_B]/([Q_A^-Q_B]+[Q_AQ_B^-])$. We tested the model using RCs from R. sphaeroides R-26 with α independently determined to be 0.065.[3] A good fit between theory and experiment was found (see Figure).

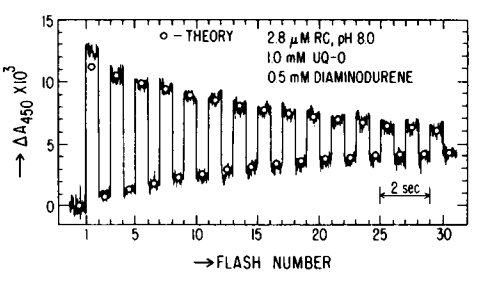

* Supported by grants from the NSF and the NIH.

[1] A. Vermeglio, Biochim. Biochem. Acta 459 (1977) 516-524.

[2] C. A. Wraight, Biochim.Biophys.Acta 459 (1977) 525-531.

[3] D. Kleinfeld, M. Y. Okamura, and G. Feher, Biophys. J. 37 (1982) 110a.

M-PM-B10 SPECTRAL AND KINETIC CHARACTERIZATION OF REDOX COMPONENTS OF LIGHT-DRIVEN ELECTRON FLOW IN PHOTOSYNTHETIC MEMBRANE GROWTH INITIATION SITES OF *RHODOPSEUDOMONAS SPHAEROIDES* J. R. Bowyer[a], C. N. Hunter[b], T. Ohnishi[a] and R. A. Niederman[b]. [a]Dept. Biochem. and Biophys., U. of Penn., Phila., PA 19104 and [b]Dept. Biochem., Rutgers Univ., Piscataway, NJ 08854

The kinetics of light-driven electron flow and the nature of redox centers at sites of intracytoplasmic photosynthetic membrane (ICM) growth initiation have been examined in an effort to elucidate stages in the development of photosynthetic competence in *R. sphaeroides*. These membrane growth initiation sites are isolated with an upper pigmented band (UPB) which sediments more slowly than the mature ICM-derived chromatophore fraction in sucrose gradients. The presence of cytochromes c_1, c_2, b_{561} and b_{566} was demonstrated in the UPB by redox potentiometry; the c-type cytochromes were confirmed in polyacrylamide gel electrophoresis. Signals characteristic for light-induced reaction center (RC) bacteriochlorophyll a (Bchl) triplet and $(Bchl)_2^+$ states were observed by EPR spectroscopy but the Rieske iron-sulfur signal of the bc_1 complex was present at a three-fold reduced level on a RC basis in comparison to chromatophores. Although flash-induced absorbance measurements demonstrated primary and secondary semiquinone anion signals, cytochrome b_{561} photoreduction and cytochrome c_1/c_2 reactions occurred at slow rates. The UPB was enriched approx. 2- and 4-fold in total b- and c-type cytochromes, respectively, but photoreducible b per RC in the UPB was lower. Moreover, none of the RC-linked respiratory systems of the UPB exhibited mature ICM kinetics. These results suggest that interaction of newly synthesized RC with respiratory membrane is insufficient to produce fully functional cyclic electron flow. Instead, subsequent synthesis and assembly of appropriate components of the chain is required, particularly those of the bc_1 segment. (Supported by PHS grant GM26248 (R.A.N.) and NSF grants PCM78-16779 (T.O.) and PCM79-03665 (R.A.N.).)

M-PM-B11 TRIPLET STATE OF BACTERIOCHLOROPHYLL AND CAROTENOID IN BACTERIAL REACTION CENTERS C.C. Schenck, P. Mathis, M. Lutz, D. Gust and T.A. Moore
Service de Biophysique, Département de Biologie, CEN Saclay, 91191 Gif-Sur-Yvette cédex, France

In the reaction center of photosynthetic bacteria, when the primary ubiquinone is reduced, the triplet state P^R of the primary electron donor (a pair of bacteriochlorophylls named P) is populated with a temperature-dependent quantum yield ; when a carotenoid is present, the energy transfer $P^R + Car \rightarrow P + {}^3Car$ takes place in a few ns. We measured by flash absorption spectroscopy the influence of temperature on the yield and kinetics of P^R and ^3Car in the reaction center of several strains of Rps Sphaeroides. The rate of T-T energy transfer, measured as the decay of P^R and as the rise of ^3Car after a flash, decreases when the temperature is lowered. Between 60 and 30 K the half-time of transfer becomes longer that the ^3Car half-time of decay (about 6 µs) and below 20 K the transfer is slower than the internal decay of P^R (about 100 µs). In several cases it is clear that P^R and ^3Car decay independently and are not in thermal equilibrium. The S-S energy transfer from carotenoid to P occurs with a high efficiency at all temperatures.

The data can be accounted for on the basis of estimated energy levels of P^R and ^3Car, in the frame of the equilibrium $^3P\text{-}BChl \rightleftharpoons {}^3[P^+\text{-}BChl^-]$ postulated by Shuvalov and Parson. We propose that both T-T and S-S energy transfers between P and the carotneoid occur via a BChl, to which the carotenoid should be tightly coupled via exchange interactions.

M-PM-C1 ELECTRO-OPTICAL STUDY OF BOVINE ROD OUTER SEGMENT DISK MEMBRANES. Taihyun Chang and Hyuk Yu. University of Wisconsin, Madison, Wisconsin 53706.

Electrophoretic light scattering and dynamic Kerr effect measurements are used to examine the electrostatic and dynamic properties of disk membrane vesicles (DMV). The output at 752.5 nm of Kr ion laser has been tested in order to make sure that it does not bleach the rhodopsins on the DMV. Surface charge of the vescile determined by monitoring the electric mobility shows no difference on photochemical state as well as calcium ion binding isotherm. Furthermore, protein dynamics on the DMV also does not show detectable dependence on photochemical state. GTP-binding protein bound DMV have also been prepared and electro-optical study is performed to examine the effect of the binding.

M-PM-C2 THE TERMINAL LOOP (TL) COMPLEX OF FROG RETINAL ROD OUTER SEGMENT (ROS) DISKS: IMPLICATIONS FOR DISK MORPHOGENESIS. J.M. Corless, Departments of Anatomy and Ophthalmology, Duke University Medical Center, Durham, N.C. 27710.

Thin sectioning and freeze-fracture techniques reveal a clustering of specific morphological elements along the perimeter of ROS disks. This TL complex (Figure) consists of (a) semi-circular to crescent-shaped densities within the TL, (b) linear interdisk densities spanning the cytoplasm near the TL, and (c) distinctive freeze-fracture particles located between (a) and (b). The TL complex appears to have an overall dimeric organization in that the upper and lower halves of the complex in projection seem related by a 2-fold axis (arrow). The TL complexes of adjacent disks preferentially interact to form axially extended rows rather than randomly distributed connections. These features of the TL complex suggest it may maintain both the high curvature and axial spacing of TLs, as well as the alignment of disk margins and incisures. We suggest that the TL complex basically reflects the spatial distribution of the large TL protein localized along the disk perimeter by Papermaster et al. (J. Cell Biol. 78:415, 1978). When the observed and implied features of the TL protein/complex are viewed from the standpoint of disk formation (Steinberg et al., J. Comp. Neurol. 190:501, 1980), the TL protein emerges as prime candidate for the morphogen which locally directs the growth and differentiation of the disk margin. In particular, the intradiskal (extracellular) and cytoplasmic domains of the TL protein/complex provide the templates which guide the development of the disk margin and incisures. Supported by U.S.P.H.S. Grant EY-01659 from the National Eye Institute.

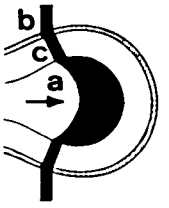

M-PM-C3 TRANSDUCTION MECHANISMS IN PHOTORECEPTOR ADAPTATION. K.N. Leibovic, Dept. of Biophysical Sciences, State University of New York at Buffalo, Buffalo, NY 14214.

It is well known that at a given level of adaptation, the photoreceptor operating range covers only some three orders of magnitude of light intensity, while the complete adaptive range is ten or more orders of magnitude. We have studied the response characteristics near threshold and near saturation by intracellular recording in Bufo rods, taking into account the effects of bleaching and backgrounds. For this purpose the isolated retina is an ideal preparation.

We have found that: (1) Bleaching and backgrounds both reduce the amplitude of the response, but bleaching, unlike backgrounds which speed up the response, leaves the response kinetics invariant within the limits of experimental error. (2) Saturated responses produced by high intensity flashes have a plateau phase, followed by a relaxation to the steady state. The duration of the plateau and the speed of relaxation provide measures of the kinetics of internal transmitter activation and inactivation. An analysis of our data reveals that the effect of the transmitter on membrane potential is reduced either with higher background intensity or with increased levels of bleaching. (3) There is a 1-1 correspondence between bleaching and backgrounds which applies to threshold elevation, response amplitude reduction and possibly also the reduction of the transmitter effect.

Our findings have implications for the internal transmitter hypothesis which will be discussed as it relates to photoreceptor adaptation. Supported by NIH Grant 1 R01 EY03672-01A1.

M-PM-C4 PHOSPHOLIPID BINDING OF ROD OUTER SEGMENT PHOSPHODIESTERASE. David F. O'Brien, Patricia N. Tyminski, Eastman Kodak Company, Research Laboratories, Rochester, NY 14650.

The rod outer segment (ROS) membrane cyclic GMP phosphodiesterase (PDE) is a surface-associated (peripheral) enzyme. The PDE is activated by light exposure of rhodopsin in the membranes in the presence of GTP and a second peripheral enzyme, the ROS GTP-binding protein. In isotonic media the PDE strongly associates with phospholipid membranes as well as with ROS, and rhodopsin: phospholipid membranes. Since only membrane associated PDE is readily light activated, the PDE activity saturates when the available binding sites are occupied. Four to five times the PDE activity is observed with rhodopsin:PC/PE (1:250/250) membranes as with rhodopsin:PC/PE (1:50/50) membranes at equal rhodopsin concentrations. Therefore, the amount of PDE bound to a membrane is dependent on the phospholipid surface, rather than the rhodopsin content. When rhodopsin:PC/PE membranes with bound PDE are mixed with PC membranes, the PDE redistributes to both membrane surfaces. A gradient separation of the rhodopsin:PC/PE and PC membranes, followed by a PDE assay, shows the PDE associated with both membrane fractions. Previous observations of ROS peripheral enzyme transfer between membranes[1] are explained in terms of PDE redistribution to newly available lipid sites, accompanied by bleached rhodopsin interaction with the GTP-binding protein.

---

[1] D. F. O'Brien and P. N. Tyminski, Biophys. J. 33, 203a (1981).

M-PM-C5 VOLTAGE DEPENDENCE OF THE LIGHT-SENSITIVE CONDUCTANCE OF SALAMANDER RETINAL RODS. D. A. Baylor & B. Nunn, Neurobiology Department, Stanford Medical School, Stanford, CA 94305.

We have examined the electrical properties of the light-sensitive conductance by recording membrane current from the outer segment of an isolated rod with a suction electrode while controlling the internal voltage with two intracellular electrodes and a voltage clamp. The ionic conductance of the outer segment appears to consist mainly of light-sensitive pores or carriers, as no residual conductance was measurable in saturating light. In darkness the instantaneous current-voltage relation of the outer segment showed strong outward-going rectification, as if the inward current at potentials negative to -40 mV were limited by an energy barrier on the outer surface of the membrane. The current reversed sign near +5 mV, in agreement with Bader et al. (J. Physiol. 296: 1 (1979)). The rapid increase of outward current with depolarization (e-fold in 13 mV) may indicate that current is carried by divalent ions or Na dimers. Steady light reduced the dark current without changing the reversal potential or form of the rectification.

Small step changes in voltage around the resting level caused slow (half time ≈0.5 sec) symmetrical relaxations in the dark current. These relaxations were faster in the presence of a background light that shortened the incremental flash response. The kinetics of the flash response showed voltage dependence, recovery being slowed by strong depolarization. Within the framework of the "Ca hypothesis" these phenomena may be consistent with voltage effects on an electrogenic Na/Ca exchanger that modulates the light-sensitive conductance by changing $[Ca_i]$. (Supported by USPHS grant EY 01543).

M-PM-C6 DEPENDENCE OF SINGLE PHOTON RESPONSE ON LONGITUDINAL POSITION OF ABSORPTION IN TOAD ROD OUTER SEGMENTS. J. L. Schnapf, Department of Neurobiology, Stanford University Medical School, Stanford, CA 94305. (Intro. by J. G. Nicholls).

Light responses were recorded from toad rods to study the dependence of the kinetics and amplitude of the single photon response on the longitudinal position of excitation within the outer segment. Membrane current was recorded from the inner segment of an isolated rod with a suction electrode while stimulating the outer segment with a dim narrow transverse slit of light.

Flashes at the tip of the outer segment gave a smaller average response than flashes at the base. Comparison of amplitude histograms of responses from the two positions revealed that the probability that an incident photon will elicit an electrical response was the same at the tip and base. Characteristic differences in flash sensitivities at the two sites are attributed to differences in the amplitude of the single photon response.

Flash responses from the tip were slower than those from the base. For both tip and base responses, the ensemble variance was proportional to the ensemble average. This indicates that the single photon responses had the same waveform as their respective averages, and that there was no significant contribution of response latency fluctuations to the waveform of the average.

The calculated cable attenuation is not sufficient to explain the observed differences between tip and base. Differences instead might be associated with a longitudinal gradient of internal sodium concentration, or aging of the outer segment discs. (Supported by USPHS grant EY 01543).

M-PM-C7 EXTERNAL CALCIUM MODULATES THE SELECTIVITY OF CATION TRANSPORT IN ROD PHOTORECEPTORS. Paul P.M. Schnetkamp and Wayne L. Hubbell, Department of Chemistry, University of California, Berkeley, CA 94720

The effects of Ca on the selectivity of cation uptake in isolated intact bovine rod outer segments (ROS) were studied. Cation transport was followed by the potential sensitive probe neutral red. This probe monitors the uptake of cations in ROS by means of their effect on the electrostatic potential at the surface of the intracellular disk membranes [Schnetkamp et al., Biochim. Biophys. Acta 642:213(1981)]. In accordance with this we observed that permeable cations (amines) or alkali cations in the presence of gramicidin affected the probe in a way only dependent on the charge, not on the species of the cation. Without added ionophores, we found that Ca inhibited Na uptake when the external pCa was lowered from 6 to 2, whereas K uptake was stimulated when pCa was lowered from 9 to 6 (subsequent further reduction to 2 had little effect). Li could to some extent replace Na, while Rb and Cs could replace K. On a time scale of ten minutes no significant uptake was observed for organic cations like choline and tetramethylammonium or for Ca and Mg. Changing the external pCa from 9 to 2 was without effect on the probe unless the divalent cation ionophore A23187 was added. In the latter case large changes of the probe were observed even by changes of free Ca in the micromolar range. Therefore, the effects of Ca on Na and K uptake noted above were most likely due to an action of Ca on the external side of the plasma membrane of ROS. The effects of Ca on cation fluxes in ROS appear to be shaped by at least three different transport modes: Ca-inhibited conductive Na transport, Ca-stimulated conductive K transport and Na-Ca exchange diffusion. (This work was supported by NIH Grant #EY 00729.)

M-PM-C8 EXTERNAL CALCIUM INHIBITS THE EFFLUX OF CALCIUM FROM ISOLATED RETINAL ROD OUTER SEGMENT DISCS IN THE DARK. H. Gilbert Smith and Peter M. Capalbo, Advance Technology Laboratory, GTE Laboratories, Inc., Waltham, MA 02254

Decreasing the concentration of free non-radioactive calcium in the external solution flowing past isolated discs which have been preloaded with radioactive calcium causes as much as a 30-fold increase in the rate of radioactivity efflux in the dark. The external calcium concentration dependence of this dark calcium efflux suggests that extradiscal calcium acts at an inhibitory site with an apparent dissociation constant of between 50 and 100 μM. The dark efflux of calcium is not altered by changes in the external sodium (0 to 100 mM), potassium (0 to 100 mM), or magnesium (0 to 2 mM) concentration if the osmolarity is kept constant. External lanthanum, on the other hand, is more effective than calcium in inhibiting the dark calcium efflux. In the presence of 100 μM lanthanum, changes in external calcium no longer alter the dark efflux rate; however, external lanthanum does not inhibit the light-induced release of calcium from discs. This suggests that there are at least two calcium efflux pathways in the disc membrane -- one that is regulated by light and not affected by external lanthanum or calcium, and another that is inhibited by either external lanthanum or calcium in the dark. Alternatively light might act to remove the ability of external lanthanum or calcium to inhibit the calcium efflux. Because the magnitude of the light-induced calcium release depends on the amount of calcium within the discs, factors which regulate the intradiscal calcium in the dark can serve to indirectly control a subsequent light-induced calcium release.

M-PM-C9 CALCIUM CONTENT AND CALCIUM EXCHANGE IN INTACT VERTEBRATE PHOTORECEPTORS W.H. Schröder, G.L. Fain, Institut für Neurobiologie, Kernforschungsanlage Jülich, 5170 Jülich, FRG

Using a new method, we have measured total calcium concentration and calcium uptake into the rods of the toad, Bufo marinus. Measurements were made using a Laser Micro Mass Analyser (LAMMA 500, Leybold-Heraeus), and in parallel with an improved energy dispersive X-ray microprobe fitted to an electron microscope. Retinas were isolated either in total darkness or in dim red light, exposed to oxygenated test solutions, and shock frozen. Frozen samples were cryo-substituted with acetone using a temperature program of stepwise increasing temperatures during a period of two weeks. Cryosubstituted retinas were embedded and sectioned at a thickness of 0.5 um. LAMMA measurements were made from rod outer segments using a beam diameter of 2 - 4 um. Rods in freshly dissectioned dark-adapted (DA) retinas unexposed to test solutions contained 3 - 5 mmol/l total Ca. No variation in [Ca] could be detected either across the ROS or in profiles from tip to base ($\pm$ 6 % SD). When dark adapted retinas were exposed either to Na or K ringers containing 44Ca (stable isotope) substituted for 40Ca no significant amount of 44Ca uptake (< 2 % of total Ca) could be detected in intact ROS, even after 45 min of exposure, though total Ca was unchanged. By contrast 5 % to ~ 50 % of total Ca was 44Ca in outer segments broken off from the retina, even after 1 min exposure to test ringer, indicating that isolation of ROS, as normally performed, may drastically change the properties of Ca transport. Exposure to low Ca ringer depletes ROS of Ca. However, this process is slow and seems not to be responsible for the major part of the decrease in the sensitivity of rods to light in low Ca.

M-PM-C10 EFFECTS OF cGMP ON THE LIGHT-SENSITIVE CA^{2+} POOL OF ROD OUTER SEGMENT DISKS. John S. George, Division of Life Sciences, Los Alamos National Laboratory, Los Alamos, NM 87545

Cytoplasmic Ca^{2+} activity (Aca) appears to control the dark current of retinal rods, but manipulations which change intracellular cGMP concentrations also affect the magnitude of the dark current and the kinetics of the photoresponse.

Distribution and metabolism of Ca^{2+} was studied in suspensions of isolated rod outer segments (ROS) with leaky plasma membranes. Preparations contained 10-100 μM Rhodopsin along with some mitochondria and nuclei. Aca of suspensions was monitored with a miniature Ca^{2+} sensitive electrode or the distribution of ^{45}Ca between particles and suspending aqueous was studied by centrifugal filtration of particles through silicone oil or radioautography of freeze-dried thin layers of ROS suspension. Light caused a rapid release of Ca^{2+} from an ionophore (A23187) sensitive pool in ROS. $>10^4$ Ca^{2+} were released per photon ($>10^3$ Ca^{2+} photon^{-1} sec^{-1}) without detectable latency in the fastest responses.

In the presence of ATP, cGMP stimulated uptake of Ca^{2+} by ROS, driving Aca below levels observed with any control nucleotide injection. Total particle Ca^{2+} increased and this additional Ca^{2+} was released by light. 10 μM Ruthenium Red blocked Ca^{45} accumulation by mitochrondria but ROS still contained enough Ca^{45} (10-20x more per unit volume than the suspending medium in the presence of cGMP) to account for observed light responses.

In the absence of added ATP, ROS retained >50% of their ionophore sensitive Ca^{2+} for >1 hr, but released it when cGMP was added. Preliminary results are consistent with the idea that protons produced by cGMP hydrolysis might exchange for Ca^{2+} ions bound within the ROS disk.

M-PM-C11 INTERFERENCE BETWEEN THREE FUNCTIONNAL SITES ON PHOTOEXCITED RHODOPSIN : THE CHROMOPHORE SITE, THE BINDING SITE FOR THE G PROTEIN, AND THE PHOSPHORYLATION SITE. Claude PFISTER, Hermann KUHN* and Marc CHABRE, DRF/Biologie Moléculaire et Cellulaire, CENG, F-38041 Grenoble and *Institut für Neurobiologie der KFA, D-5170 Jülich.

Photoexcited rhodopsin interacts with the GTP binding protein (G or Transducin) as a first step to the activation of cGMP phosphodiesterase in the rods. Meta II is the intermediate R* to which G binds prior to GDP/GTP exchange (Emeis et al, FEBS Letters, 143, 29 (1982), Bennett et al, Eur. J. Biochem., 127, 97 (1982)). We demonstrate that, at physiological temperature and pH, in frog rods, the binding of G to R* perturbs two reactions that Meta II normally undergoes : The spectral post-Meta II decay of the chromophore and the phosphorylation of the protein by an ATP dependent kinase. The evolution of R*-G complexes, obtained upon less than 10% bleaching in absence of GTP, was compared to that of free R* obtained upon strong bleaching and/or in presence of GTP : i) By linear dichroism measurements on magnetically oriented frog rods suspensions, a strong reduction of the amount of Meta III formed is observed for the R*-G complex, as compared to free R*, and the rate of the reversal reaction Meta III → Meta II is much enhanced. ii) The phosphorylation rate of complexed R* is reduced by a large factor as compared to that of free R*.

The interferences between the reactions at the three sites identified in R* will be discussed : The retinal site, in the hydrophobic core, is sensitive to the presence of G bound to its site on the cytoplasmic surface; the kinase and the G protein compete for the access to their respective binding sites, both located on the surface.

Supported by CNRS (Equipe de recherche 199).

M-PM-D1 REGULATION OF ADIPOCYTE TRIGLYCERIDE METABOLISM MONITORED BY ^{13}C NMR. L. O. Sillerud and C. H. Han*, Los Alamos National Laboratory, University of California, Los Alamos NM 87545

The fat droplet within the isolated rat epididymal fat pad adipocyte contains triglycerides at a concentration high enough so that high-resolution ^{13}C NMR signals can be obtained in a few minutes with an excellent signal-to-noise ratio from about 10^6 cells. We have utilized these resonances to study the synthesis and degradation of triglycerides and their regulation by the hormones insulin, glucagon and epinephrine, and have correlated these data with parallel experiments using ^{14}C labeled substrates. The synthesis of triglyceride from 5.5 mM glucose was stimulated by about 4-fold by 10 nM insulin. Measurements of the triglyceride spin-lattice relaxation times and nuclear overhauser enhancements at 37°C in situ within the adipocyte were used to correct the NMR data in order to determine absolute metabolic rates. For example, triglyceride synthesis from glucose in the presence of insulin occured at a rate of 330 nmol/hr/10^6 cells. Since the NMR signals from free and esterified fatty acids and glycerol are distinct we could directly measure the rate of hormone-stimulated lipolysis. Epinephrine (10 μM) gave a lipolytic rate of 0.30 μmol/hr/10^6 cells as monitored by free glycerol appearance in the medium. ^{13}C NMR provides a superior method for the measurement of triglyceride metabolism since it directly measures the changes in the substrates and products in situ. These results will be useful for the application of NMR to humans in vivo as a result of the findings that the ^{13}C NMR spectrum of, for example, a human arm (Alger, Sillerud, et al. Science 214 (1981)660) consists primarily of resonances from fats.

This work was performed under the auspices of the Department of Energy.

M-PM-D2 NMR STUDIES OF INTRACELLULAR ^{23}Na IN AMPHIBIAN OOCYTES, OVULATED EGGS, AND EARLY EMBRYOS. Raj K. Gupta, Adele B. Kostellow, and Gene A. Morrill, Department of Physiology and Biophysics, Albert Einstein College of Medicine, 1300 Morris Park Avenue, New York, NY 10461

The anionic complex of dysprosium(III) with tripolyphosphate has been used as a paramagnetic shift reagent for separating the resonances of intra- and extracellular Na ions in suspensions of Rana oocytes, ovulated eggs, and early cleavage embryos. This technique allows accurate determination of both extracellular space and $[Na]_i$. In prophase oocytes, only 14-17% of the total Na (40 mmols/kg cells) was NMR-visible. Homogenizing oocytes in 0.24 M sucrose did not significantly affect the Na-resonance but addition of nitric acid markedly increased the Na-signal. NMR analysis of Na in medium and oocyte suspensions yielded identical pulse widths for the same nutation angle showing that the coupling of the rf to the coil is not affected by the presence of oocytes in the sample tube. In contrast, the relaxation time (T_1) for intracellular Na was only 4-5 msec compared with the value of 57 msec for Na in medium without shift reagent. In Ca-free medium the oocyte gained 16-20 mmols Na/kg cells with a corresponding increase of 17-20 mmols of NMR-visible Na, suggesting "free" and "bound" compartments within the oocyte. Progesterone reinitiates the meiotic divisions and by second metaphase the eggs gain Na with about 30% of the total Na being NMR-visible. Following fertilization there is a 10-15% loss of cell Na and by the 2-4 cell stage about 70% of the total Na is NMR-visible. These results cannot be readily explained by a uniform first order quadrupolar interaction involving the entire Na pool, and suggest that: 1) a large fraction of the prophase oocyte Na is "bound" and/or compartmentalized, and 2) changes in NMR-visible Na occur following hormonal and developmental stimuli.(Supported in part by AM-32030 and HD-10463).

M-PM-D3 PERPENDICULAR ALIGNMENT AND CATHODAL GALVANOTAXIS OF FIBROBLASTIC CELLS IN DC ELECTRICAL FIELDS. M.S. Cooper, Biophysics Group and R.E. Keller, Department of Zoology, University of California, Berkeley, CA 94720. (Intro. by H.J. Bremermann)

The effects of DC electrical fields on cultured amphibian (Ambystoma mexicanum and Xenopus laevis) neural crest cells were studied. Seconds after fields are applied, saltatory movements of intracellular particles throughout the cell accelerate. Subsequently, anode (hyperpolarized) and cathode (depolarized) facing margins of the cells withdraw, breaking contacts with other cells and/or the substratum. This withdrawl is believed to be caused by cytoskeletal contractions in response to modified ion fluxes through the cell membrane at these sites. The bipolar cells which result are aligned perpendicular to the electric field, a shape which minimizes the voltage drop across the cell's exterior and thus reduces the induced transmembrane potential perturbations. Perpendicular alignment has been observed in fields as low as 1-2 V/cm. In larger fields (>10 V/cm), the perpendicular cells migrate sideways towards the cathode. The cells appear to be constrained to remain perpendicular to the field during this galvanotaxis even though virtually all protrusive activity is confined to the cathode side of the cells. We propose that the perpendicular orientation is maintained by the same mechanism which generates the perpendicular orientation initially; very likely the chronic hyperpolarization and depolarization of the anode and cathode facing cell membranes. Membrane depolarization and electrophoretic accumulation of integral membrane components are considered as reasons for protrusion formation on the cathode sides of the cells. We suggest that confluence disruption produced by DC electrical fields may stimulate cell proliferation in fibroblastic cell types which exhibit density-dependent contact inhibition.

M-PM-D4 HETEROGENEITY OF CELLULAR DYE ENVIRONMENTS IN AN EPITHELIAL CELL LINE DETERMINED BY FLUORESCENCE LIFETIMES. Beverly S. Packard, Kerry K. Karukstis, and Melvin P. Klein, Division of Chemical Biodynamics, LBL, University of California, Berkeley, CA. 94720. (Intr. by Melvin Calvin)

The cellular localization and distribution of fluorescent probe molecules depend on their chemical structure and cellular environment. To study the number and types of environments in an epithelial (Madin-Darby Canine Kidney) cell line, we have measured the fluorescence lifetimes of three structurally different fluorescent dyes -- the indocarbocyanine diI C16(3), rhodamine-B, and Collarein. The latter is a rhodamine-cardiolipin conjugate we have recently designed and synthesized to localize in the plasma membrane. The former two dyes required at least two exponentials to fit their decay curves while a single exponential with a time constant of 1.85 nsec. sufficed to fit the Collarein decay. These data are consistent with fluorescence microscopic observations in which diI and rhodamine-B exhibit heterogeneous spatial distributions while Collarein appears to be located exclusively on the cell surface. (This work was supported by NIH Training Grant T32 AM07349Z, NIH Research Service Award 1 F32 GM08617-01, and the U.S. Department of Energy, Contract No. DE-AC03-76SF00098.)

M-PM-D5 INWARD RECTIFICATION IN NEANTHES OOCYTES. R. Gunning and S. Ciani. Dept. of Physiology, UCLA, Los Angeles, Calif. 90024. USPHS GM 27042-06 and MDA.

Inward rectifying potassium current in the eggs of the marine polychaete Neanthes arenaceodentata was studied under voltage-clamp conditions. The steady-state conductance, the time-constant of current relaxation and the "instantaneous" conductance, defined as the conductance 1msec after the beginning of the voltage-step, were analyzed as functions of external potassium and transmembrane voltage. As seen in other preparations, the steady-state and instantaneous conductances increased sigmoidally about E_K as the membrane potential was hyperpolarized. Also, the current relaxed exponentially between the instantaneous and steady-state values. However, the time-constant of current relaxation in Neanthes increased sigmoidally with hyperpolarization throughout an 80mV range centered at E_K, in contrast to the exponential decrease seen in starfish eggs (Hagiwara, Miyazaki & Rosenthal, 1976, Journal of General Physiology, 67:621) and skeletal muscle (Hestrin, 1981, Journal of Physiology, 317:497; Leech and Stanfield, 1981, Journal of Physiology, 319:295). The Neanthes results are best described by a three-state kinetic model where O is the only conducting state, x and w are independent of both voltage and external potassium, the single-channel conductance is voltage-independent, and a fast process is responsible for the apparent instantaneous rectification.

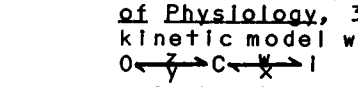

M-PM-D6 ELECTROPHYSIOLOGICAL CHANGES IN STARFISH OOCYTES DURING HORMONE-INDUCED MATURATION. WJ Moody, JB Lansman,& MM Bosma. Jerry Lewis Center, UCLA, Los Angeles, CA 90024

Electrical properties of oocytes of the starfish L.hexactis were studied under voltage clamp during induction of meiotic maturation by 1-methyladenine (1-MA). The immature oocyte showed three ionic currents:(1) An inwardly rectifying K current (I_{ir}), activated at potentials negative to -70mV; (2) An inward Ca current (I_{Ca}) activated at potentials positive to -50mV; and (3) A transient outward K current (I_A), activated at potentials positive to -20mV. During the first hour of exposure to 1-MA, the amplitudes of each of the three currents were changed. I_A and I_{ir} were consistently decreased (by 50-90% & 30-60%, respectively), while I_{Ca} was increased. The change in I_{Ca} occurred in about 70% of the cells. Kinetics of the currents appeared unchanged, as were the steady-state inactivation curves for I_A and I_{Ca}. The changes were gradual, with 50% effect at about 30 min (15°C). With the same time course, the total membrane capacitance (C_m) decreased by 50-60%, from ca. 3.6 to 1.5 $\mu F/cm^2$. The C_m change may be related to retraction of microvilli during maturation. During longer exposures to 1-MA, a slow partial reversal of the changes in C_m, I_{ir}, and I_A was seen. Recovery could be as much as 50% in 5 hours. The similarity in time course of I_A and C_m decrease and recovery was particularly striking, and suggests that membrane removal during maturation may serve to modulate I_A. The fact that the percentage decrease in C_m was consistently larger than I_A suggests that the membrane removed may have a high density of I_A channels. I_{Ca} showed no reversal at long times, and sometimes continued to increase long after the first hour, indicating that a separate mechanism for its change is probably involved.

M-PM-D7 ENDOPLASMIC RETICULUM FROM SEA URCHIN EMBRYOS CONTAINS AN ATPase ACTIVATED BY MICROMOLAR CALCIUM. K.W. Anderson, A.C. Charles, and W.Z. Cande, Department of Botany, University of California, Berkeley, CA 94720.

Since changes in intracellular Ca^{2+} concentration have been implicated in the control of mitosis and cytokinesis, we have examined homogenates of unfertilized and fertilized sea urchin eggs and two-cell stage embryos for Ca^{2+} pump activity. Homogenates were fractionated on 30-50% sucrose density gradients, and the fractions were assayed for Mg-ATPase activity activated by μM Ca^{2+}. A fraction identified by marker enzymes as endoplasmic reticulum (ER) was found to have the highest specific (Ca^{2+} + Mg^{2+}) ATPase activity. Both A23187 and oxalate enhanced this activity, while vanadate, azide, and stelazine (a calmodulin inhibitor) had no effect. As viewed by negative stain electron microscopy, the ER appeared to form closed, unilamellar vesicles 130-200 nm in diameter. Two-cell stage embryos showed a higher content of (Ca^{2+} + Mg^{2+}) ATPase than did either fertilized or unfertilized eggs. A vesicular plasma membrane fraction was also obtained from the sucrose gradient. Its Mg-ATPase activity was inhibited 10% by 5 μM Ca^{2+} and 40% by 100 μM Ca^{2+}. ATPase rate with mM Mg^{2+} was the same as with mM Ca^{2+}. We are presently determining ATP-dependent Ca^{2+} uptake, the relation of Ca^{2+} concentration to enzyme activation, and the coupling ratio for Ca^{2+} transport. Since we have previously shown (Silver et al., 1980, Cell 19:505) that isolated mitotic apparatus can actively accumulate Ca^{2+}, we are examining such preparations for the presence of Ca^{2+}-sequestering ER. (Supported by NIH grant GM23238.)

M-PM-D8 CURRENT PATTERNS GENERATED DURING SPERM-EGG INTERACTION IN VOLTAGE CLAMPED EGGS OF THE SEA URCHIN, LYTECHINUS VARIEGATUS. E. L. Chambers and J. W. Lynn. Physiology and Biophysics, Univ. Miami, School of Medicine, Miami, FL 33101. (Intr. by D. Landowne).

Unfertilized eggs were voltage clamped (VC) using either a fast 2-electrode clamp or a 1-electrode switched clamp. Eggs were continuously VC 3-5 min prior to insemination and 15 min following sperm initiated activation. At potentials (E) from +15 to -75 mV, for eggs penetrated by sperm which subsequently cleave, characteristic inward current (I) patterns (the activation current, Iact) are generated comprising : a) a sharp initial onset and shoulder of 11.7±0.3s duration, both with I amplitude dependent on E; b)a major I peak at 30.6±0.9s; and c) a decline of I to 10% of the I peak, the rate being exponentially related to E. As E becomes more negative, the percentage of cleaving eggs decreases as a consequence of suppressed sperm entry. The Iact of noncleaving eggs also comprises a sharp onset, a shoulder and a major peak. However, shoulder I returns towards the holding level prior to the I peak, I peak is delayed, and I returns rapidly to the holding level independently of E. Additional I patterns (sperm transient currents) are generated at E between -30 and -80 mV which are initiated by interaction of non-penetrating sperm with the egg with no subsequent morphological signs of activation. These currents show a sharp onset, a maximum I dependent on E, and a sharp return to the holding level after 10.0±0.7s. At clamped potentials of +20 mV and above, sperm attach to the egg and no activation whatsoever occurs. The approximate linear relationship between E and the magnitude of the shoulder of Iact and of the sperm transients are consistent with the presence of receptor type channels in the egg membrane which open in response to a sperm ligand. [NSF PCM 78-6178, NIH RR-05363-20, NIH HD-07129].

M-PM-D9 CELL GROWTH ON LIQUID-LIQUID INTERFACES, C. R. Keese and I. Giaever, General Electric Research & Development Center, P.O. Box 8, Schenectady, NY 12301.

We have cultured a wide variety of both normal and transformed cells on a phase boundary between tissue culture medium and a fluorocarbon fluid. The immediate substrate is the layer of denatured protein that spontaneously forms on the interface. Growth patterns observed on these interfaces differ from those seen on conventional solid substrates. Depending on the cell strain and the composition of the fluorocarbon fluid, cells will tend to clump into isolated aggregates or form nearly confluent cell monolayers containing "lake-like" openings. We demonstrate that these growth patterns can be attributed to the ability of cultured cells to stress and break the protein monolayer on which they grow.

In addition we have applied our understanding of these substrates to devise a new type of microcarrier system for mass culturing in which anchorage-dependent cells are grown on the surface of small droplets (∿200μm dia.) of emulsified fluorocarbon fluids.

In both this microcarrier system and with growth of cells on planar interfaces, the cell mass may be mechanically harvested without the use of proteolytic enzymes or chelating agents, thus avoiding the uncertain effects of such treatment.

(Supported, in part, by a grant from the National Foundation for Cancer Research, Bethesda, MD.)

M-PM-D10 POROUS BOTTOM CULTURE DISHES AND APPARATUS FOR GROWTH AND STERILE MEASUREMENT OF SHEETS OF EPITHELIAL CELLS. Roderic E. Steele, NHLBI, NIH, Bethesda, MD 20205.

Epithelial cells normally obtain most of their nutrients from the basolateral side which faces the blood stream. When these cells are grown in culture on a surface, it is this basolateral side that is found attached to the surface. Thus when the cells grow into a confluent layer on a solid surface, they tend to isolate their basolateral sides from the nutrient containing medium on the opposite side of the cells. The normal development of tight junctions between these epithelial cells will increase this isolation.

We have developed porous bottom culture dishes (PBCDs) which allow the cells to exchange nutrients and wastes at their basolateral sides. When the PBCDs are made with feet about 1.5 mm tall, the culture medium can circulate freely beneath the PBCDs. The bottom of the PBCDs have been made from three types of porous membranes made from cellulose esters, collagens or polycarbonate coated with collagen. The sides of the PBCDs provide chemical and electrical isolation between the solution which contact the two sides of the membranes. This makes it possible to bath the basolateral and apical sides of the cell layers with different solutions. The electical isolation greatly simplifies the task of measuring potential difference and short circuit current of the epithelia under sterile conditions. We have designed apparatus for rapid measurement of these electrical parameters under sterile conditions.

M-PM-D11 SUSPENSION POLYMERIZATION TO ADAPT MICROSPHERES TO CONJUGATE FORMATION. George Czerlinski and June Tow, Northwestern University, Chicago, Illinois 60611.

In contrast to emulsion polymerization, suspension polymerization only uses one liquid phase. The conditions of polymerization are such that dense coats are obtained with high reduction in interparticle connections and improved definition of coating thickness, thereby allowing quantitative investigations. The coatings carry charged residues (such as CH_2-COO^- or CH_2-NH_3^+), thereby promoting reversibility of suspending the particles in aqueous media and diminishing aggregation behavior. These residues may also be used to link the particles chemically to other molecules, including proteins (and immunoglobulins). As the interior of these coated particles consists of magentizable materials, magnetic manipulation of these particles may be used in many applications in molecular and cellular biochemistry. One such application deals with the magnetic sorting of cells according to surface density of antigenic sites.

M-PM-D12 CIRCULAR INTENSITY DIFFERENTIAL SCATTERING, (CIDS), STUDIES OF THE SPERM OF ELEDONE CIRRHOSA. (Marcos F. Maestre, Carlos J. Bustamante, and Ignacio Tinoco, Jr.) Lawrence Berkeley Laboratory and Chemistry Department, University of California, Berkeley, CA 94720.

The angular dependence of differential scattering of circularly polarized light can provide detailed information about the structures of chiral objects with dimensions the same order as the wavelength of light. The pitch, radius and sense (right- or left-handed) of helices can be determined. CIDS is defined as $(I_L - I_R)/(I_L + I_R)$ where I_L, I_R are the scattered intensities when left and right circularly polarized light is incident. The angular dependence of the CIDS has been measured for the sperm of the mediterranean octopus Eledone cirrhosa (1) and compared with theoretical calculations (2). A reasonable fit to the measured scattering pattern was obtained for a left-handed helical structure of pitch 0.65 microns and radius 0.25 microns. High voltage electron micrographs of the sperm show a helical structure which corresponds approximately to the helix deduced from the differential scattering of circularly polarized light. (1) M. F. Maestre, C. J. Bustamante, T. L. Hayes, J. A. Subirana, and I. Tinoco, Jr., Nature 298, 773 (1982); (2) C. J. Bustamante, et al., J. Chem. Phys. 73, 4273 (1980); 73, 6046 (1980); 74, 4839 (1981); 76, 3440, (1982).

M-PM-D13 QUANTITATIVE ANALYSIS OF THE RELATIONSHIP BETWEEN RECEPTOR OCCUPANCY AND CELLULAR RESPONSE IN THE HUMAN NEUTROPHIL. L.A. Sklar, A.J. Jesaitis, R.G. Painter, and C.G. Cochrane. Department of Immunology, Scripps Clinic and Research Foundation, La Jolla, CA 92037

The neutrophil is a key participant in inflammation and inflammatory disease. In order to understand the mechanism by which the occupancy of its cell surface receptors leads to its physiological responses, we devised techniques to relate quantitatively the occupancy of the receptors to the responses. First, we developed spectroscopic and flow cytometric methods to evaluate the interaction of fluorescent ligands with their receptors (Cytometry 3:161, 1982; J. Cell. Biochem., in press, 1983). These methods permit a real-time analysis of ligand internalization and an essentially continuous analysis of association and dissociation of the ligand and receptor. Second, we measured cell responses with a time resolution of a few seconds under conditions where receptor occupancy can be controlled and analyzed (P.N.A.S. 78:7540, 1981; J.B.C. 257:5471, 1982). The occupancy of the neutrophil formyl peptide receptor is controlled by a "stimulus pulse" consisting of fluoresceinated peptide and, after a defined time interval, a high affinity antibody to fluorescein. The antibody inhibits ligand binding to the receptor and resolves receptor-bound and free ligand. From pulse experiments we have constructed "occupancy-response" curves. The secretory function and potential transduction events ("membrane depolarization" and cyclic nucleotide elevation) depends on 5-10 percent occupancy. In contrast, the production of superoxide anion depends on occupancy of at least 50 percent of the receptors. The initial phase of the occupancy-response curve is nearly linear in all cases. A comparison of the occupancy-response and internalization kinetics indicates that the responses are elicited prior to the internalization of the ligand-receptor complex. Supported by NIH Grant AI 17354.

M-PM-E1 MULTIPLE EFFECTS OF D-600 ON ACETYLCHOLINE CATIONIC CHANNEL ACTIVATION AND DESENSITIZATION IN APLYSIA. N.T.Slater, H.L.Haas* and D.O.Carpenter, Center for Laboratories and Research, New York State Department of Health, Albany,NY 12201 and Univ. of Zürich, Switzerland.

The effects of the calcium antagonist D-600 on excitatory acetylcholine (ACh) receptor activation and desensitization were studied in Aplysia abdominal RB cells voltage clamped with two microelectrodes. ACh was applied by ionophoresis and D-600 was bath perfused. The steady-state ACh induced current (I_{ss}) was reduced by D-600 in a voltage dependent manner, the degree of antagonism increasing with hyperpolarization (-50 to -130 mV). The time constant of voltage jump-induced ACh current relaxations (τ_f), which approximate the mean single channel lifetime, were also reduced in a voltage dependent manner by D-600, the degree of reduction of τ_f increasing with membrane potential. In the absence of D-600 the ACh-induced inward current exhibited a single exponential relaxation to a stable plateau (I_{ss}) following voltage command steps from -50 mV to between -70 and -130 mV. In the presence of D-600 (10-100 μM) a slower inverse relaxation appeared following the accelerated inward relaxation. The time constant of this inverse relaxation (τ_s) was inversely related to both ACh and D-600 dose. High doses of ACh evoke inward currents which decrement with a time course which displays two exponential components. D-600 (20 μM) accelerated the time constant of the slow component (control: 215 ± 6 sec; D-600: 99 ± 5 sec) without affecting the fast component (control: 25 ± 2 sec; D-600: 23 ± 3 sec). These results suggest that, in addition to any effects on calcium channels, D-600 may block the open state of the ACh-activated cationic channel. The acceleration of the slow component of desensitization may provide support for the suggested dependence on intracellular free calcium of this process.

M-PM-E2 AGONISTS BLOCK CURRENT THROUGH ACETYLCHOLINE RECEPTOR CHANNELS ON BC3H1 CELLS. Sine, S.M. and J.H. Steinbach, Molecular Neurobiology Lab, The Salk Institute, La Jolla, CA.

We have examined the effects of raised agonist concentration on single channel currents elicited by cholinergic agonists across membrane patches from BC3H1 cells. Suberyldicholine (Sub) at concentrations above 10^{-6}M reduces the apparent mean channel open-time in a concentration- and voltage-dependent fashion. The closed times within a burst show a major component whose time constant is independent of Sub concentration but increases with hyperpolarization. Carbamylcholine (Carb, $1\text{-}5\times10^{-3}$M) and acetylcholine (ACh, $0.3\text{-}5\times10^{-3}$M) produce a voltage- and concentration-dependent decrease in apparent mean single channel conductance. The data are well-described by a simple sequential blocking model in which agonist occludes the ion channel. Sub shows a "slow block" similar to local anesthetics, whereas ACh and Carb show a "fast block". When the data are analyzed in terms of this model, the forward and backward rates for the action of Sub are estimated to be 1×10^{6} exp (-Vx.025)M^{-1} sec^{-1} and 1.1×10^{4}xexp (Vx.018) sec^{-1} (V in mV). The dissociation constants for Sub, Carb and ACh are estimated to be 12×10^{-3}xexp (Vx.043)M, 72×10^{-3}xexp (Vx.028)M and 35×10^{-3}xexp (Vx.034)M respectively. These apparent dissociation constants are several orders of magnitude greater than the apparent dissociation constants for receptor activation (Sine and Taylor, J. Biol. Chem. 254:3315, 1979). The voltage dependences indicate, in terms of the sequential model, that the charge on Carb or ACh senses 70-80% of the applied membrane field at the binding site whereas both charges of Sub sense, on the average, 55% of the membrane field. Supported by grants NS 13719, BNS-79-06013, and ONR contract N00014-79-C-0798. SMS was supported by fellowships from the MDA and the NIH. JHS is a Sloan Foundation Fellow.

M-PM-E3 APPARENT CHANNEL OPENING AND AGONIST DISSOCIATION RATES OF THE ACETYLCHOLINE RECEPTOR ON BC3H1 CELLS. Sine, S.M. and J.H. Steinbach. Molecular Neurobiology Lab, The Salk Institute, La Jolla, CA.

Activation of the nicotinic acetylcholine receptor was examined in BC3H-1 clonal muscle cells using the gigaseal patch clamp technique. Three agonists, acetylcholine, carbamylcholine, and suberyldicholine were applied at low concentrations and currents measured through single channels. For each agonist, channel opening events were interrupted by brief closings ("nachschlags"). The mean duration of nachschlags was unique for each agonist as was the mean number of nachschlags per burst of openings. The rate of channel opening, β, and the agonist dissociation rate, k_{-2}, were estimted as described by Colquhoun and Hawkes (Proc. Roy. Soc. B 211:204, 1981). At potentials of -60mV to -90mV and temperatures of 9-12°C we obtained the following estimated rates (mean ± S.D.; sec^{-1}).

	N	β	k-2	α (corrected)	conc. range
Carb	2	4378 (3680,4895)	7862 (6126,9237)	113 (111,114)	5×10^{-6}M
ACh	4	13050 ± 2050	4350 ± 550	175 ± 50	2×10^{-8}M - 10^{-6}M
Sub	8	9050 ± 3500	4500 ± 1200	99 ± 40	10^{-8}M - 2×10^{-7}M

Using "outside-out" patches, we have examined receptor activation kinetics across a range of agonist concentrations. At high agonist concentrations the analysis is complicated by the appearance of additional effects of agonists, which we interpret as due to agonist blocking of the receptor channel (abstract submitted). This research supported by grants NS 13719, BNS-79-06013 and ONR contract N-00014-79-C-0798. S.M.S. was supported by fellowships from the MDA and the NIH. J.H.S. is a Sloan Foundation Fellow.

M-PM-E4 KINETICS OF ENDPLATE ACETYLCHOLINE RECEPTOR SINGLE CHANNEL CURRENTS.

M.D. Leibowitz and V.E. Dionne, Departments of Biology and Medicine, University of California at San Diego, La Jolla, CA 92093

The kinetics and amplitudes of single channel currents elicited by different agonists from acetylcholine receptors at the same neuromuscular junctions have been compared using an analytical method described previously (Leibowitz & Dionne, Biophys. J. (1982) 37:18a; Dionne & Leibowitz, Biophys. J. (1982) 39:253-261). Events were recorded from junctional regions of garter snake (sp. Thamnophis) twitch fiber membrane using conventional patch-clamp techniques. Preparations of intact m. costocutaneous were enzymatically treated to remove the nerve terminals and connective tissues. Patches formed in this way contained many acetylcholine receptors. The rate of single channel activity was kept small using low concentrations of the agonists carbamylcholine (1-20 μM) or acetylcholine (0.1-1 μM).

The single channel current-voltage relation for any cell was linear, and its slope-conductance was independent of agonist. However, the activation kinetics depended upon the agonist used. The kinetic differences seemed to stem from agonist dependent lifetimes of both the open channel state and the doubly liganded closed state from which channels open. Both of these lifetimes were smaller when carbamylcholine was used to activate channels than when acetylcholine was used.

(Supported by NIH:NS 15344 and ONR:N00014-79-C-079)

M-PM-E5 HALOTHANE SHORTENS ACETYLCHOLINE RECEPTOR SINGLE CHANNEL OPENTIMES IN CULTURED XENOPUS MYOCYTES. James Lechleiter and Raphael Gruener. (Intr. by Stuart Hameroff). Dept. Physiology, University of Arizona College of Medicine, Tucson, AZ 85724.

We are interested in the effects of membrane fluidity on the acetylcholine receptor (AChR). Modulation of receptor function may occur during development or in response to pharmacologic agents as a result of changes in membrane fluidity. General anesthetics, with a wide variety of molecular structures, increase membrane fluidity (Pang et al. Mol.Pharm.15:729,1979). These anesthetics also reduce nerve-evoked postsynaptic depolarizations (Gage & Hamil, Int.Rev.Physiol.25:1:1981). This effect results from an increase in the decay rate of endplate currents, possibly due to the shortening of AChR channel opentime. To investigate this, we measured single channel currents using the extracellular patch clamp technique.

Uninnervated muscle cells from Xenopus embryos were grown in culture for 1 to 3 days. During experiments, cultures were continuously superfused with recording medium bubbled with air (control) or air with vaporized halothane. Single channel events showed two distinct control populations on the basis of current amplitudes. The mean opentime of the larger current channels was shorter than that of the smaller current channels. Exposure to halothane resulted in a significant reduction in the mean channel opentime of both populations. Since halothane is freely soluble in membrane lipids and since it is strongly hydrophobic, it is unlikely that the observed effects are due to direct interaction of anesthetics with the receptor. Our results are consistent with the idea that an increase in membrane fluidity allows more rapid relaxation of open receptor channels and are in agreement with the hypothesis of Gage & Hamil (Neurosci.Let.1:61:1975). Supported by BRSG and COG grants and by training grant #842122.

M-PM-E6 ION PERMEATION AND SELECTIVITY OF THE ACETYLCHOLINE RECEPTOR CHANNEL

H.M. Hoffman and V.E. Dionne, Department of Medicine, University of California at San Diego, La Jolla, CA 92093

The mean conductance of acetylcholine receptor channels at garter snake neuromuscular junctions depends monotonically on temperature with an apparent activation enthalpy ca. 11 kcal/mol at -90 mV and between 0-23 C (Hoffman & Dionne, Biophys. J. (1982) 37:19a). The temperature dependence was independent of the permeant ions (Li, Na, Rb, Cs), although the mean conductance was less with Li and increased according to the sequence above.

Both the conductance data and its temperature dependence were fit by an energy-barrier model consisting of one dominant barrier with a shallow well on its extracellular side. Ion selectivity appeared to be produced by different well depths for different ions and not by different barrier heights with this model. Given a constant barrier enthalpy for the different ions, the well free energy depth was least for Li and increased with the observed conductance sequence: Li, Na, Rb, Cs. For these ions the correlation between greater well depth and increased conductance can be accounted for by the exponential distribution of thermal energy which drives the ion permeation process.

(Supported by NIH:NS 15344)

M-PM-E7 PATCH-RECORDING OF PURIFIED AND RECONSTITUTED TORPEDO ACETYLCHOLINE RECEPTORS.
David W. Tank*, Richard L. Huganir+, Paul Greengard+, and Watt W. Webb†, *Dept. of Physics and †Applied and Engineering Physics, Cornell University, Ithaca, NY 14853, and +Dept. of Pharmacology, Yale University School of Medicine, New Haven, CT 06510.

We have applied our methods of patch-clamp recording ion channels reconstituted into large liposomes (D.W. Tank, C. Miller, and W.W. Webb (1982) PNAS 80, in press) to the purified Torpedo acetylcholine receptor (AChR). Asolectin detergent-dialysis vesicles containing acetylcholine-affinity-column purified electroplax AChRs were fused to form large (>10μ) liposomes by rapid freezing and subsequent thawing. In membrane patches isolated from these liposomes, we reproducibly record single AChR channels. For acetylcholine (ACh), carbamylcholine (carb), and suberyldicholine, the main conductance state is agonist independent, being 42pS when the patch separates symmetrical salt solutions of 150mM NaCl, 1mM $CaCl_2$, 1mM $MgCl_2$, 10mM Hepes, pH 7.2, T=22°C. With increasing [NaCl], single channel currents at 100mV show a first-order saturation (I_{max}=9.1pA, K_d= 129mM Na^+). Even at low agonist concentrations (1μM ACh, 20μM carb), a slow inactivation process (desensitization) leads, within several minutes, to an extremely low equilibrium rate of channel opening. At higher agonist concentrations (10μM ACh), this inactivation is more rapid; also, observed openings display obvious burst-kinetics. Open channel lifetime distributions require two exponentials for accurate fitting. The time constants for channels activated by 20μM carb (150mM NaCl; +100mV) are τ_{fast}=.4ms and τ_{slow}=3ms; for ACh (1μM), these time constants are ~2 fold larger. Hence, Torpedo AChRs have channel properties similar to those of mammalian muscle AChRs. This provides further support for the idea of structural homology among vertebrate nicotinic AChRs.

M-PM-E8 CHOLINE BLOCKS INHIBITORY CHOLINERGIC RECEPTORS OF APLYSIA, REVEALING A VOLTAGE-DEPENDENT SYNAPTIC CONDUCTANCE.
Daniel Gardner. Dept. of Physiology & Biophysics, Cornell University Medical College, New York City, N.Y. 10021.

Inhibitory cholinergic receptors of Aplysia are similarly sensitive to both ACh and choline (Ruff, White and Gardner, Soc. Neurosci. Abstr. 7:838, 1981). I now report that 1 mM bath choline blocks PSCs mediated via these receptors. In conventional inhibitory followers, choline reduces IPSC amplitude by 42 ± 6 % without significant effect on the single exponential decay, suggesting that choline acts via receptor block or desensitization, rather than channel block. On self-inhibitory cells, choline partially blocked in 6 cases, but not in 2 others. Use of choline as a Na-substitute thus may involve unwanted partial agonist action; even where activation is inapparent or transient, choline may alter PSPs. In cells BL7 and BR7, cholinergic depolarizing-hyperpolarizing PSPs are produced by early inward (D) and late outward (H) currents. Choline activates only the H receptor. Similarly, choline fully blocks only the H component, revealing an exponentially-decaying D-component, with decay strongly dependent upon membrane potential (V) over the range -10 to -80 mV. Rate constant $\alpha = 1/\tau_D = B \exp(AV)$, with A = 0.021 ± 0.003 mV^{-1} and B = 0.26 ± 0.07 ms^{-1}. Subtraction yields the H-component, which decays exponentially with time constant τ_H = 48 ± 3 ms. Choline and eserine uncover identical time constants, suggesting that voltage-dependence is a property of the native τ_D decay process, not a voltage-dependent drug block. Voltage-dependent duration, as well as amplitude, diminishes excitation at depolarized V, uncovering underlying inhibition. In this dual excitatory-inhibitory synapse, voltage-dependence of one component thus serves an easily-identified function. Supported by NS11555.

M-PM-E9 DESENSITIZATION OF PURIFIED ACETYLCHOLINE RECEPTORS RECONSTITUTED IN PLANAR LIPID BILAYERS.
P. Labarca+, D.R. Fredkin+, J. Lindstrom* and M. Montal+. UCSD+ and Salk Institute*, La Jolla, CA 92093

Single channel currents induced by addition of agonists to planar lipid bilayers containing purified Acetylcholine Receptor (AChR) occur in paroxysms of channel activity followed by quiescent periods. This pattern is more pronounced as the agonist concentration increases and is reflected in histograms of channel opening frequencies (Fig. A). Computer simulations with a three-state model, consisting of two closed (unbound C and bound CL) and one open state, OL, do not resemble the recorded pattern of channel activity, especially at high agonist concentration (Fig. C). Inclusion of fast desensitization to a fourth state, DL, does reproduce the qualitative features of channel recordings (Fig. B). Consequently, the occurrence of paroxysms of channel activity is interpreted, in agreement with others (1), as being due to the transit of AChR through its active conformation, from which it can open several times before desensitizing. Supported by NIH, MDA, ONR, DAMR.

1) Sakmann, B., Patlak, J. & Neher, E. (1980) Nature 286:71-73

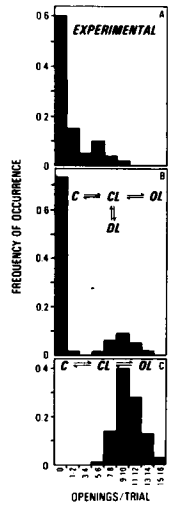

Fig. legend: A) Single channel records were divided in 100 intervals, 100 ms long, and the number of channel openings per trial were measured at 1 mM carbachol. B) and C) computer simulations for the 4-state and 3-state models, respectively. Parameters: agonist dissociation, 30 μM; desensitization rate, $5s^{-1}$; reactivation rate, $0.5s^{-1}$; opening rate = closing rate, 0.22 ms^{-1}.

M-PM-E10 A NOVEL USE OF CAMPBELL'S THEOREM TO DETERMINE THE AMPLITUDE, TIME COURSE AND FREQUENCY OF OCCURRENCE OF MINIATURE ENDPLATE POTENTIALS DURING PROTRACTED PERIODS OF INTENSE SECRETION. J.R. Segal, B. Ceccarelli and W.P. Hurlbut. (Intr. by C.M. Connelly.) Veterans Administration Medical Center, N.Y., N.Y. 10010; Dept. of Pharmacology, Univ. of Milano, Italy, and Rockefeller Univ., N.Y., N.Y., 10021.

The rate of secretion of quanta of acetylcholine at the neuromuscular junction has been measured by counting individual miniature endplate potentials (mepp's) or by applying Campbell's theorem to the mean and variance, M_2, of the junctional voltage. Since neither of these methods can be used during protracted periods of intense secretion, we have developed a technique which uses M_2 and the third central moment (skew), M_3, to measure the mepp frequency, ν. When the junctional potential is due to the summation of randomly occurring mepp's of time course $h[\exp(-t/\theta_1) - \exp(-t/\theta_2)]$, then $M_2 = \nu h^2 K_2$ and $M_3 = \nu h^3 K_3$, where the K's are functions only of θ_1 and θ_2. θ_1 and θ_2 can be obtained from power spectral analysis and combined with parallel measurements of M_2 and M_3 to yield ν and h. Calculations based upon computer-simulated random sequences of mepp's demonstrate that the measurement of M_3 becomes unreliable when ν exceeds ca. 3000/sec, a limit also predicted by simple theory. The method has been applied successfully to junctions of frog cutaneous pectoris muscles stimulated by exposure to La^{3+} in either Ca^{2+}-containing or Ca^{2+}-free solutions. The resulting estimates of the total number of quanta secreted will be correlated with changes in the ultrastructure of the nerve terminals. Supported by the Veterans Administration (JRS) and by grants from Muscular Dystrophy Association (BC and WPH) and by NIH Grant NS-18354 (WPH).

M-PM-E11 RESTING POTENTIAL MODULATES TRANSMITTER RELEASE IN SQUID GIANT SYNAPSE. S. M. Simon, M. Sugimori, R. Llinás. Dept. Physiol. & Biophys., New York Univ. Med. Ctr., New York 10016.

Transmitter released by a presynaptic terminal can be modulated by axo-axonic junctions terminating on its surface. The mechanism behind such modulation is unknown due to the inaccessibility of most presynaptic terminals to direct electrophysiological analysis. We studied the role of resting potential on transmitter release from the giant synapse of the stellate ganglia of the squid, Loligo pealeii, where we can voltage-clamp both pre- and postsynaptic terminals simultaneously (Llinás et al., Biol. Bull. 155:454, 1978). This allowed control of the resting membrane potential, the action potential (a.p.) profile , and the determination of presynaptic calcium current (I_{Ca}) and postsynaptic current (p.c.). The amplitude of the p.c. was found to be affected by the presynaptic resting membrane potential by: (1) A direct effect on the activation kinetics of the calcium current (depolarization primes the activation kinetics and hyperpolarization slows down the activation of I_{Ca}), and (2) an effect independent of changes in a.p. profile or I_{Ca} in which a small depolarization has a significant facilitatory effect on the p.c. (This effect cannot be explained solely on the basis of increase in free calcium near the release site, but may be related to the immediately releasable transmitter store).

In studies of modulation effects of the a.p. waveform on transmitter release, increase of a.p. amplitude increased I_{Ca} and p.c.; increase of a.p. duration increased I_{Ca} and p.c. duration but not necessarily I_{Ca} amplitude. The data support a close-to-linear relationship of calcium and transmitter release (Llinás et al., Biophys. J. 33:289 & 323, 1981) which is unaffected by changes in resting potential or a.p. profile. [Supported by USPHS grant NS141014]

M-PM-E12 PHOSPHORYLATION OF THE NICOTINIC ACETYLCHOLINE RECEPTOR BY cAMP-DEPENDENT PROTEIN KINASE. Richard L. Huganir and Paul Greengard, Dept. Pharmacology, Yale University School of Medicine, New Haven, CT 06510. (Intr. by Richard W. Aldrich)

The nicotinic acetylcholine receptor from Torpedo californica was phosphorylated by an endogenous membrane-bound cAMP-dependent protein kinase. The endogenous cAMP-dependent protein kinase phosphorylated the γ and δ subunits of the acetylcholine receptor which were identified after purification of the acetylcholine receptor by affinity chromatography. Protein kinase inhibitor, a specific inhibitor of the catalytic subunit of cAMP-dependent protein kinase, abolished the basal endogenous phosphorylation of the γ and δ subunits of the receptor. cAMP activation of the endogenous phosphorylation of the γ and δ subunits was dose dependent with a half-maximal response at 25 nM. In contrast, calcium/calmodulin did not stimulate the phosphorylation of the acetylcholine receptor. Experiments using purified acetylcholine receptor and purified catalytic subunit of cAMP-dependent protein kinase demonstrated that the purified receptor was rapidly and specifically phosphorylated on the γ and δ subunits by the purified catalytic subunit to a stoichiometry of 1.0 and 0.89 mol ^{32}P/mol receptor, respectively. The initial rates of phosphorylation of the γ and δ subunits of the receptor were comparable to those of histone f2B and Synapsin I (Protein I), two of the most effective substrates for the catalytic subunit. Under the conditions used, the γ and δ subunits had K_m values of 4.0 μM and 3.3 μM and V_{max} values of 2.7 μmol/min/mg and 2.1 μmol/min/mg, respectively. The results are consistent with the idea that the acetylcholine receptor is phosphorylated in vivo by a cAMP-dependent protein. The possible effect of this phosphorylation on the function of the acetylcholine receptor and its associated channel will be discussed.

M-PM-E13 MUSCARINIC ACETYLCHOLINE RECEPTORS IN BULLFROG ATRIUM: ^{3}H-QNB BINDING, VOLTAGE-CLAMP AND PATCH-CLAMP STUDIES. D. Baker, Y. Momose, W. Giles, G. Szabo. University of Texas Medical Branch, Galveston, Texas 77550.

Suspensions of free cells from bullfrog atria were prepared by enzymatic dispersion. Equilibrium binding of ^{3}H-QNB, a specific muscarinic antagonist, was measured using a filtration technique. Cells were counted in a hemacytometer. All QNB binding to cells was inhibited by atropine (10^{-6}M). Maximum specific binding averaged 6.73×10^5 molecules/cell, or 171 molecules/μm^2 of cell surface. The K_d was 48±10 pM. K^+ and Ca^{++} channel blockers (Ba^{++} 5×10^{-5}M; and Cd^{++} 10^{-4}M or D-600 10^{-5}M, respectively) did not influence QNB binding.

A single microelectrode technique was applied to individual cells from the same suspensions for quantitative measurement of an acetylcholine-induced K^+ current (I_{ACh}). Dose-response curves obtained by holding the cell near E_{rest} (-85 mV) and bath applying ACh yielded a maximum I_{ACh} of 120±20 pA. The reversal potential for I_{ACh} was about -100 mV; hence, the maximum ACh-induced conductance change was approx. 8.0 nS. From patch clamp measurements of ACh-induced single channel currents, the single channel conductance was calculated to be 2.3 pS. Therefore, the maximum number of K^+ channels open in the steady state is approx. 3,500/cell, or about 1 μm^2 of cell surface.

Summary: The number of muscarinic ACh receptors per cell exceeds the maximum number of K^+ channels that can be kept open by ACh by 200 fold. Previously identified muscarinic receptors which inhibit Ca^{++} channels probably cannot account for this difference. Thus, there may be a considerable 'receptor reserve'. (Supported by NIH HL-27454, HL-24820, and AHA 81-835).

M-PM-E14 SITE-SPECIFIC FLUORESCEIN-LABELED COBRA α-TOXIN: KINETICS OF INTERACTION WITH THE ACETYLCHOLINE RECEPTOR. Albert T. Cheung*, David A. Johnson, Palmer Taylor* (intro. by M.B. Bolger), Div. of Pharmacology, Dept. of Medicine, University of California, San Diego, La Jolla, CA 92093

Previous studies of the interaction between α-toxins and the nicotinic acetylcholine receptor (AChR) utilized primarily radiolabeled α-toxins that do not allow continuous monitoring of binding events. To develop a nondestructive method to explore the α-toxin receptor interaction, we studied the binding kinetics of N^ϵ-fluorescein isothiocyanate-lys-23 cobra α-toxin (FITC-TX) to the membrane-associated AChR from the Torpedo californica electric organ using fluorescence techniques. Two spectroscopic parameters monitored the reaction: total fluorescence and steady-state polarization of the fluorescein fluorescence. Both parameters revealed identical kinetic information. Analysis of the initial rate of the reaction as a function of reactant concentrations showed that the reaction was first-order with respect to both toxin and AChR. An integrated rate expression for a reversible bimolecular mechanism best fit an analysis of the total reaction; however, the apparent second-order association rat constant derived from the integrated rate analysis varied between 4 and 8×10^8 $M^{-1}sec^{-1}$ as the ratio of AChR to FITC-TX increased. Examination of the relationship between toxin occupation and association rate suggested that the degree of AChR occupation did not affect association kinetics. The variation in second-order association rate constants calculated from the integrated rate analysis appeared to be due to a time-dependent change in the dissociation rate. The dissociation kinetics exhibit either unimolecular or complex behavior that depends upon the lifetime of the α-toxin-AChR complex. The unimolecular dissociation rate constant was 3×10^{-5} sec^{-1}. A kinetic scheme has been developed to explain these observations.

M-PM-E15 PERMEABILITY OF SINGLE ACETYLCHOLINE CHANNELS IN CHICK MYOTUBES. Terry M. Dwyer and Jerry Farley, Depts. of Physiology and Biophysics and Pharmacology and Toxicology, U. Miss. Med. Ctr., Jackson, Ms 39216.

The permeability of the acetylcholine (ACh) channel of the neuromuscular junction is determined in part by laws of diffusion in bulk solution and in part by specific characteristics of the internal structure of that channel. Single channel ACh currents were recorded from a gigohm patch clamp using an inside-out membrane plucked from 21 day old chick myotubes. The external permeant cation was cesium throughout the experiments. Four properties of these currents behaved as in bulk solution. First, the I-V relation was linear in the nearly symmetrical solutions of 108 CsCl, 2 $BaCl_2$ and 5 HEPES outside and 120 CsF and 5 HEPES inside. Second, at 11 C the reversal potential was shifted as predicted, 23.9 mV for an e-fold change in cesium concentration from 360 mM to 40 mM. The 40 mM cesium was diluted with mannitol. Third, the permeability relative to cesium for NH_4, methylamine, ethylamine, and arginine (1.87:0.93:0.65:0.02) fell as expected by target theory, and was fit by the functions as used for the frog endplate channel, scaled by factors of 2/3, 1/2, and 1/3 for equations 3,4, and 5 of Dwyer et. al., J. Gen. Physiol., 75:469-492. Fourth, the Q_{10} of the single channel current amplitude was 1.3 for 120 cesium inside and 1.4 for 120 methylamine inside, as expected for diffusion in free solution.

In contrast, diluting internal cesium, ammonia, or methylamine with the poorly permeant cation arginine yielded currents smaller than expected from the independence principle. The block was equal whether 80 mM of either internal or external cesium was replaced by arginine.

(Supported by NIH grants NS-16462 and NS-17789.)

M-PM-F1 Thiol oxidizing reagents inhibit H^+-ATPase and coupling factor B.

Lakshmi Kantham, B.C., Michael Pringle and D.Rao Sanadi.

Although sulfhydryls of H^+-ATPase have been studied in detail with alkylating reagents (NEM), organomercurials (pCMB, mersalyl) and dithiol reagents (Cd^{2+}, phenylarsine oxide), no experiments have been reported with thiol oxidizing agents. Since Cd^{2+} and the arsenical bind H^+-ATPase and promote discharge of membrane potential ($\Delta\psi$), we have examined the effects of dithiol-disulfide interconversion on the H^+-ATPase. The exchange activity of H^+-ATPase (1) was inhibited by 80 and 51% at 0.1 and 1.5mM o-phenanthroline/Cu^{2+} and iodosobenzoate respectively whereas ATPase activity remained unaffected. $\Delta\psi$ was monitored using a voltage sensitive dye, oxonol VI. ATP induced $\Delta\psi$ was inhibited by 72 and 65% in the presence of o-phe/Cu^{2+} and iodosobenzoate respectively at above concentrations. With increasing concentrations of these reagents there was also a corresponding increase in the rate of decay of $\Delta\psi$ which was measured after addition of oligomycin. Inhibition of exchange activity without any effect on ATPase activity would indicate that the thiols oxidized are in coupling factor B (F_B)(2). Confirmatory studies on isolated F_B showed similar inactivation of coupling activity. Our results indicate that the F_B may have a role in regulating H^+-permeability by undergoing dithiol-disulfide interconversion. (1) Joshi, S. et al, JBC, 254, 10145-10152, 1979. (2) Joshi, S. and Hughes, J.B. JBC, 256, 11112-11116, 1981.

M-PM-F2 ISOLATION AND CHARACTERIZATION OF THREE HEME C-CONTAINING PROTEINS FROM CHROMATIUM VINOSUM. Dale F. Gaul, Gary O. Gray and David B. Knaff, Department of Chemistry, Texas Tech University, Lubbock, TX 79409.

The photosynthetic purple sulfur bacterium Chromatium vinosum has been shown to contain two previously uncharacterized c-type cytochromes. One cytochrome, with an α-band maximum at 550 nm, a molecular weight of 15 kD and an oxidation-reduction midpoint potential (E_m) of +240 mV, appears to function as an electron carrier in cyclic electron flow. This cytochrome appears to be analagous to cytochrome c_2 of the photosynthetic purple non-sulfur bacteria and mitochondrial cytochrome c. The second C. vinosum cytochrome, previously undetected, has an α-band maximum at 551 nm, a molecular weight of 18.8 kD and E_m = -300 mV at pH 8.0. This low potential C. vinosum cytochrome is similar in some respects to cytochromes of the c_3 type.

In addition to the two c-type cytochromes, C. vinosum contains a high-spin heme c-containing protein with optical and EPR spectral properties very similar to those of myoglobin. The high-spin hemoprotein is a monomeric protein with a molecular weight of 11.9 kD and E_m = -110 mV (n = 1) at pH 8.0. The protein binds CO and O_2 and these complexes have absorbance spectra very similar to those of carbonmonoxy- and oxy-myoglobin respectively. The protein may serve to control O_2 concentrations in C. vinosum cells during micro- or semiaerobic growth.

Research supported by grants from the R. A. Welch (D-710) and National Science (PCM-8109635) Foundations to D.B.K.

M-PM-F3 ELECTRIC FIELD INDUCED ATP SYNTHESIS IN RESPIRATION INHIBITED SUBMITOCHONDRIAL PARTICLES FROM BEEF HEART. Tian Yow Tsong & Barry E. Knox, Department of Physiological Chemistry, The Johns Hopkins University School of Medicine, Baltimore, Maryland 21205

According to the chemiosmotic hypothesis, the final step in the energy transduction of the mitochondrion involves the conversion of a proton electrochemical potential energy into the chemical bond energy of ATP. F_oF_1 ATPase catalyses this energy conversion process. The proton electrochemical potential is composed of the Nernst diffusion potential of protons (-2.3RTΔpH/F, F being the Faraday constant) and the membrane potential ($\Delta\psi$). To assess the role of $\Delta\psi$ and to study rapid kinetics of ATP synthesis, we have employed a high voltage pulsation method with which a membrane potential of controlled magnitude and duration can be imposed on cells or organelles in suspension. Respiration inhibited submitochondrial particles (mean diameter of 200±50 nm) when exposed to electric pulses in the order of 10-30 kV/cm (that generate maximal $\Delta\psi$ of 150-450 mV), and of duration 10-100 μs induced synthesis of ATP. With one 30 kV/cm-100 μs pulse, the yield was roughly 1-3 ATP per F_oF_1 complex, and as many as 8-20 ATP per F_oF_1 complex was produced by repeating electric pulses with the same sample. By varying the ionic strength of the suspending medium and the pulse width, it is unequivocally shown that the synthesis was electrically driven (i.e. Joule heating played no part in the synthesis). The voltage induced ATP synthesis was completely inhibited by specific inhibitors of F_oF_1 ATPase, oligomycin and DCCD. Ionophores and uncouplers have varying degrees of inhibition. The dependence of ATP synthesis on pulse length was non-linear, exhibiting a threshold at 10 μs and a biphasic behavior above this value. The meaning of these observations will be discussed. (Supported by NIH Grant GM 28795).

M-PM-F4 EFFECT OF PHENYLARSINE OXIDE ON MITOCHONDRIAL K^+ FLUX. Jyoti Srivastava and Joyce J. Diwan, Biology Department, Rensselaer Polytechnic Institute, Troy, NY 12181.

Phenylarsine oxide (PheAsO), a dithiol-reactive reagent, uncouples oxidative phosphorylation and activates K^+-dependent H^+ efflux from mitochondria (Sanadi et al., J. Bioenerg. Biomembr. 13: 425, 1981). PheAsO is reported to react with a dithiol group on Coupling Factor B (Joshi & Hughes, J. Biol. Chem. 256:11112, 1981; Stiggall et al., Arch. Biochem. Biophys. 196:638, 1979). It was earlier shown that mercurial sulfhydryl reagents enhance rates of respiration-dependent K^+ flux into mitochondria (e.g. Jung et al., Arch. Biochem. Biophys. 183:452, 1977; Diwan et al., Indian J. Biochem. Biophys. 14:342, 1977). In the present studies, the unidirectional K^+ flux into rat liver mitochondria was measured by means of ^{42}K, with succinate present as energy source during the 7-8 minute incubations. PheAsO is found to stimulate K^+ influx. Subsequent treatment with BAL (2,3-dimercaptopropanol), a dithiol, largely reverses the effect of PheAsO on K^+ influx. The monothiol β-mercaptoethanol (MEt) also reverses the effect of PheAsO, but consistently to a slightly lesser extent. For example, in one experiment 6 nmol PheAsO/mg protein (50 μM) increased the K^+ influx rate from 0.94±0.12 to 1.57±0.14 nmol K^+/mg protein(min) (means ± SD). Addition of 12 nmol BAL/mg protein (100 μM) 1 minute after addition of the PheAsO resulted in K^+ influx rates of 1.15 and 1.11 nmol K^+/mg protein(min). MEt at 24 nmol/mg protein (200 μM) added 1 minute after the PheAsO resulted in K^+ influx rates of 1.20 and 1.23 nmol./mg protein (min). It remains to be determined whether the PheAsO-sensitive K^+ transport mechanism involves Coupling Factor B. (Supported in part by USPHS Grant GM-20726)

M-PM-F5 GENERAL ANESTHETICS: A NEW CLASS OF UNCOUPLERS IN MITOCHONDRIA. HAGAI ROTTENBERG, PATHOLOGY DEPARTMENT, HAHNEMANN UNIVERSITY, SCHOOL OF MEDICINE, PHILADELPHIA, PA 19102

General anesthetics such as halothane and chloroform uncouple oxidative phosphorylation in rat liver mitochondria at mM concentrations (1-10 mM). These uncouplers differ markedly from classical (protonophoric) uncouplers. Similar to classical uncouplers general anesthetics inhibit phosphorylation while stimulating state 4 respiration. However, in contrast to protonophors, general anestetics stimulate both coupled and uncoupler-stimulated ATPase activity. Moreover, unlike protonophores, general anesthetics have little effect on the proton electrochemical potential gradient when generated by electron transport or ATP hydrolysis. General anesthetics, in the mM concentration range, increase inner membrane fluidity. The order parameter of the lipid spin probe 5-doxyl stearate is decreased, the partition of 5-doxyl-decan into the mitochondrial membranes is increased and the fluorescence of membrane probes is depolarized by general anesthetics. These and other findings suggest that uncoupling by general anesthetics is not the result of the collapse of the proton electrochemical potential but is associated with the disruption of lipid-protein and/or protein-protein interactions in the mitochondrial inner membrane.

Supported by Grant GM28173 from the National Institute of General Medical Science and AA3442 from the National Institute of Alcohol Abuse and Alcoholism.

M-PM-F6 REDOX-LINKED HYDROGEN BOND STRENGTH CHANGES IN CYTOCHROME *a* OF CYTOCHROME OXIDASE. Patricia M. Callahan and Gerald T. Babcock, Department of Chemistry, Michigan State University, East Lansing, MI 48824-1322.

We have recently presented evidence which indicates that the formyl group of the heme *a* of cytochrome *a* is involved in a hydrogen bond interaction (Callahan and Babcock, Biochemistry, in press). The hydrogen donor to the bond is associated with the polypeptide backbone. This structure rationalizes the anomalous optical red-shift and formyl vibrational properties of the protein bound chromophore. Because the visible absorption bands of cytochrome *a* arise from π-π^* transitions, we expect that the absorption maxima will shift to lower frequencies as the strength of the hydrogen bond increases. Concomitantly, the vibrational frequency of the formyl acceptor should decrease as the hydrogen bond becomes stronger. Finally, because there is an approximately linear relationship between hydrogen bond strength and the resulting formyl vibrational frequency decrease, it should be possible to estimate the strength of the hydrogen bond *in situ*. By using a series of hydrogen donors with oxidized and reduced low-spin heme *a* model compounds and with a copper porphyrin *a* analog, we have tested these predictions. Our results confirm the relationship between formyl vibrational frequency and absorption red-shift and allow us to estimate hydrogen bond strengths in the protein. For oxidized cytochrome *a* we find that the strength is ~3.0 kcal/mole which increases to ~5.4 kcal/mole upon reduction. The implications of this redox-linked hydrogen bond strength change for proton pumping in cytochrome oxidase will be considered. (Supported by NIH GM25480).

M-PM-F7 DUAL EFFECT OF FCCP AND CCCP ON MITOCHONDRIAL OXYGEN CONSUMPTION. Juan Reyes and Dale J. Benos. Department of Physiology and Biophysics, LHRRB, Harvard Medical School, Boston, MA 02115.

Carbonyl cyanide phenyl-hydrazone compounds (FCCP, CCCP) have been used as proton ionophores in studies of cell bioenergetics, membrane transport, and to estimate pools of intracellular calcium.

We report here that these two compounds have a dual effect on the rate of oxygen consumption of isolated mammalian liver cells in suspension and on the rate of oxygen consumption of energized mitochondria (state 4). The biphasic dose response curve of oxygen consumption versus CCCP and FCCP concentration is characterized first, by an increase in the rate of O_2 (Qo_2) consumption which is paralleled by a decrease in the stimulation by 0.6 mM ADP of state 4 mitochondrial respiration (i.e., increased mitochondrial uncoupling) at low concentration of CCCP (< 1μM) and FCCP (< 0.5μM). This initial increase in Qo_2 is followed by a reduction in the O_2 consumption rate without a change in the uncoupled state of the mitochondria (i.e., no stimulation of respiration by ADP) at higher concentrations of CCCP and FCCP.

Binding of either the charged or uncharged form of FCCP (>0.5μM) and CCCP (>1μM) to phospholipid monolayers produces a negative interfacial potential that correlates well with the effect that these compounds produce on Qo_2 of uncoupled mitochondria. This negative interfacial potential could be responsible for the observed decrease in Qo_2 at high FCCP or CCCP concentrations in a number of ways, e.g., by directly affecting the electron transport system and/or by decreasing the substrate availability for electron transport. Side effects such as the one described here should be carefully considered when using these compounds as tools in cell physiology research. Supported by NIH Grant AM 25886 and by funds from the Andrew W. Mellon Foundation.

M-PM-F8 CHEMICAL MODIFICATION OF PLASTOCYANIN. Gross, E. L., Pan, R.L., Draheim, J., Rellick, L., and Duane, J. Depts. of Biochemistry and Engineering Graphics and Biophysics Program, The Ohio State University, Columbus, Ohio 43210.

Chemical modification of spinach plastocyanin (PC) with ethylene diamine (EDA) and a water-soluble carbodiimide produces four forms of chemically-modified plastocyanin containing 2.1, 3.2, 4.1 and 6.3 moles of EDA/mole PC. All four forms show a + 40 mV shift in redox potential. However, the affinity for P700 increases with increasing extents of modification. The minimal modification which shifts the redox potential occurs at residues 41-45 approximately 18A^{o} distant from the copper. Both chemical modification and reduction of the protein cause conformational changes as determined by changes in absorption, fluorescence and circular dichroism.

Reaction of PC with 4-chloro-7 nitrobenzofurazan (NBD-Cl) modified approximately one lysine residue. Energy transfer has been observed between typsines on the protein and the NBD derivative. Modification affected its interaction with P700.

M-PM-F9 DELAYED FLUORESCENCE AND ELECTRON EXCHANGE OF EXCITED ZINC CYTOCHROME C B.P.S.N. Dixit, T. Horie and J. M. Vanderkooi, Department of Biochemistry and Biophysics, Univ. Penn. Philadelphia PA 19104

Reactions of the excited triplet state of zinc cytochrome c were measured by monitoring transient absorption and emission. At room temperature the excited singlet state can be thermally populated from the triplet state as can be seen by emission of fluorescence which has the same spectrum as prompt fluorescence but decays with the lifetime of phosphorescence. The emission intensity is temperature dependent; the activation energy derived from an Arrhenius plot is 0.4 eV, in agreement with the energy difference between the first excited singlet and triplet states. The decay of emission is independent of concentration and laser intensity which indicates that the emission is E-type. Owing to its strong intensity (eg., at 25 C is 17 times more than phosphorescence), delayed fluorescence offers a sensitive method to study the triplet state. As a model for electron transfer in cytochromes we have studied the reactions of triplet zinc cytochrome c with methyl viologen, propylene viologen sulfite, iron cytochrome c and ferricyanide. These electron acceptors quench the triplet with rate constants in the range of 10^6 to 10^9/ M/sec, rates which approach the diffusion limit. The decay kinetics are complex and are interpreted to involve electron exchange and protein rearrangement.
(Supported by NIH grant GM12202)

M-PM-F10 PROTON-TRANSLOCATING ATPase COMPLEX OF E. COLI: REACTION WITH EDC, A WATER SOLUBLE CARBODIIMIDE.

Hansruedi Loetscher (introduced by Walter Baase). Institute of Molecular Biology, University of Oregon, Eugene, OR 97403

The F_0F_1-ATPase of E. coli is purified after induction of a λ-transducing phage carrying the ATPase genes of the unc operon. (Foster et al. (1980) J. Biol. Chem. 255, 12037-12041). Incubation of either F_0F_1 or F_1 alone with EDC leads to a time-dependent inhibition of ATPase activity. The inhibition is more efficient in the intact F_0F_1-complex than in F_1. During inactivation of F_1-ATPase several crosslinks are formed. The predominant crosslink is tentatively identified to be β-ε with a molecular weight of 65 k. Treatment of F_0F_1-ATPase with EDC results in the formation of the same crosslinks as seen with F_1. In addition, a modification of subunit b leading to a change in mobility on SDS gels is also observed. The formation of the major crosslinks is not affected by the nucleophile glycine ethyl ester. Preliminary experiments using [^{14}C]CH_3EDC indicate a modification of different subunits by EDC. Most of the label is found to be in subunit β whereas subunits α,δ, b and eventually c (the DCCD-binding protein) are modified to a lesser extent. The possibility that the water-soluble EDC might react with the DCCD-sensitive sites in subunit β and/or c is of particular interest. The consequences of such a reaction for the structural arrangement and function of proton-translocating ATPases will be discussed.

Abbreviations: EDC, 1-ethyl-3-[3-(dimethylamino)propyl] carbodiimide
DCCD, dicyclohexylcarbodiimide

WITHDRAWN

M-PM-F12 Phosphodiester Differences in Differentiating Excitatory Tissue. C. Tyler Burt, Malcolm Pluskal, Frank Sreter; Dept. Radiology, Mass. General Hospital; Dept. of Muscle Research, Boston Biomedical Research Institute.

Some mammalian species, particularly man, contain the phosphodiester-glycerolphosphorylcholine. Early studies showed interesting organ specificities and later ones, variation of levels within a particular organ class. Burt and Ribolow have used these observations to speculate that the variation of GPC levels can play an active role in tissue differentiation. We extend results on this phenomena in two ways. First, surface coil studies verify in vivo the previously reported results that GPC appears in electrically stimulated muscle at roughly the same time as the light chains begin to change from fast to slow type. In such muscles, a slight alkalinization was seen between stimulated and contralateral muscle. Phosphocreatine to inorganic phosphate ratio (PCr/Pi) is decreased in the transformed muscle. Phosphomonoester levels can be initially high, but this seems to be a stress effect because they fall to lower levels with continued sampling.

Preliminary observations on calf brain show differences between gray and white matter. In particular, for one animal, a strong residence was seen in white matter but not gray. All samples show a very broad peak ($\nu_{\frac{1}{2}}$~5ppm) center at -13ppm. This result tends to verify that phosphodiesters can at least be used to categorize the state of excitatory tissue differentiation and may help explain the events which are happening in the differentiation process. In particular, they may play a role in controlling the percent loss of phospholipid seen in the differentiated tissue.

Acknowledgement: We wish to thank Dr. Britton Chance and his colleagues at the Johnson Foundation and also Dr. Jungalwalla of the Shriver center for providing brain samples.

M-PM-G1 UNITARY CURRENT FLUCTUATIONS DUE TO SAXITOXIN BLOCK OF SODIUM CHANNELS IN PLANAR BILAYERS. Robert J. French[1], Jennings F. Worley, III*[2], and Bruce K. Krueger[2]. Depts. of Biophysics[1] and Physiology[2], Univ. of Maryland Sch. of Med., Baltimore, MD 21201.

Saxitoxin (STX)-blockable, voltage-gated Na channels from rat brain were incorporated into planar lipid bilayers as described in the previous abstract. In the presence of batrachotoxin (0.6 μM) on the trans side (the side opposite that of vesicle addition), and with >5 channels incorporated, a steady-state, ohmic current was observed at potentials < 80 mV (cis minus trans). This multi-channel, "macroscopic" Na current was blocked by STX from the cis side only with a K_i of 5 nM at +30 mV. Although most of the current was blocked with 320 nM STX (cis) at 30 mV, we observed occasional, stepwise current fluctuations that showed a unitary conductance of 30 pS in 500 mM NaCl. These single-channel records suggested that the individual channels were blocked about 99% of the time. The mean duration of the opening steps decreased as the STX concentration was raised. The apparent mean open time at 320 nM STX and 30 mV (about 240 msec, records low pass filtered at 30 Hz) was consistent with an association rate constant of about 10^7 M^{-1}-sec^{-1}. This suggests that most of the stepwise fluctuations reflected the blocking and unblocking of individual Na channels by STX rather than the intrinsic gating of the channels. Block of Na channels by STX was voltage-dependent, with potency decreasing about 10-fold when the voltage was changed from +30 mV to -60 mV. This contrasts with observations in nerve under physiological conditions that showed Na channel block by STX to be independent of membrane potential. The voltage-dependence in our experiments, rather than being an intrinsic characteristic of STX binding, may be a secondary consequence of the high concentrations of Na (500 mM) and Ca (0.1 mM) on the trans side, much greater than the levels normally present at the cytoplasmic surface of the membrane. Supported by NIH, U.S. Army Res. Dev. Comm., and A. P. Sloan Fndn.

M-PM-G2 SODIUM CHANNELS FROM RAT BRAIN IN PLANAR LIPID BILAYERS.
Bruce K. Krueger[1], Jennings F. Worley, III*[1], and Robert J. French[2]. Depts. of Physiology[1] and Biophysics[2], Univ. Maryland Sch. of Med. Baltimore, MD 21201.

Voltage-gated, saxitoxin (STX)-blockable, Na channels have been identified in planar lipid bilayers that were exposed to membrane vesicles prepared from rat brain. We measured both macroscopic (multichannel) currents and the underlying single-channel currents. Bilayers (0.25 mm diameter) were formed from solutions of phosphatidylethanolamine and phosphatidylserine in decane. Membrane vesicles, which were enriched 5-fold in ^{3}H-STX binding (compared to crude brain homogenate), were added to the cis side. Normally, solutions on both sides of the bilayer contained 500 mM NaCl, 0.1 mM $CaCl_2$, and 0.1 mM $MgCl_2$. Batrachotoxin (0.6 μM) was added to the trans side to activate the channels which were then open most of the time at potentials < 80 mV (cis minus trans) and were almost completely closed at potentials >110 mV. STX blocked the channels in the nanomolar range from the cis side only. In membranes with very few channels incorporated, we observed single-channel fluctuations indicating a unitary conductance of about 30 pS in symmetrical 500 mM NaCl solutions. Reversal potentials for single-channel currents measured after replacing some of the Na on the cis side by K, suggested a P_K/P_{Na} of about 0.07. In similar experiments, we detected no permeability to Cs. Thus, with respect to voltage-dependence, neurotoxin sensitivity, and ion selectivity, these channels resemble Na channels in native nerve and muscle membranes. The sidedness of STX block and the voltage-dependence of these channels indicate that they were incorporated into the planar bilayer with their extracellular sides facing cis. Supported by NIH, U.S. Army Res. Dev. Comm., and A. P. Sloan Fndn.

M-PM-G3 FUNCTIONAL RECONSTITUION OF THE SODIUM CHANNEL PURIFIED FROM RAT BRAIN. M.M. Tamkun, J.A. Talvenheimo, and W.A. Catterall (Intr. by C. Stirling), Dept. of Pharmacology, University of Washington, Seattle, WA 98195.

Voltage-sensitive sodium channels were solubilized from rat brain membranes with Triton X-100 and purified to 50-90% homogeneity using either 3 or 4 of the purification steps of Hartshorne et al (J. Biol. Chem., in press). The most highly purified preparation consists of three polypeptide subunits (α, β1, and β2) with molecular weights of 270,000, 39,000 and 37,000. The purified sodium channel retains [^{3}H]saxitoxin ([^{3}H]STX) binding activity that is labile at 36° but lacks the veratridine and scorpion toxin binding characteristic of the native channels. Purified sodium channels were incorporated into egg phosphatidyl choline vesicles by adsorption of detergent with Bio-Beads SM-2. The reconstituted vesicles contain 20 to 40% of the purified sodium channels, all of which regain stability of STX binding at 36°. Veratridine (100 μM) increased the rate of $^{22}Na^+$ influx into reconstituted vesicles up to 10-fold. However, in phosphatidyl choline vesicles, the reconstituted sodium channels did not bind [^{125}I]scorpion toxin. In contrast, when reconstituted into a protein-free, rat brain phospholipid extract, ∿ 50% of the purified sodium channels bound [^{125}I]scorpion toxin specifically (K_D = 30 to 80 nM at $V_M \sim 0$). Denaturation of the purified sodium channel by incubation at 36° before incorporation into vesicles causes a parallel loss of both STX binding and scorpion toxin binding. These results suggest that the α, β1, and β2 subunits of the sodium channel are sufficient for reconstitution of STX and scorpion toxin binding as well as veratridine-stimulated $^{22}Na^+$ transport. Restoration of high affinity scorpion toxin binding is dependent on the lipid composition of the vesicle membrane.

M-PM-G4 NERVE SODIUM CHANNEL IN MEMBRANE VESICLES AND IN RECONSTITUTED PROTEOLIPOSOMES: EFFECT OF ANEMONE TOXIN II. Ana M. Correa, Gloria M. Villegas and R. Villegas. Instituto Internacional de Estudios Avanzados (IDEA), Apartado 17606, Caracas 1015A, Venezuela, & Instituto Venezolano de Investigaciones Científicas (IVIC), Apartado 1827, Caracas, Venezuela.

It is known that the ^{22}Na flux through the Na channels of lobster nerve plasma membrane vesicles is increased by the lipid soluble neurotoxins, i.e. veratridine (VER), batrachotoxin, grayanotoxin I and aconitine, and that this increment is abolished by tetrodotoxin (TTX). In the present experiments the presence of the polypeptide neurotoxin receptor was demonstrated by using sea anemone toxin II (ATX). Essays were carried out in the presence of a K^+ gradient. Vesicles were prepared in 0.3 M KPi and diluted 20-fold in 0.3 M ChCl or 0.3 M ChPi (Ch=choline). $K_{0.5}$ obtained from the dose-response curves are 20-40 μM for VER and 0.1-0.2 μM for ATX. The maximum increment of the ^{22}Na flux is produced by VER concentrations as low as 3 μM when additioned with 50 nM ATX. Substitution of Ch^+ by K^+ in the diluting medium or of K^+ by Ch^+ in the preparative medium diminishes the effect of VER and abolishes that of ATX. TTX blocks the ^{22}Na fluxes stimulated by VER, by ATX, and by VER plus ATX ($K_{0.5}$ 10-30 nM). Na channels of particles obtained by detergent treatment of the membrane (0.5% cholate + 30 mM octylglucoside) and centrifugation, when incorporated into soybean liposomes, also respond to the toxins. However, the $K_{0.5}$ of VER stimulation is 40-50 μM, and the effect of ATX is only observed at high ATX concentrations (> 1 μM) in the presence of VER and the K^+ gradient. The ^{22}Na flux increments are abolished by TTX ($K_{0.5}$ 1-3 nM). The results reveal the existence of the polypeptide neurotoxin receptor in addition to the receptors for the lipid soluble neurotoxins and for TTX.

M-PM-G5 THE SUBUNIT COMPOSITION OF THE SAXITOXIN RECEPTOR OF THE SODIUM CHANNEL FROM RAT BRAIN. R.P. Hartshorne, D.J. Messner, J.C. Coppersmith, and W.A. Catterall (Intr. by J. Sanchez), Dept. of Pharmacology, University of Washington, Seattle, WA 98195.

The saxitoxin (STX) receptor of the sodium channel was purified from rat brain by chromatography on DEAE-Sephadex, hydroxylapatite, and wheat germ agglutinin-Sepharose followed by sedimentation through sucrose gradients. The final specific activity was 2900 pmol STX bound/mg protein or 0.92 mol STX bound per STX receptor of $M_r \sim 316{,}000$. Analysis by SDS gel electrophoresis shows that subunits α ($M_r \sim 270{,}000$), β1 ($M_r \sim 39{,}000$) and β2 ($M_r \sim 37{,}000$), which comprise > 90% of the protein in purified STX receptor preparations, are the only polypeptides which quantitatively comigrate with the purified STX receptor during velocity sedimentation through sucrose gradients. β1 and β2 are often poorly resolved by SDS gel electrophoresis but chromatography of SDS denatured STX receptor on Sepharose 4b followed by gel electrophoresis ± β-mercaptoethanol (βME) shows that β1 and β2 are separate entities and that β2 is covalently linked to α by disulfide bonds while β1 is not. The α and β subunits of the sodium channel were covalently labeled in situ in synaptosomes using a photoreactive derivative of scorpion toxin. Analysis of the effect of βME on the migration of the labeled subunits indicates that the α and β1 subunits are labeled by scorpion toxin while β2 is not and that the β2 subunit is covalently attached to α by disulfide bonds in situ as well as in purified preparations.

M-PM-G6 SODIUM CHANNELS AND THEIR SURFACE CHARGE HAVE NO MEASURABLE "ELECTROPHORETIC" MOBILITY IN FROG SARCOLEMMA. W. Stühmer, P.R. Stanfield, and W. Almers. Dept. Physiology and Biophysics, Univ. of Washington Medical School, Seattle, WA 98195.

In embryonic toad muscle, many integral membrane proteins readily re-distribute under an electric field in the plane of the membrane (Poo, Ann. Rev. Biophys. Bioeng. 10, p. 245, 1981). Sodium channels might behave similarly, as they are known to bear a large negative charge. To test this, we pressed the tips (10-20 μm diameter) of firepolished glass micropipettes against the sarcolemma of frog sartorius muscle fibers, and explored whether steady potentials across the rim of the pipette tip caused local accumulation or depletion of sodium channels. Such potentials could be applied without changing the membrane potential across the patch of sarcolemma covered by the pipette tip. The sarcolemma patch was voltage-clamped, and peak sodium current (I_{Na}) across the patch served as an assay for the number of functional channels there. With a 25 mV p.d. across the pipette rim, I_{Na} changed by less than 10% over 80 min, and the h_∞ curve shifted by 2 mV or less. Hence (1) re-distribution of Na^+ channels did not occur, suggesting that lateral mobility of Na^+ channels is restricted (Stühmer & Almers, 1982, PNAS 79, 946); and (2) the "surface charge" acting on the inactivation mechanism is largely unaffected by a lateral electric field, and is thus not likely to result from mobile lipids. However, it was also found that steady depolarizing potential across the patch membrane causes an ultra-slow inactivation of I_{Na} occurring independently of a lateral electric field, and with rate constants of 0.1-1/min at 15-17°C. The steady-state dependence on membrane potential E could be described by $u_\infty = 1/\{1 + \exp[(E - 71\ mV)/7.7\ mV]\}$. Supported by the MDA, USPHS (AM-17803), and the Wellcome and Max Kade Foundations.

M-PM-G7 DENSITY OF AMILORIDE-SENSITIVE SODIUM CHANNELS IN RABBIT URINARY BLADDER INCREASES WITH URINARY STONE FORMATION. D.D.F. Loo and J.M. Diamond. Dept. of Physiology, U.C.L.A. Medical School, Los Angeles, California 90024.

Crystalline material is frequently found in the urinary sediment of New Zealand white rabbits. Occasionally the crystals aggregate to form stones. We have compared the sodium transport properties of bladders with and without urinary stone formation. In a modified Ussing chamber (tissue area, 2 cm^2) with NaCl-$NaHCO_3$ Ringer's solution bathing both the mucosal and serosal membranes, the magnitude of the sodium transport was determined by measuring the total trans-epithelial short circuit current I_{sc}, the amiloride-sensitive current I_{am}, and the non-selective amiloride-insensitive current I_o. In stone-free bladders, I_o was approximately 1.5 uA with little variation, while I_{am} varied from 0.5 to a maximum of 10 uA. In bladders containing stones, I_o remained essentially constant at 1.5 uA, but I_{am} was found to range from 10 uA to 100 uA. Using fluctuation analysis we have found that this enormous increase in I_{am} is due to an increase in the density of amiloride-sensitive sodium channels. The single channel I_{am} currents remained unchanged. Mechanisms for such an observed increase in channel density will be discussed.

Supported by grants GM 14772 and AM 17328 (UCLA Center for Ulcer Research and Education).

M-PM-G8 MONOVALENT AND DIVALENT GUANIDINIUM IONS AS PROBES OF THE SODIUM CHANNEL IN SQUID GIANT AXONS. Catherine Smith, Leslie Mc Kinney, Miklos Danko and Ted Begenisich. Department of Physiology, University of Rochester, Rochester, NY 14642

We have investigated the interactions of several guanidinium derivatives with the sodium channels of squid giant axons using voltage-clamp and internal perfusion techniques. The main focus of the study was on the monovalent cations guanidinium, n-propylguanidinium, and nonylguanidinium and the divalent cations, 1,8 bis-guanidino-n-octane (bisG8), $bisG_2$, and $bisG_3$. All these compounds reduced peak transient and especially steady state sodium channel currents. The results summarized here pertain to steady state currents: either the naturally occurring non-inactivating currents or currents from axons with sodium channel inactivation removed with proteolytic enzymes. The potency of the n-alkylguanidinium derivations increased with alkyl chain lengths as has been previously described. The bisG8 compound was more effective than nonylgunidinium and $bisG_2$ and $bisG_3$ blocked more than n-propyl guanidine. The effective voltage dependence of the block produced by $bisG_2$ and $bisG_3$ was greater than that of n-propyl guanidine and guanidine. There was little difference in the voltage dependence of block produced by bisG8 and nonylguanidine. One (simple) interpretation of these results is that near the inner end of the sodium pore something like 15% of the membrane voltage drops over a linear distance of 6 to 12 Å. We also found that raising the internal sodium concentation dramatically increased the effective potency of these compounds while changes in external sodium were without effect. These latter data may result from the multi-ion nature of the pore.

M-PM-G9 SODIUM CHANNEL ACTIVATION IN PRONASE TREATED SQUID AXON. Stimers, J. R., Bezanilla, F., Taylor, R. E. Dept. Physiology, University of California, Los Angeles, CA 90024 and Lab. Biophysics, NINCDS, NIH, Bethesda, MD 20205.

Sodium (I_{Na}) and gating (I_g) current were measured in internally perfused, voltage clamped squid axons pretreated with pronase to remove inactivation. Pronase treatment makes steady state activation measurements possible and simplifies the kinetics. The fraction of open channels versus voltage curve (F-V), determined in 10 axons, 1) increased e-fold for a 7mV depolarization, suggesting that 4 electronic charges (e^-) must move across the membrane field to open each channel, 2) reached half maximum at -20 to -10mV and 3) saturated near +50mV. The charge versus voltage curve (Q-V), determined in the same axons, also saturated at +50mV and was always greater than or equal to the F-V curve. This is expected if the charge movement recorded is associated with Na channel gating. In axons not treated with pronase the F-V curve is greater than the Q-V curve for potentials positive to 0mV. The total charge in these experiments was about 1850e^-/um^2.

Kinetic analysis of Na channel activation has revealed that the transition between the last closed and first open states is not the slowest. In 10mM Ca^{2+} the time constant of the last transition is at least 2.3 times faster than the rate limiting step. However, in the presence of 50mM Ca^{2+} the ratio of time constants is reduced to 1.5. When the time constants of Na channel activation are compared with those of I_{g-ON} it was found that there is a component of I_{g-ON} which has the same time constant as activation from -20 to +50mV. This is also true for the Na tail currents and I_{g-OFF}. Kinetic models for the Na channel will be discussed.

Supported by USPHS grant GM30376. Grass and American Heart Association fellowships awarded to JRS.

M-PM-G10 PRESSURE REVERSAL OF INERT GAS NARCOSIS AT NODE OF RANVIER SODIUM CHANNELS. Joan J. Kendig, Dept. of Anesthesia, Stanford University School of Medicine, Stanford, CA, 94305
Two common assumptions are that the membrane actions of inert gases are fundamentally similar to those of general anesthetics and that pressure reversal of anesthesia is a direct antagonism between pressure and the anesthetic agent. To test these assumptions experiments were designed to compare hyperbaric nitrogen with other anesthetic agents, and to explore the basis for pressure antagonism to anesthetic block of sodium channels. Axons of frog sciatic nerve were prepared for vaseline gap voltage clamp by standard methods and placed in a pressure vessel. Temperature was maintained near 10°C. Nitrogen (N_2) at 7 and 14 atmospheres (atm) depressed sodium current amplitude, shifted steady-state inactivation (h_∞) in the hyperpolarizing direction, and decreased the time constant of inactivation (T_h) at potentials positive to the holding potential, but not at more negative potentials. Nitrogen resembles general anesthetics in these respects. Hyperbaric helium to 100 atm had little effect on Na current maximum amplitude. The h_∞ curve was shifted 5-15 mV in the depolarizing direction. T_h was increased at positive, but unaffected at negative potentials. Helium pressure and nitrogen thus exert opposite effects on h_∞ and T_h. At a total pressure of 100 atm, the actions of 14 atm N_2 on h_∞ and T_h were reversed. Since all classes of anesthetic agents, now including inert gases, produce some sodium channel block by decreasing h_∞, opposing effects on sodium inactivation may be the basis for the limited pressure reversal of anesthetic conduction block observed in vertebrate axons. For inert gases and volatile agents, the results are consistent with direct antagonism.
Supported by PHS Grant NS13108, NSF BNS 8020497, and ONR N00014-75-C-1021.

M-PM-G11 A MODEL OF INTERACTION OF LOCAL ANESTHETICS WITH NA CHANNELS. CF Starmer, AO Grant, and HC Strauss. Duke University Medical Center, Durham, North Carolina.

We have developed a model of local anesthetic blockade of sodium channels that does not require modification of gating kinetics. By considering the population of sodium channels as a mixture of homogeneous subgroups of channels, a kinetic relationship of channel-drug binding can be derived that provides results consistent with use dependence, voltage dependence, frequency dependence and slow channel inactivation. Each subgroup of channels is determined by the position of the activation (m) and inactivation (h) gates. The level of channel block, based on the two most favorable channel gate configurations, can be represented by:

$$db/dt = (k_1 m^3 h + k_0 m^3 (1-h))[D] (1-b) - (r_0(1-h) + r_1 h)b \exp(-ZVF/RT)$$

where b is the fraction of blocked channels, k_0 is the forward rate of constant for channels with m^3 = open, h = closed, k_1 is the rate constant for channels with m^3 = open, h = open, [D] is the drug concentration, r_0 and r_1 are dissociation rate constants for channels with h = closed and h = open and V is the transmembrane potential. Gating models (e.g., Hodgkin-Huxley) are used to estimate the channel partition coefficients which modulate the forward and reverse flux of drug. I_{Na} is reduced by the fraction of blocked channels according to: $I_{Na} = \bar{g}_{Na} m^3 h(1-b) (V-V_{Na})$. The model (1) describes relief of block with hyperpolarizing potentials without requiring a shifted h_∞ curve for blocked channels; (2) describes a dependence of I_{Na} reduction on the resting transmembrane potential when using repetitive stimuli; (3) describes tonic block without requiring specialized binding sites; and (4) demonstrates the confounding effects of channel inactivation and drug blocking as a function of stimulus protocols. (Supported by NIH grants HL-19216, HL-17670.)

M-PM-H1 AXIAL FORCE from TRANSVERSE MOTIONS of the CROSSBRIDGE, by Peter R. Greene, Johns Hopkins University; Baltimore, Maryland, 21218

Three distinctly different types of transverse crossbridge motion are examined. The first, called the "snap-through hinge", is a co-ordinated motion of the two myosin heads transverse to the axis of the thick and thin filaments. This motion requires that the two heads be attached to adjacent actin filaments (Borejdo & Oplatka, 1981). The second type of transverse crossbridge motion, called "actin-bending", arises from the thermally excited bending modes of the thin filaments, (Greene, 1981). The third type of motion, called "S2-bending", also arises from the thermally excited bending modes of S2. Calculations indicate that the axial force generated by the snap-through hinge can exceed 5×10^{-12} newtons per crossbridge, a rather high value; the other two schemes produce considerably less force than the usual 2×10^{-12} N/XB calculated for skeletal muscle (Huxley & Simmons, 1971). The three different types of motion can be superimposed on one another, since they involve three different structures, i.e. the S1 heads, the thin filaments, and the S2 chain, respectively. Experimental implications will be discussed.

REFERENCES

(1) Borejdo, J. and Oplatka, A., Nature, V 291, p. 322, 1981.

(2) Greene, P.R., J. Gen. Physiol., V 78, p. 17a, 1981.

(3) Huxley, A.F. and Simmons, R.M., Nature, V 233, p. 533, 1971.

M-PM-H2 PHOSPHORESCENCE ANISOTROPY MEASUREMENTS OF SLOW MOTIONS IN EOSIN-LABELED MYOSIN
Thomas Eads, Robert Austin*, Brian Citak, David Momont & David Thomas, Dept. Biochem., Univ. Minn. Med. School, Minneapolis, MN 55455; *Physics Dept., Princeton University, Princeton, NJ 08544.

Polarization of transitions of the long-lived triplet state of eosin-iodoacetamide (E51A) covalently bound to myosin was observed by time-resolved triplet-triplet absorption dichroism (start observation at 100ns) and by emission anisotropy (start at 1μs). These methods probe previously unobservable motions and complement fluorescence and EPR methods by extending the time range and providing time resolution, respectively. Myosin*E51A was characterized by enzymatic activity, distribution of label in subunits and proteolytic fragments, and optical properties. Monomeric myosin and myosin filaments show complex polarization decay with characteristic times ranging from 100's of ns to 10's of μs in myosin, and to tens of ms in filaments. Reasonably high initial anisotropies (r_i~0.2 at 100 ns) show that probe and/or protein segmental motions which are fast but restricted account for about half of the decay amplitude. Early observable decay components have characteristic times consistent with those determined in fluorescence depolarization and EPR experiments. Subsequent components have small amplitudes and characteristic times of μs in myosin and somewhat larger amplitudes and much longer times (ms) in filaments. Thus the submicrosecond motions are restricted in amplitude. We estimated angular ranges of restricted motion using simple models. Preliminary results with labeled glycerinated muscle fibers are presented. An acceptable degree of labeling specificity was achieved despite the binding properties of eosin. The anisotropy decay is shown to be complex and characteristic of the state of the fiber.

M-PM-H3 ORDER & ORIENTATION OF MUSCLE CROSSBRIDGES USING FLUORESCENCE POLARIZATION. M.G.A. Wilson and Robert Mendelson. C.V.R.I. and Biochem./Biophys., U. Calif., San Francisco, CA 94143.

We have reexamined the question of the order and orientation of muscle crossbridges in relaxation and rigor using chemically skinned rabbit psoas fibers labelled with SH_1 reacting fluorophore 1,5 IAEDANS. We find that portions of carefully handled, relaxed fibers selected by laser diffraction show considerable order. This is in qualitative agreement with X-ray diffraction experiments on living muscle. Exercise of the muscle decreases this order. To model these data, we have extended and corrected the theory of Weill & Sturm (Biopolymers 14:2537-2553) to apply to crossbridges having Gaussian or uniform disorder about their mean declination with or without the torsional degree of freedom. Exhaustive calculations using these models and others on our data and Yanagida's ethenonucleotide data (J.M.B. 146:639-560) indicate that the change in declination of the crossbridges between rigor and relaxation is small: usually less than 5° and nearly always less than 10°. The similarity of model fits from two very different fluorophores at different S1 locations and with different reactivities suggests that this conclusion is valid. Supported by USPHS grant HL-16683 and NSF grant 79-22174.

M-PM-H4 EFFECTS OF ADP AND VANADATE ON TENSION TRANSIENTS INITIATED BY PHOTOLYSIS OF CAGED-ATP WITHIN SKELETAL MUSCLE FIBERS. Y.E. Goldman, J.A. Dantzig, M.G. Hibberd and D.R. Trentham. Depts. of Physiol. and Biochem. & Biophys., Univ. of Penna., Phila., PA 19104.

We have studied the decay of rigor tension and stiffness in single fibers of rabbit glycerinated psoas muscle which occurs after liberation of up to 1 mM ATP from caged-ATP by a pulse of 347 nm radiation (Goldman, Hibberd, McCray and Trentham, Nature, in Press). Incubation of fibers in MgADP (1-5 mM) prior to ATP release slows relaxation. The slower relaxation may be limited by the rate of the reaction A.M.ADP→A.M or by a reduction of the effective A.M concentration due to a rapid equilibrium between A.M.ADP and A.M. Reattaching cross-bridges produce a substantial rise in tension before the final relaxation. If a fiber is incubated in a solution of MgADP (5 mM), vanadate (V_i, 1 mM) and MgATP (50 μM) and then relaxed with 100 μM ATP in the absence of ADP and V_i, the tension of the next rigor contraction is suppressed. The suppression is probably due to formation of stable M.ADP.V_i complexes (Goodno and Taylor, P.N.A.S. 79:21, 1982). Cross-bridges can apparently attach in this tension-suppressed state as judged by stiffness measurements using quick stretches and measurement of sarcomere length change by white light diffraction (Goldman, Biophys. J., 1983, this volume). When caged-ATP is photolyzed in the ADP, V_i, low ATP solution, the relaxation is slow, as with ADP alone, but the initial tension rise is strongly inhibited. This supports the conclusion that M.ADP.V_i complexes can reattach to actin but produce little force. To the extent that V_i is an analog of P_i these results suggest that full force generation by a cross-bridge requires phosphate release. Supported by NIH grants HL15835 to the Penna. Muscle Institute, AM00745, AM26846 & a British-American Heart Fellowship to MGH.

M-PM-H5 **TRANSIENT KINETICS OF MgATP CLEAVAGE IN SINGLE GLYCERINATED MUSCLE FIBERS.** Michael A. Ferenczi, Earl Homsher *, David R. Trentham. Department of Biochemistry and Biophysics, School of Medicine, University of Pennsylvania, Philadelphia PA 19104 .* Department of Physiology, School of Medicine, UCLA, Los Angeles CA 90024.

Transient kinetic measurements of ATP cleavage within single glycerinated muscle fibers from rabbit psoas have been made. A fiber was attached to a tension transducer and put into rigor in the presence of 0.5 to 10.0 mM P^3-1-(2-nitro)phenylethyl-[2-^{3}H]adenosine 5'-triphosphate (caged-ATP) a photolabile precursor of ATP. Flash photolysis of caged-ATP results in ATP formation within the fiber at 100 s^{-1} (Goldman,Hibberd,McCray & Trentham, 1982, Nature, in press). The solution also contained 100 mM TES, 51 mM EGTA ($[Ca^{2+}]<10^{-8}$M), 3.2 mM $MgCl_2$ and 10 mM glutathione at pH 7.1 and 22 °C. The solution was lowered from beneath the fiber and after 400 ms a 50 ns light pulse from a frequency-doubled ruby laser (347 nm) was focussed on the fiber. At a predetermined time following the pulse, the fiber was rapidly frozen between copper blocks at 77 °K to stop ATP cleavage. Tension was recorded throughout. [2-^{3}H]-ADP, [2-^{3}H]-ATP and [2-^{3}H]-caged-ATP were extracted from the fiber at -18 °C in a 2 mM EDTA solution of 50 % aqueous methanol which denatures the ATPase. The relative amounts of nucleotides were quantified following their separation on HPLC. Up to 5 mM ATP was formed from 10 mM caged-ATP with a single laser pulse. The fiber was almost completely relaxed 350 ms after a laser pulse which released 1 mM ATP. 350 ms after the release of 0.25 to 1 mM ATP, 150 μM ADP had formed within the fiber. This compares with a myosin head concentration of 280 μM.

(Supported by MDA and NIH).

M-PM-H6 MECHANICAL PROPERTIES OF SINGLE CARDIAC MYOCYTES. C. Pasternak, G.G. Ahumada* and E.L. Elson (Intr. by L.J. Banaszak), Dept. of Biol. Chem. and *Cardiovascular Division, Washington University School of Medicine, St. Louis, MO 63110.

A newly developed method for measuring cellular deformability is applied to analyze the mechanical properties of cultured ventricular myocytes from 3 day old rats. The "cell poker" tests the resistance to indentation of areas of the cell with a glass probe tip 2 μM in diameter (1). The cells are indented perpendicular to their surface and forces of a few millidynes recorded. The myocytes adhere to glass coverslips and contract spontaneously under the measurement conditions. They show normal physiological response to isoproterenol, ouabain and Ca^{+2}. The force of contraction, it's time dependence and frequency are recorded. The "cell poker" alternately samples the resistance to indentation of the contracted and relaxed states. The amplitude of contraction can be related to the difference in resistance at a certain level of indentation. The ability to measure directly forces developed in parts of a cell gives new insights into contractility, by characterizing the viscoelastic properties of the relaxed and contracted states. Increasing the external Ca^{+2} concentration intensifies contraction mainly by increasing the resistance of the contracted state, but it also decreases the resistance of the relaxed state to fast indentations, and may have a more general effect on the cell's cytoskeleton.

(1) N.O. Petersen, W.B. McConnaughey and E.L. Elson, PNAS 79, 5327-5331 (1982).

M-PM-H7 RESPONSE OF THE SINGLE FROG CARDIAC CELL TO STRETCHES AND RELEASES. M. Tarr, J.W. Trank, and K.K. Goertz*. Physiology Dept., Univ. of Kansas College of Health Sciences and Hospital, Kansas City, KS. 66103.

The response of the single isolated frog atrial cell following stretches or releases applied during twitch contractions was investigated to determine the effects of releases and stretches on contraction dynamics. Families of auxotonic contractions were obtained by initiating contractions from different initial sarcomere lengths above the unloaded resting length or by allowing the cell to take up various amounts of slack prior to auxotonic force development. From these contractions the velocities of shortening and forces at a given time but at different lengths were determined to obtain force-velocity points; each point associated with a different curve in the family of length-dependent force-velocity relationships existing at that time. A similar analysis was done on contractions in which stretches and releases were imposed on the cell at various times following stimulation. Comparison of the force-velocity data indicated that following both releases and stretches there was a depression of the force-velocity relationship compared to that apppropriate for a given length and time had the stretch or release not been imposed on the cell during contraction. These data indicate either that 1) the force-velocity relationship at a given length and time during contraction depends on the previous history of contraction or 2) the disruption of attached cross-bridges which can result from imposing a release or stretch on the cell during the contraction process produces long-term changes in the level of contractile activation. (Supported by NHLI Grant 18943 and by a Grant-in-Aid from the American Heart Association with funds contributed in part by the Kansas Affiliate, Inc.).

M-PM-H8 THE EFFECT OF REMOVING TROPONIN C FROM SKINNED SKELETAL MUSCLE FIBERS AND ADDING BACK EXOGENOUS CARDIAC OR SKELETAL MUSCLE TROPONIN C W.G.L. Kerrick*, H. Zot+, P.E. Hoar* and J.D. Potter+; *Univ. of Miami, Miami FL., +Univ. of Cincinnati, Cincinnati, OH.

Troponin C was removed from skinned adductor magnus (fast-twitch) fibers of the rabbit by treating them with a low ionic strength EDTA solution similar to that used for selectively extracting troponin C from rabbit skeletal muscle myofibrils (Zot, H. & Potter, J.D., J. Biol. Chem. 257: 7678-7683 (1982)). The fibers were no longer activated in the presence of Ca^{2+}. Adding back either cardiac or skeletal muscle troponin C caused the fibers to regain their Ca^{2+}-sensitivity. The reactivated fibers responded in a graded manner to increasing concentrations of either Ca^{2+} or Sr^{2+}. Approximately 8 times more Sr^{2+} was required for half maximal activation of the reconstituted fibers whether skeletal or cardiac troponin C were used for substitution. In untreated skinned cardiac and slow twitch fibers approximately the same concentrations of Ca^{2+} or Sr^{2+} were required for activation of tension in contrast to fast twitch fibers which require 8 times more Sr^{2+} than Ca^{2+} for activation. Thus substitution of cardiac troponin C for fast twitch troponin C did not affect the activation properties of skinned fast twitch fibers. These data suggest that differential activation by Ca^{2+} or Sr^{2+} in skinned fast twitch muscle fibers is not affected by the substitution of cardiac troponin C. Therefore the difference observed in the activation of cardiac and fast twitch skeletal muscle fibers by Ca^{2+} and Sr^{2+} cannot be due to differences in troponin C but may be due to one or more of the other thin filament proteins. Supported by grants from the National Institutes of Health, American Heart Association, and Muscular Dystrophy Association.

M-PM-H9 MYOSIN LC2 PHOSPHORYLATION MODULATES ACTOMYOSIN INTERACTION IN SKINNED PSOAS FIBERS.

H. Lee Sweeney, J.D. Potter* and M.J. Kushmerick, Dept. of Physiology and Biophysics, Harvard Medical School and *Dept. of Pharmacology and Cell Biophysics, University of Cincinnati.

Bundles of rabbit psoas fibers were stored at 2°C for 24 hours in a relaxing solution containing 110 mM free K^+, 5 mM ATP, 5 mM EGTA, 1 mM free Mg^{++} and sufficient immidazole to bring the ionic strength to 0.2 M at pH 7.1. Single fiber segments were mounted between a lever and a tension transducer. The fibers were briefly (10 min) treated with 0.5% lubrol in relaxing solution. Maximal activation at 20°C in pCa 5.0 with 15 mM PCr and 5 mM ATP at pH 7.1 produced an isometric tension between 1.5 and 2.0 kg/cm^2. The extent of 18,000 dalton light chain (LC2) phosphorylation was no more than 10% even after 30 min of full activation. The unloaded velocity of shortening, as assessed by the slack test, ranged between 3.0 and 3.5 fiber lengths per second and was well maintained in repeated contractions. If, however, after a control contraction, the fiber was relaxed in a solution containing 1 μM calmodulin and 3 μM myosin light chain kinase, and was then activated in normal pCa 5.0 solution, the unloaded shortening velocity fell to a stable but depressed level that was 50-60% of the control value. Under these conditions, LC2 is 50-60% phosphorylated. This data provides further evidence that myosin light chain 2 phosphorylation plays a modulatory role in the actin myosin ATPase cycle of mammalian skeletal muscle.

Supported by #H22619-3E and AM14485.

M-PM-H10 THE EFFECT OF MYOSIN SULFHYDRYL MODIFICATION ON FIBER TENSION, STIFFNESS AND VELOCITY OF CONTRACTION. M.S. Crowder and R. Cooke, Department of Biochemistry/Biophysics and the CVRI, University of California, San Francisco, CA 94143.

Glycerinated rabbit psoas muscle fibers have been modified with a paramagnetic probe (IASL) that reacts specifically at a sulfhydryl (SH_1) on the myosin head. The extent of SH_1 modification was determined by extracting myosin and measuring its ATPase in the presence of EDTA. Reaction of 30-40% of SH_1 produced no change in fiber properties, while reaction of 60-70% of SH_1 caused small decreases ($\lesssim$10%) in tension and stiffness. Further reaction with IASL to modify 80-90% of SH_1 caused $\sim$20% decrease in tension, and stiffness, however analysis of EPR spectra showed that a significant number of sulfhydryl groups other than SH_1 are modified in these fibers. Reaction of 50% of the SH_1 causes no measurable effect on the velocity of contraction, measured by load steps at 10°C. Extrapolation to zero load gave a maximum contraction velocity of about 2 length/sec for both control and labeled fibers. In solution the actin activated ATPase of HMM or S1 is decreased significantly by SH_1 modification (Mulhern and Eisenberg (1978) Biochem. 17:4419). Thus the effect of SH_1 modification on the actomyosin interaction depends strongly on whether this interaction is taking place in solution or in the organized array of the muscle fiber. Supported by grants from the USPHS, AM00479 and AM30668.

M-PM-H11 MYOSIN LIGHT CHAIN PHOSPHORYLATION DURING CONTRACTION OF CHICKEN FAST AND SLOW SKELETAL MUSCLES. K. Bárány, D.L. VanderMeulen, R.F. Ledvora* and M. Bárány. Dept. of Physiology and Biophysics, and Dept. of Biological Chemistry, College of Medicine, Univ. of Illinois at Chicago, Chicago, IL 60612

A modified automatic freezing apparatus (Kretzschmar and Wilkie, J. Physiol. 202, 66P, 1962) was used for studying light chain (LC) phosphorylation during contraction of the fast posterior latissimus dorsi (PLD), and slow, anterior latissumus dorsi (ALD), muscles of chicken. With this apparatus the muscles were frozen within 100 ms at various stages of the contraction-relaxation cycle. The frozen muscles were pulverized using a liquid nitrogen-chilled mortar containing frozen perchloric acid. After thawing and centrifugation, the residue was dissolved in an SDS-containing solution and the phosphorylated and unphosphorylated forms of P-light chain (LC) were separated by two dimensional gel electrophoresis. The intensities of the Coomassie blue stained LC spots were measured with a laser scanning densitometer. The PLD muscle reached its maximal isometric tetanic tension in 0.2 sec at 37°C and this was accompanied by maximal LC phosphorylation. On the other hand, in case of ALD muscle, tetanic tension was developed in 1.5-2.0 sec at 37°C and also LC phosphorylation proceeded at a much slower rate than in the PLD. When contralateral PLD muscles were stimulated for 0.2 sec and one muscle was frozen at the height of the tetanus while the other muscle was allowed to relax and frozen immediately, both contracted and relaxed muscles exhibited maximal LC phosphorylation. However, when the muscle was allowed to relax for about 1 sec, LC dephosphorylation occurred. These data suggest that LC phosphorylation is associated with the contractile phase of the mechanical activity and LC dephosphorylaton plays no role in relaxation. (Supported by Chicago Heart Association and NIH NS-12172).

M-PM-H12 EXTRACELLULAR CALCIUM AND TONIC TENSION IN RAT EXTRAOCULAR MUSCLES.

Dante J. Chiarandini, Departments of Ophthalmology and Physiology and Biophysics, New York University Medical Center, New York, NY 10016

Extraocular muscles (EOMs) of mammals possess in addition to twitch or singly innervated fibers a population of multiply innervated fibers (global MIFs) which have many structural, contractile and electrophysiological similarities with slow or tonic fibers of amphibians. In vitro exposure of rat EOM (inferior rectus) to a $[K]_o$=20-75 mM induces a long lasting tonic tension. Exposure of the muscles to Ca-free saline (1 mM EGTA + 2-3 mM Mg) practically abolishes the tonic tension whether applied before increasing $[K]_o$ or during the tension. These effects cannot be explained by a change in the surface potential. NO_3 (40 mM) and SCN (3-12 mM) potentiate tonic tensions. SCN enhances tension without shifting to the left the log $[K]_o$-tension curve. SCN induces an increase of the basal tension of the muscle, which is abolished by Ca-free saline but not affected by depolarization. Cadmium (0.5-1.0 mM) depresses tonic tension without displacing the log $[K]_o$-tension curve. Mg (10 mM) reduces tension and, in contrast, shifts to the right the log $[K]_o$-tension curve. Nifedipine (1-10 μM) and felodipine (10 μM) do not modify the tonic tension. These results suggest that the tension generated by global MIFs of rat EOM depends on extracellular Ca and that SCN and Cd modify tension amplitude by increasing and decreasing a membrane Ca permeability. Supported by USPHS grant EY 01297.

M-PM-H13 DEPLETION OF Ca_0 DURING CARDIAC MUSCLE TWITCHES MEASURE WITH Ca SELECTIVE MICROELECTRODES: Ca INFLUX DURING SINGLE BEATS. Donald M. Bers. Division of Biomedical Sciences, University of California, Riverside, CA 92521-0121.

Double barreled Ca-selective microelectrodes (tip diameters 4-12 μm) were used to monitor changes of $[Ca]_0$ which occur during rabbit papillary muscle twitches. The Ca selective barrel utilized Simon's neutral Ca exchange resin (ETH 1001) and reference barrels were filled with 140 mM NaCl or 1 M KCl. Transient depletions of Ca_0 were seen during the early phases of the action potential and preceded tension development. When the inotropic state of the muscle is modified by various interventions, the magnitude of the Ca_0 depletion changes in parallel with tension development. The Ca_0 depletion and tension are decreased by Co, verapamil and long rest intervals. The Ca_0 depletion and tension are increased by 10^{-8} M isoproterenol, reduction of $[Na]_0$, 5 mM Caffeine, continued pacing at a given frequency after a rest interval, and increasing $[Ca]_0$ (e.g., 8.5 ± 1.0 μM at 0.2 mM Ca_0, 16.9 ± 1.6 μM at 0.5 mM Ca_0 and 44.7 ± 3.7 μM at 2.0 mM Ca_0). The Ca_0 depletion measured most probably represents Ca influx which occurs during single beats and this technique may be very useful in the study of cardiac excitation-contraction coupling. Rough estimations of the Ca influx represented by the Ca_0 depletion are in the range which would be required for direct activation of the myofilaments. (Supported by the American Heart Association, Greater Los Angeles Affiliate and USPHS HL 11351-15 and 28589-01).

M-PM-H14 IS THE RELAXANT EFFECT OF EPINEPHRINE IN HEART MUSCLE RELATED TO STIMULATION OF THE Na-K PUMP? L. Cleemann and M. Morad, Depts. of Physiology, School of Dental Medicine and Medical School, Univ. of Penna., Phila., PA 19104

Experiments were carried out to examine whether the relaxant effect of adrenaline in frog ventricular muscle is mediated by a Na^+-Ca^{2+} counter transport system through alterations of the Na^+ gradient induced by stimulation of Na^+-K^+-pump. A single sucrose gap voltage clamp technique was used to monitor the effect of adrenaline on tension and membrane currents. Changes in Na^+-K^+ pump activity were estimated by measurements of either total K^+ activity (^{42}K content) or paracellular K^+ concentration (K^+-selective microelectrodes). In order to separate the positive inotropic effect from the relaxant effect of the drug I_{si} (Ca^{2+} channel) was blocked either by long depolarizing clamp pulses or by addition of Ni^{2+}. Under these conditions the relaxant effect of adrenaline was consistently seen as suppression of developed tension. Stimulation of the pump by adrenaline was indicated by the increased rate of K^+ depletion following a period of rapid stimulation. ^{42}K measurements showed that the relaxant effect of the drug was accompanied by a 1-5 mM net gain in $[K]_i$. Both the relaxant effect and the gain in $[K]_i$ were blocked by addition of strophanthidine. A large increase in Na-gradient will occur if the gain in K^+ content is accompanied by an equivalent loss in $[Na]_i$. In Na^+-depleted strips, although epinephrine had its positive inotropic effect, it failed to enhance the rate of relaxation, suggesting that a large Na^+ gradient was necessary for the relaxant effect of the drug. Our results are consistent with the hypothesis that changes in the Na^+ gradient induced by stimulation of the Na^+-pump may be responsible for enhanced relaxation seen in the presence of epinephrine. It is likely, therefore, that Na^+-Ca^{2+} counter transport system plays a central role in the relaxation process.

M-PM-I1 ^{31}P - NMR STUDIES OF SMOOTH MUSCLE ENERGY METABOLISM. Hans J. Vogel, Sture Forsén and Per Hellstrand, Depts of Physical Chemistry 2 and of Physiology and Biophysics, University of Lund, Sweden (Intr. by K.A.P. Edman).

^{31}P - NMR spectra at 103 MHZ were obtained from smooth muscle preparations isometrically mounted in a horizontal probe and superfused with tris-buffered PSS at pH 7.4 and 23°C. Spectral accumulation time was 1.5 hrs to 15 min depending on sample size (70 - 800 mg). Preparations remained viable for at least 24 hrs. Spectra, from rabbit urinary bladder, portal vein and taenia coli or guinea pig taenia coli, all showed resonances corresponding to PCr and ATP at a ratio of 1.5 - 2.0, consistent with chemical analysis. P_i and phosphomonoesters were normally low and increased after prolonged superfusion. Spectra obtained during 15 - 60 min high-K^+ induced contractions showed a small reversible decrease in PCr (10 - 30 %) with no change in ATP. NaCN (1 - 2 mM) lowered PCr with little change in ATP. Intracellular pH (6.9 - 7.0) did not change appreciably with these treatments. Determined from the positions of the ATP peaks, intracellular Mg^{2+}/ATP was below 1.5 and did not change upon perfusion with high [Mg^{2+}], high osmolarity, or Mg^{2+}-free, EDTA containing medium. Despite low levels of phosphorylated compounds smooth muscle preparations, because of a comparatively low metabolic rate and slow contractile characteristics, seem suitable for ^{31}P - NMR analysis.

Supported by Swedish MRC (00028) and AB Hässle, Mölndal.

M-PM-I2 A NEW METHOD FOR ASSESSING MYOSIN PHOSPHORYLATION IN SMOOTH MUSCLE: ELECTROPHORESIS AND IMMUNOBLOTTING. David R. Hathaway and Joe R. Haeberle, Depts. Medicine and Pharmacology, Ind. Univ. School Med, Indianapolis, Indiana 46223

The 20,000 dalton light chain subunits (LC_{20}) of bovine aortic smooth muscle myosin have been purified to homogeneity by a new procedure. These light chains were used to immunize rabbits by intramuscular and subcutaneous injection of 90 μg of LC_{20} per animal at 3 week intervals. Serum from these animals was found to react strongly with aortic LC_{20} transferred to nitrocellulose sheets electrophoretically, using ^{125}I-Protein A and autoradiography to identify protein bands. In addition to bovine aortic LC_{20}, the antiserum was found to cross-react with LC_{20} from rat uterine and chicken gizzard myosins. In all cases, serum dilutions of 1:5000 were found to be adequate for quantitative studies. Whole muscle samples (eg. uterine and vascular) have been subjected to isoelectric focusing and urea gel electrophoresis followed by immunoblotting. Both the unphosphorylated (UP-LC_{20}) and the phosphorylated (P-LC_{20}) species could be identified by autoradiography and quantitated by two methods: densitometric scanning and direct counting for ^{125}I. Reasonably good agreement in the % LC_{20} phosphorylation was obtained over the range of 10-80% when compared to urea gels alone. Preliminary studies suggest that the immunoblot can detect less than 100 ng of LC_{20}. In conclusion, separation of P-LC_{20} and UP-LC_{20} by electrophoretic methods and quantitation by immunoblotting is a sensitive and specific method for assessing myosin LC_{20} phosphorylation which can be applied to intact muscle studies.

M-PM-I3 THE ROLE OF MYOSIN LIGHT CHAIN PHOSPHORYLATION IN THE REGULATION OF STEADY-STATE ISOMETRIC TENSION AND UNLOADED SHORTENING VELOCITY IN RAT UTERINE SMOOTH MUSCLE. Joe R. Haeberle, David R. Hathaway, and Richard A. Meiss (Intr. by H. R. Besch), Depts. Medicine, Pharmacology and Physiology, Indiana Univ. Sch. Med., Indianapolis, IN 46223.

Myosin light chain (LC_{20}) phosphorylation in uterine smooth muscle has been examined as a function of: 1) time during isometric contraction, and 2) extracellular Ca^{2+} during steady-state contraction. Rat uterine longitudinal muscle (50-100 um thick) was contracted isometrically by K^+-depolarization in 10 mM Ca^{2+}. Muscles were frozen in acetone + 10% TCA (-78°C) and warmed to 21°C in the same solution. LC_{20} was isolated by two-dimensional gel-electrophoresis utilizing SDS-PAGE followed by isoelectric focusing (IEF). Phosphorylation was quantitated by densitometric scanning of silver-stained IEF gels. LC_{20} phosphorylation peaked at 10 sec after stimulation with 0.64 ± 0.050 mol PO_4/mol LC_{20} (mean ± S.E., n=5) and fell to 0.53 ± 0.009 mol PO_4/mol LC_{20} (n=4) at two min. No significant change ($p>0.05$) in LC_{20} phosphorylation occurred between 30 sec and 90 min of contraction with an average of 0.53 ± 0.013 mol PO_4/mol LC_{20} (n=27). However, unloaded shortening velocity (V_o), measured by isotonic quick-releases, declined from a peak of 0.021 ± 0.0028 L_o/sec (n=4) at 30 sec to 0.010 ± 0.0015 L_o/sec (n=9) at 45 min ($p<0.01$). During steady-state contraction (10 min) both LC_{20} phosphorylation and tension changed as a function of extracellular Ca^{2+}. Phosphorylation declined from 0.51 ± 0.019 mol PO_4/mol LC_{20} (n=8) with 10 mM Ca^{2+} to 0.38 ± 0.008 mol PO_4/mol LC_{20} (n=3) with 0.01 mM Ca^{2+} ($p<0.01$); isometric tension fell to 13.8 ± 0.05% of the high calcium level. In summary, for the K^+-depolarized uterus, V_o decreased with constant LC_{20} phosphorylation, whereas changes in phosphorylation paralleled changes in steady-state tension. (Supported in part by the American Heart Association, Indiana Affiliate).

M-PM-I4 THE FUNCTIONAL EFFECT OF Ca^{2+}-INSENSITIVE MYOSIN LIGHT-CHAIN KINASE, PHOSPHATASE, AND CATALYTIC SUBUNIT OF THE cAMP-DEPENDENT PROTEIN KINASE ON TENSION IN SKINNED GIZZARD SMOOTH MUSCLE FIBERS. P.E. Hoar**, M.P. Walsh#, M.D. Pato@, R.S Adelstein+, D.J Hartshorne~, W.G.L. Kerrick**. **Univ. of Miami, FL. 33101; #Univ. of Alberta, Edmonton, Alberta; @Univ of Saskatchewan, Saskatoon, Sask. 57NOWO; ~Univ. of Arizona, Tucson, AZ. 85721; +National Institutes of Health, Bethesda, MD. 20205

Skinned fibers exposed to Ca^{2+}-insensitive myosin light-chain kinase (MLCK) in the absence of Ca^{2+} can be maximally activated. This tension response can be inhibited by the addition of an exogenous smooth muscle phosphatase. This response correlates with phosphorylation and dephosphorylation of the myosin light-chains. Fibers which have been inhibited by trifluoperazine (TFP) (50 uM) in the presence of high Ca^{2+} are caused to contract by the addition of Ca^{2+}-insensitive MLCK. The concentration of Ca^{2+}-insensitive MLCK needed for this activation was less than that required in the absence of Ca^{2+} and TFP. This suggests that high Ca^{2+} may inhibit the endogenous phosphatase. Fibers activated by the Ca^{2+}-insensitive MLCK are not inhibited by the catalytic subunit of the cAMP-dependent protein kinase. In contrast Ca^{2+}-activated fibers are inhibited by the catalytic subunit. However the rate of inhibition is much slower in the presence of high Ca^{2+} than in its absence. This suggests that the inhibitory site is protected in the presence of high Ca^{2+} or that the phosphatase is inhibited by high Ca^{2+}. These data are consistent with the proposed model that smooth muscle skinned fibers are regulated by a Ca^{2+}-sensitive MLCK/phosphatase system which can be modulated by the cAMP-dependent protein kinase. Supported by the National Institutes of Health, American Heart Association, and Muscular Dystrophy Association.

M-PM-I5 PHOSPHORYLATION OF MAMMALIAN MYOSIN KINASES BY THE CATALYTIC SUBUNIT OF cAMP-DEPENDENT PROTEIN KINASE OR cGMP-DEPENDENT PROTEIN KINASE. M. Nishikawa, P. de Lanerolle, *T.M. Lincoln, & R.S. Adelstein, *Univ. of South Carolina Sch. of Med., Columbia, SC 29208, & NHLBI, NIH Bethesda, MD 20205

Bovine tracheal myosin kinase (T·MK, MW=160,000) and human platelet myosin kinase (P·MK, MW=105,000) have been purified to apparent homogeneity. We have investigated the phosphorylation of these two myosin kinases (MK) by the catalytic subunit of cAMP-dependent protein kinase (cA·PK) and by cGMP-dependent protein kinase (cG·PK). When MK is phosphorylated by cA·PK in the presence of bound calmodulin, one mole of phosphate is incorporated per mole of T·MK or P·MK with no effect on MK activity. Phosphorylation of MK by cA·PK in the absence of bound calmodulin results in the incorporation of two moles of phosphate per mole of MK and decreases the MK activity. These data obtained with T·MK and P·MK are similar to those obtained for phosphorylation of gizzard MK (MW=130,000) although the molecular weights differ among these three enzymes. In contrast to cA·PK, cG·PK cannot phosphorylate T·MK in the presence of bound calmodulin. In the absence of bound calmodulin, cG·PK can phosphorylate only one site in T·MK and this phosphorylation has no effect on MK activity. Extensive tryptic digestion of phosphorylated T·MK yields the same single phosphopeptide as that found following phosphorylation of T·MK by cA·PK in the presence of bound calmodulin. On the other hand, cG·PK incorporates phosphate into two sites in P·MK, when calmodulin is not bound to P·MK. In the presence of bound calmodulin, phosphate is incorporated into a single site in P·MK by cG·PK.

M-PM-I6 PROTEIN PHOSPHORYLATION AND cAMP-LEVELS IN FORSKOLIN-TREATED TRACHEAL SMOOTH MUSCLE. P. de Lanerolle, M. Nishikawa & R.S. Adesltein, Laboratory of Molecular Cardiology, NHLBI, NIH, Bethesda, MD 20205

Data from biochemical and physiological experiments have demonstrated that myosin phosphorylation plays an important role in regulating smooth muscle contraction. The mechanisms that regulate smooth muscle relaxation, on the other hand, are less well understood. Since data from *in vitro* experiments have demonstrated that phosphorylation of myosin kinase (MK) by cAMP-dependent protein kinase decreases the activity of MK, it has been suggested that myosin dephosphorylation, subsequent to MK phosphorylation, is a step in cAMP-mediated relaxation of smooth muscles. We are presently testing this hypothesis by studying the relationships among an increase in cAMP-levels, MK phosphorylation and myosin dephosphorylation in forskolin-treated intact tracheal smooth muscle (TSM). Muscles were either contracted with 10^{-6}M methacholine and relaxed with 4 x 10^{-5}M forskolin or treated with forskolin alone. TSM were frozen at various times following the addition of forskolin and assayed for cAMP levels, myosin phosphate content (in the 20,000 dalton light chain) or MK phosphate content. MK phosphate content was determined by incubating TSM strips with ^{32}P and immunoprecipitating MK from tissue frozen following forskolin treatment. The data demonstrate an increase in cAMP and a decrease in myosin phosphate content within 15 secs of adding forskolin. The immunoprecipitation experiments demonstrate that canine TSM MK has a Mr=155,000 (while bovine TSM MK has a Mr=160,000-See Nishikawa *et al.*, this volume) and that MK is partially phosphorylated in resting muscle. We are presently performing experiments to determine the stoichiometry of MK phosphorylation following forskolin treatment.

M-PM-I7 COOPERATIVE INTERACTIONS BETWEEN THE TWO HEADS OF SMOOTH MUSCLE MYOSIN. J.R. Sellers, P.B. Chock and R.S. Adelstein, NHLBI,NIH Bethesda, MD 20205

The correlation curve between phosphorylation and MgATPase activity suggests that both heads of a smooth muscle myosin or heavy meromyosin (HMM) molecule must be phosphorylated before the Mg-ATPase activity of either head can be activated by actin. The two heads of HMM appear to be phosphorylated randomly, while those of myosin are phosphorylated in an ordered manner (Persechini & Hartshorne, Science, 213,1382,1981; Sellers & Adelstein, Biophys. J. 37, 262a, 1982, Ikebe et al, J. Biochem. 91, 1809, 1982.). We have investigated the cause of this difference between HMM and myosin. We find that if myosin is first phosphorylated at high ionic strength (0.6M KCl), where it is monomeric, and then assayed for MgATPase activity (in 0.05M KCl) the data support a model where the two heads are phosphorylated randomly (i.e. similar to HMM). Direct analyses of the time courses of phosphorylation of HMM, and myosin at high ionic strength, show that a single rate constant is sufficient to fit the data through greater than 90% of the reaction. However, when phosphorylation is carried out at low ionic strength (0.02M KCl), where myosin is present as filaments, the data can be fitted to the sum of two rate constants. This suggests that when myosin is polymerized into filaments the two previously identical heads become nonequivalent leading to an apparently ordered phosphorylation reaction. The correlation curves between MgATPase activity and dephosphorylation of fully phosphorylated myosin, both in a filamentous and monomeric state, is best explained by a model where dephosphorylation of one head is sufficient to deactivate the entire molecule. In the case of monomeric myosin the dephosphorylation appears to be random whereas in the case of filamentous myosin the dephosphorylation appears to be ordered, presumably for the reasons discussed above.

M-PM-I8 REGULATION OF MOLLUSCAN ACTOMYOSIN ATPASE BY Ca^{2+}. Chalovich, J.M., Chantler, P.D., Szent-Gyorgyi, A.G., and Eisenberg, E. NIH, Bethesda, MD and Brandeis University, Waltham, MA.

The interaction of myosin and actin in many invertebrate muscles is mediated by the direct binding of Ca^{2+} to myosin, in contrast to modes of regulation in vertebrate skeletal and smooth muscles. Earlier work showed that the binding of skeletal muscle myosin subfragment-1 to the actin-troponin-tropomyosin complex in the presence of ATP is weakened by less than a factor of 2 by removal of Ca^{2+} although the maximum rate of ATP hydrolysis decreases by 96% (Chalovich et al., J. Biol. Chem., 1981 and 1982). We have now studied the invertebrate type of regulation using HMM prepared from both the scallop Aequipectin irradians and the squid Loligo pealii. Binding of these HMM's to rabbit skeletal actin was determined by measuring the ATPase activity present in the supernatant after sedimenting acto·HMM in an Airfuge ultracentrifuge. Binding was measured at 25°C in 1 mM ATP, 1.8 mM $MgCl_2$, 10 mM imidazole, 0.5 mM DTT, 0.1 mM Ca EGTA or 0.5 mM EGTA. Even in the absence of Ca^{2+}, the HMM of both species bound to actin in the presence of ATP; the binding constant in the absence of Ca^{2+} (4.8×10^3 M^{-1}) being about one-fourth of that in the presence of Ca^{2+} (2.2×10^4 M^{-1}). Studies of the steady-state ATPase activity of these HMM's as a function of actin concentration revealed that the major kinetic effect of removing Ca^{2+} was to decrease the maximum velocity (4- to 6-fold in Aequipectin and 5- to 7-fold in Loligo). Furthermore, at 400 μM actin where about 65% of the Aequipectin HMM was bound to actin in the absence of Ca^{2+}, the rate of ATP hydrolysis was only one-fourth of that in the presence of Ca^{2+}. Therefore, inhibition of the ATPase rate in the absence of Ca^{2+} cannot be due simply to effects of Ca^{2+} on the binding of S-1 to actin; rather, Ca^{2+} must also alter a kinetic step in the cycle.

M-PM-I9 DO SMOOTH MUSCLE'S CONTRACTILE CAPABILITIES REFLECT UNIQUE CROSS-BRIDGE PROPERTIES? D. Warshaw & F. Fay, U. Mass. Med. Sch., Physiol. Dept., Worcester, MA 01605

Smooth muscle's slow, economical force production may reflect differences in cross-bridge (X-B) mechanics and kinetics relative to that in fast striated muscle (SKM). We have recently presented data (Science, in press) demonstrating that tension transients recorded in response to small rapid step length changes (ΔL=0.3-2.0%L_{cell} in 2.0$_{ms}$) in single smooth muscle cells (SMC) from the toad stomach muscularis (Bufo marinus) do reflect these X-B properties. The transients are characterized by a linear elastic response coincident with the ΔL followed by a biphasic tension recovery comprised of two exponential components (τ_{fast} = 5-20ms, τ_{slow} = 50-300ms). Since stiffness (K) may reflect the number of attached X-Bs, we studied possible changes in the population of attached X-Bs during the recovery phase by imposing small (ΔL=0.5%L_{cell}) sinusoidal ΔLs (250Hz) superimposed upon the step length changes as an estimate of K. The results from both the step and sinusoidal ΔL studies were interpreted in terms of a X-B cycle having at least one detached and two attached (low and high force) X-B states. Significant differences observed for SMC X-B mechanics and kinetics as compared to SKM were: 1) 3 x more compliant X-B; 2) longer cycle time; 3) as much as 90% of X-B cycle time spent in high force X-B state. These results suggest that the longer cycle time may be due largely to a decreased detachment rate resulting from the ability of the X-B in SMC to remain attached over longer distances due to the increased compliance. Furthermore, we propose that the high economy of force maintainance in SMC may be largely accounted for by the increased duty time of the high force X-B state as well as the overall slowing of the cycle. (Supported by: DW, MDA; FF, HL 14523.)

M-PM-I10 **DEPENDENCE OF UNLOADED SHORTENING VELOCITY (V_{us}) ON Ca^{2+}, CALMODULIN AND CONTRACTION DURATION IN "CHEMICALLY SKINNED" SMOOTH MUSCLE.** Richard J. Paul, Glenn Doerman, Claudia Zeugner* and J. Caspar Rüegg*. II. Physiology Institute, University of Heidelberg* (FRG) and Dept. of Physiology, University of Cincinnati, College of Medicine, Cincinnati, OH 45267 USA.

V_{us}, a mechanical parameter associated with the rate of cross bridge cycling, was investigated in chemically-skinned guinea pig taenia coli and hog carotid artery. V_{us} was measured by the technique whereby large (5 to 20%) length steps are rapidly imposed on the muscle and the time under unloaded conditions determined from the isometric myograms. V_{us} determined in this manner was similar to V_{max} determined from Hill force-velocity relations as reported for both living and skinned muscles. The behavior of V_{us} was qualitatively similar for both preparations. V_{us} was strongly temperature dependent with a Q_{10} of 3.6. V_{us} was dependent on both the Ca^{2+} and calmodulin concentrations. In contrast to the dependence of isometric force (P_o) on Ca^{2+}-calmodulin, V_{us} could be further increased by addition of Ca^{2+} and/or calmodulin under conditions when P_o was maximized. Incubation with ATP-γS, which presumably maximizes the phosphorylation of myosin, did not increase V_{us} beyond the maximum value obtained in the presence of Ca^{2+}-calmodulin alone. The development of V_{us} following exposure to a high Ca^{2+} solution was found to preceed that of P_o. V_{us} reached a steady state value before the attainment of maximum isometric force. The steady state value tended to be slightly lower than the maximum V_{us}, the largest difference observed being less than 1.5-fold. Thus while both P_o and V_{us} are dependent on the Ca^{2+}-calmodulin concentration in skinned smooth muscle, the dependencies are not identical, differing with respect to temporal development and concentration. These differences may underlie the decline in velocity with maintained isometric force observed in living smooth muscle. Supported by NIH HL23240, HL22619, AHA EI 81-148 (RJP) and the Deutche Forschungsgemeinschaft.

M-PM-I11 **PHOSPHORYLASE AND MYOSIN LIGHT CHAIN PHOSPHATASE ACTIVITIES FROM AORTIC SMOOTH MUSCLE.** J. DiSalvo and D. Gifford*. Dept. Physiol. Univ. of Cincinnati, Coll. Med. and Univ. of Leuven, Belgium.

Both phosphorylase and the 20,000 dalton myosin light chains (MLC) are phosphorylated when vascular smooth muscle contracts. Conceivably, phosphatases which are effective against these substrates may participate in coordinating arterial metabolism and contractility. Procedures involving ion exchange chromatography, gel filtration and affinity chromotography of extracts from bovine aortic muscularis yielded a spontaneously active (Mr>350,000 daltons) and an ATP-Mg dependent phosphatase (Mr≃140,000 daltons). Spontaneously active phosphatase was effective in dephosphorylating both phosphorylase a (240nmol^{32}P/min/mg) and phosphorylated bovine cardiac MLC (1μmol^{32}P/min/mg). In contrast, ATP-Mg dependent phosphatase was only effective in dephosphorylating phosphorylase a (100nmol^{32}P/min/mg). Spontaneous phosphatase activity against phosphorylase a was markedly stimulated by Mg^{2+} (0.5-10mM), whereas activity against MLC was unaffected at low Mg^{2+} (0.5-2.5mM) and inhibited 25% by high Mg^{2+} (10mM). High concentrations (10mM) of Mn^{2+} or Co^{2+} inhibited sponatenous phosphatase activity against both substrates. No evidence for conversion of spontaneous phosphatase activity to an ATP-Mg dependent form was obtained. These findings suggest that spontaneous and ATP-Mg dependent phosphatase activities present in mammalian vascular smooth muscle are ascribable to separate enzymes which show different substrate specificities. The spontaneously active form may participate in coordinating arterial metabolism and contractility since it dephosphorylates both phosphorylase a and phosphorylated MLC.
This work was supported by NIH grants HL 20196 and HL 22619.

M-PM-I12 ACTIN-ACTIVATED ATPase ACTIVITY OF PHOSPHORYLATED MYOSIN FROM PULMONARY ARTERY AT LOW Mg^{2+} CONCENTRATIONS; EFFECT OF ACTIN AND TROPOMYOSIN FROM DIFFERENT SOURCES. N. Nath, A. Carlos, and J.C. Seidel, Department of Muscle Res., Boston Biomed. Res. Inst., Boston, MA 02114.

In the presence of 2mM $MgCl_2$ and 2mM ATP the ATPase activity of phosphorylated bovine pulmonary myosin was activated by actins from rabbit skeletal muscle, chicken gizzard, or pulmonary artery in the presence or in the absence of micromolar concentrations of Ca^{2+}. There was little difference among the three actins in the extent of activation but tropomyosins from these three muscles differed markedly in their ability to stimulate activity. Their effectiveness decreased in the order: gizzard tropomyosin > skeletal tropomyosin > pulmonary tropomyosin. There is only a small effect of Ca^{2+} on the activity in the presence or absence of tropomyosin as found by Chacko and Rosenfeld (Proc. Natl. Acad. Sci. USA. 79: 292 (1982)). This effect does not depend on the source of the actin and therefore differs from the Ca^{2+} and tropomyosin dependent activation of phosphorylated gizzard myosin by gizzard actin (Nag et al. Biophys. J. 37: 48, 1982). These observations suggest that the phosphorylated forms of myosin from gizzard and pulmonary artery differ in their interactions with actins from these two muscles. (Supported by grants from NIH (HL 23249, HL 15391) and Muscular Dystrophy Association).

M-PM-I13 CHYMOTRYPTIC DIGESTION OF PHOSPHORYLATED GIZZARD MYOSIN ALTERS ITS Ca^{2+} AND TROPOMYOSIN DEPENDENT ACTIN ACTIVATED ATPase ACTIVITY. Sumitra Nag and John C. Seidel. Department of Muscle Research, Boston Biomedical Research Institute, Boston, MA 02114 and Department of Neurology, Harvard Medical School, Boston, MA.

At low concentrations of Mg^{2+}, less than 1mM, the activation of ATPase activity of phosphorylated gizzard myosin by gizzard actin requires both gizzard tropomyosin and μM concentrations of Ca^{2+} (Nag et. al., Biophysical J., 37, 48, 1982). The dependence of activity on Ca^{2+} and tropomyosin is partially lost if either actin or myosin is replaced by the corresponding proteins from skeletal muscle, showing that both myosin and actin play a role in this regulation. 6-10 mM $MgCl_2$ will enhance activity in the presence of tropomyosin to the same extent as does Ca^{2+}. Digestion of phosphorylated gizzard myosin by α chymotrypsin leads to an increase in activity in the presence of EGTA and tropomyosin with resulting partial loss in dependence of activity on Ca^{2+}. Tropomyosin stimulates the actin activated ATPase activity of the complete digest two to three times. The activity of phosphorylated gizzard HMM isolated from a chymotryptic digest of phosphorylated myosin is no longer dependent on Ca^{2+} or tropomyosin. Chymotryptic cleavage either in the presence or in the absence of ATP leads to loss of Ca^{2+} sensitivity, suggesting that the site 5K daltons from the N terminus of the myosin heavy chain, at which cleavage is promoted by ATP (Okamoto and Sekine, Biochem. J., 90, 833, 1981), is not involved in the loss of Ca^{2+} sensitivity. (Supported by grants from NIH (HL 23249, HL 15391) and Muscular Dystrophy Association).

M-PM-I14 PURIFICATION AND PROPERTIES OF DICTYOSTELIUM MYOSIN LIGHT CHAIN KINASE. Linda M. Griffith and James A. Spudich. Department of Structural Biology, Stanford University School of Medicine, Stanford, CA 94305.

Myosin isolated from Dictyostelium discoideum grown in ^{32}P-phosphate has 0.2-0.3 mole Pi/mole 210,000 MW heavy chain and 0.1 mole Pi/mole 18,000 MW light chain (Kuczmarski and Spudich. 1980. PNAS 77, 7292.). From extracts of log phase cells we have purified 1000-fold an enzyme which phosphorylates the 18,000 MW light chain of Dictyostelium myosin. We measured myosin light chain kinase (MLCK) activity by incubating purified myosin and MLCK in 20 mM Tris pH 7.5, 5 mM $MgCl_2$, and 1.5 mM γ-^{32}P-ATP. Autoradiograms of samples run on SDS polyacrylamide microgels detect as little as 0.025 pmole ^{32}P/pmole 18,000 MW light chain. Amoebae were lysed under conditions which minimize proteolysis (Uyemura, Brown and Spudich. 1978. JBC 253, 9088.). Proteolysis inhibitors were also added (Adelstein and Klee. 1981. JBC 256, 7501.) MLCK activity fractionates in 80-100% ammonium sulfate, elutes from DE-52 at 0.15 M KCl, and from hydroxylapatite (HAP) at 0.07 M H_3PO_4. 100 gm wet cells yield about 1 mg of partially purified MLCK. We have no evidence for separation during purification of two components which might be required for enzyme activity. The peak of MLCK activity from HAP has 6-10 proteins by SDS gel electrophoresis and elutes from A0.5m as a single peak of K_d = 0.6. The activity of the enzyme is enhanced by 5 mM Mg^{++} and inhibited by KCl and 1 mM Ca^{++}. Serine is the site of phosphorylation both in vivo and in vitro. Dictyostelium MLCK will also phosphorylate the 18,500 MW alkali light chain of rabbit skeletal muscle myosin, but not histone or casein. (Supported by NIH 1 F32 GM07781 to L.M.G. and GM 25240 to J.A.S.)

M-PM-I15 MOVEMENT OF MYOSIN MEASURED IN VITRO. Michael P. Sheetz* and James A. Spudich. Department of Structural Biology, Stanford University School of Medicine, Stanford CA 94305. *On leave from Department of Physiology, University of Connecticut Health Center, Farmington, CT 06032

Movement of myosin along actin fibers is believed to be the basis for most motile activities in muscle and nonmuscle cells. No method has been described, however, for measuring myosin movement on actin in vitro because of the difficulties of obtaining an organized actin substratum and of monitoring the position of myosin. We have utilized the well organized arrays of actin filaments in cells of characean algae as an actin substratum. The filament polarity is known in Nitella and there are regions where filaments of opposite polarity are in close proximity at the zones of indifference. Cells were cut open to expose the actin filaments to the medium. Fluorescent polymer beads (0.7 μ in diameter) were coated with rabbit skeletal muscle HMM by a covalent reaction. When these HMM-beads were applied to the actin filaments of the Nitella an ATP-dependent motion of the beads was observed that always followed the path of the actin filaments. With 1 mM ATP the HMM-beads moved at a rate of 2-5 μ/sec. Simultaneous movement of HMM-beads in opposite directions on opposite sides of the zone of indifference was observed. The direction of HMM-bead movement was the same as that of cytoplasmic streaming in Nitella prior to dissection. Motion was prevented by pretreatment of HMM-beads with 1 mM N-ethylmaleimide (NEM) followed by 2 mM dithiothreitol (DTT) whereas pretreatment with 2 mM DTT followed by 1 mM NEM did not block motility. NEM pretreatment of the Nitella did not block motility of the HMM-beads. We suggest that the ATP dependent movement of the beads on Nitella actin is driven by the rabbit skeletal muscle HMM.

M-PM-J1 THE FOLDING OF RIBOSOMAL RNA IS DETERMINED BY THE RIBONUCLEOTIDE SEQUENCE
Wong, Kin-Ping; Nguyen, Luc Sinh; Wong, Andrew; Fox, J. Wesley; and Hung, Chun-Ho. Dept. of Biochem., Univ. of Kansas Med. Ctr., K.C., KS 66103

The mechanism in which ribosomal 5S, 16S, and 23S RNAs acquire their native conformation has been investigated by unfolding and refolding studies using circular dichroism, hydrodynamic measurements, and thermal denaturation to monitor the changes in conformation, hydrodynamic shape, and stability, respectively. Furthermore, the refolded RNAs were examined for their protein binding properties and in vitro reconstitution behavior. The results showed that ribosomal RNAs can be denatured by 5M urea and EDTA (molar ratio of EDTA to RNA: 3.25×10^3) to an unfolded state which is consistent with a single stranded highly helically stacked polyribonucleotide. Removal of the denaturant (urea and EDTA) by exhaustive dialysis against native and reconstitution buffers results in refolded RNAs whose conformation and stability are indistinguishable from the native RNAs. Sedimentation velocity and intrinsic viscosity measurements demonstrated that the refolded RNAs have the same hydrodynamic properties as the native RNAs under the same buffer conditions. Difference two-dimensional gel electrophoresis showed that both refolded 16S and 23S RNAs bind their corresponding ribosomal proteins to form reconstitution particles which are very similar to those reconstituted from their corresponding native RNAs. However, some subtle but significant differences were observed in comparing the steps of in vitro reconstitution of the refolded RNAs and those of the native RNAs. These results indicate that the folding of the ribosomal RNAs into their native conformations free in solution is determined solely by their ribonucleotide sequences.

M-PM-J2 DEMONSTRATION OF ORDERED RNA STRUCTURE AND RNA-CAPSID INTERACTIONS IN COWPEA CHLOROTIC MOTTLE VIRUS BY DIFFERENCE RAMAN SPECTROSCOPY. B.J.M. Verduin, Dept. of Virology, Agricultural Univ., Wageningen, The Netherlands; B. Prescott and G.J. Thomas, Jr., Dept. of Chemistry Southeastern Mass. Univ., N. Dartmouth, MA 02747.

Laser Raman spectra have been recorded for the following states of the bromovirus CCMV and its components in aqueous solution: native virus particles, swollen virus particles which retain RNA, empty capsids which are devoid of RNA, coat protein dimers which result from capsid disassembly, and coat protein core molecules which lack a 25 residue fragment of the N-terminus. The Raman spectrum of encapsidated viral RNA has also been generated by computer subtraction of the spectra of whole virus and empty capsids or subunits. The data reveal a number of structural characteristics of the viral genome and coat subunits, including the following: (i) CCMV RNA manifests a highly ordered secondary structure in the native virion, which is perturbed slightly by pH-induced swelling of the capsid; (ii) conversion of the native virus (pH 5.0) to swollen particles (pH 7.5) causes elimination of specific RNA base interactions; (iii) the secondary structure of the coat protein is predominantly a β-sheet structure in all assembly states mentioned above; (iv) the secondary structure of the N-terminal fragment does not differ appreciably from that of the coat protein. Raman difference spectroscopy also reveals that amino acid side chains of the capsid subunit are involved in the structure transition which accompanies swelling of the virion.

Supported by N.I.H. Grant AI 11855.

M-PM-J3 THE STRUCTURE AND STABILITY OF A DOUBLE-STRAND HELIX WITH AN EXTRA CYTIDINE. (Kathleen M. Morden and Ignacio Tinoco, Jr., Chemistry Department, University of California, Berkeley, CA 94720.)

Three deoxyribo-oligonucleotides have been compared to determine the effects of a perturbation on the structure and dynamics of a double-stranded DNA helix: I) $dCA_6G + dCT_6G$, II) $dCA_3CA_3G + dCT_6G$, and III) $dCA_5G + dCT_5G$. Thermodynamic parameters have been measured from optical melting curves. The extra cytidine in helix II significantly destabilizes the double strand compared to helix I; an increase in free energy of 2.9 Kcal/mol at 25°C is found. Double-strand formation in the perturbed helix II is destabilized by 1.7 Kcal/mol at 25°C relative to helix III with one less base pair. Nuclear magnetic resonance has been used to study the conformation of these three helices in solution. The temperature dependence of the chemical shifts has been investigated for the aromatic base protons in each of the double helices as well as in the single strands. The base-pairing imino protons from helix II have been observed in H_2O and show that one of the A·T imino resonances has an upfield shift of more than 0.4 ppm relative to helix III. The properties of the three helices are compared to determine their conformations and the effects of the extra cytidine.

M-PM-J4 PHOTOCHEMICAL DEMONSTRATION OF EXTRAHELICAL BASES IN A NOVEL DNA SECONDARY STRUCTURE. Daniel M. Brown, Donald M. Gray, Michael H. Patrick, and Robert L. Ratliff*. Program in Molecular Biology, University of Texas at Dallas, P.O. Box 688, Richardson, TX, 75080 and *Genetics Group, Life Sciences Division, Los Alamos National Laboratory, Los Alamos, NM 87545.

In previous work, circular dichroism (CD) spectra of the alternating sequence polynucleotide poly[d(C-T)] have been interpreted as evidence that this polymer forms a self-complex in solution at pH 5; it was proposed that this is due to the formation of a core of stacked, protonated cytosine base pairs ($C \cdot C^+$ base pairs) which forces the thymidine residues to loop-out into the solution (Gray, D.M., Vaughan, M., Ratliff, R.L., & Hayes, F.N. (1980) Nucleic Acids Res. 8, 3695-3707). We have exploited the known photochemical properties of Thy and Cyt in polynucleotides in order to correlate a possible stacked cytosine structure in the poly[d(C-T)] self-complex with the observed CD spectrum. Poly[d(C-T)] labeled with [5-^{3}H]Cyt and [methyl-^{3}H]Thy was irradiated with 280 nm light at pH values both above and below the conformational transition point (monitored by CD spectroscopy). The formation of Cyt<>Cyt only at pH 4-5, with a concomitant reduction in the formation of Cyt<>Thy, is interpreted as proof that a stable acid structure does in fact contain stacked, alternate deoxycytidine residues. A small fraction of the extrahelical thymidine residues also photodimerize, resulting in destabilization of the structure. Although the pK_a for formation of such a conformation with a core of $C \cdot C^+$ base pairs is base sequence-dependent, this conformation (monitored by CD spectroscopy) is not otherwise limited by the composition of alternating sequence copolymers. Supported by NIH Research Grant GM19060 and Grant AT-503 from the Robert A. Welch Foundation.

M-PM-J5 THREE- AND FOUR-STRANDED NUCLEIC ACID STRUCTURES FROM A NEW DNA MODEL, R. C. Hopkins and S. M. Hopkins, Division of Chemistry, University of Houston at Clear Lake City, Houston, TX 77058

Many of the advances in molecular biology of the past three decades are based on the family of Watson-Crick models for DNA, although not all experimental data are consistent with these canonical structures. A new family of double-helical models (Configuration II) having deoxyribophosphate chain directions opposite to those in the Watson-Crick models (Configuration I) have been proposed recently (1). The Configuration II models offer alternative explanations for many observed phenomena for DNA in living systems. Most importantly, these new models lend themselves to the formation of homologous multi-stranded nucleic acid structures.

A homologous model complex of RNA lying in the major groove of left-handed duplex DNA (II) can be built using a specific triplex base-pairing scheme (2). Interestingly, the 2'OH of each ribose on RNA can form a favorable hydrogen bond to N3 of an attached purine or to O2 of an attached pyrimidine. It is suggested that such a complex could be used for direct transcription of duplex DNA.

Both right- and left-handed four-stranded structures can be formed from specific base-pair pairing (3) of two homologous duplex DNA (II) models. Practically all base-pair information is occluded in these complexes which might provide semi-permanent gene inactivation. Any abnormal process involved in unpairing tetraplexes may suggest a mechanism of carcinogenesis. Such tetraplexes might also be involved in replication, recombination, plasmid insertion and stem and loop formation. (Supported in part by grant E-889 from the Robert A. Welch Foundation). 1.) Hopkins, R.(1981) Sci. 211, 289; (1982) Biophys. J. 37, 33a. 2.) Zubay, G.(1958) Nature 182, 1290. 3.) Löwdin, P.(1964) in Electronic Aspects of Biochemistry, B. Pullman, ed. (Academic Press, New York), p. 167.

M-PM-J6 STRUCTURES FOR COVALENTLY CLOSED SINGLE-STRANDED DNA IN FILAMENTOUS PHAGE: INVERTED HELICES WITH BASES OUT (I-DNA) FOR Pf1 AND Pf3, BUT HELICES WITH BASES IN FOR fd and Xf. L.A. Day, D.G. Putterman, A. Casadevall & C.J. Marzec, The Public Health Research Institute, New York, New York 10016.

The loop of DNA in a filamentous bacterial virus is held in a protein sheath made of thousands of identical subunits, such that two antiparallel chains interact with each other and with the protein sheath. Four viruses, Pf1, Pf3, fd and Xf vary greatly in these interactions. Their subunit sequences and sheath symmetries differ. The most unusual DNA structure, in the Pf1 virion, has an extreme axial nucleotide translation, h, of 5.3 A as well as spectroscopic properties suggesting base-tyrosine stacking. Model structures having inverted helices with phosphates in the center (I-DNA) are being considered for the DNA in this virus. In Pf3, the protein has too few basic residues to neutralize the phosphate charges yet it does have phenylalanyl and tryptophyl residues well located to provide an aromatic DNA-protein interface. This and other considerations also lead to I-form DNA models for Pf3 even though h for Pf3 is only 2.3 Å. Spectral properties of Pf1 and Pf3 DNAs are similar. In the fd and Xf virions, the DNAs have h values near 2.7 Å and spectral properties like those of base-base stacked structures. Ag^+ induced CD changes indicate right-handed DNA helices with bases in; hydrogen bonds can occur between bases in opposite chains, although uniform Watson-Crick pairing does not occur. The DNA-protein interfaces in fd and Xf models are highly electrostatic rather than aromatic as in Pf1 and Pf3. The average number of nucleotides per protein subunit (n/s) is nearly integer for Pf1 and Xf, yet non-integer for fd and Pf3. Our models quantitatively unify the different DNA structures, n/s values, and protein sheath symmetries via a concept we call "the pitch connection."

M-PM-J7 EVIDENCE FOR ANOTHER DNA CONFORMATION

Kenneth H. Downing Donner Laboratory, Lawrence Berkeley Laboratory, Berkeley, CA 94720

Variability of the conformation of DNA has been recognized since before Watson and Crick published the first DNA structural model. Many recent experiments have added to our understanding of the range of conformations which DNA can adopt. We have been studying the conformation of DNA (calf thymus and poly(dA-dT) in a crystalline form, mainly by electron diffraction and electron microscopy, as well as by circular dichroism. Even without solving the structure, we find that our data are not consistent with any of the previously reported conformations of DNA. DNA crystals are grown in a hexagonal platelet form. Electron diffraction patterns, obtained from crystals in the frozen hydrated state, extend to at least 3.5 Angstroms, and show 6-fold symmetry. The lattice parameters indicate that the DNA strands are aligned perpendicular to the broad face of the crystals. Thus it appears that the DNA is in an environment with 6-fold symmetry. The only nucleic acid conformations so far seen with 6- (or 12-) fold symmetry are the A' form of RNA and Z DNA. Either of these conformations might be favored by the conditions under which our crystals are grown (0.5 M sodium acetate, ~50% ethanol). However, we have been unable to form crystals with either poly(rI-rC) or poly(dG-dC), which we would expect to adopt the A' and Z conformations, respectively, more readily than the DNAs which do form the crystals. In addition, we have made CD measurements from single crystals, with the light beam perpendicular to the crystal faces. The CD spectra obtained are very similar to spectra from DNA in solution (B form), and are distinct from A or Z spectra. We can conclude that the crystallization conditions induce a change to a new DNA conformation. Our data are consistent with a helix in the B family, with 12 base pairs per turn.

M-PM-J8 SPONTANEOUS ORDERING OF DNA--EFFECTS OF INTERMOLECULAR INTERACTIONS ON DNA MOTIONAL DYNAMICS MONITORED BY ^{13}C and ^{31}P NMR SPECTROSCOPY. R.L. Rill, P.R. Hilliard, Jr., and G.C. Levy, Departments of Chemistry, The Florida State University and Syracuse University.

Solutions of defined length DNA fragments form an ordered, liquid crystalline-like phase at a high critical concentration varying inversely with DNA length. Ordering occurs at near physiological ionic strength, in the absence of heavy metals or neutral polymers, and is accompanied by the appearance of distinct opalescence. An apparent standard heat of fusion of -38 Kcal/mole helix and an entropy change of -0.13 eu (per mole helix) were determined from the temperature dependence of the phase transition of 147 nucleotide pair (np) DNA. The average phosphodiester configuration, monitored by Raman spectroscopy, was typical of B form DNA above and below the critical concentration. Effects of intermolecular DNA interactions on the motional dynamics of 147 np DNA were examined by ^{13}C and ^{31}P NMR. NMR spectra and relaxation data showed that interactions are strong at concentrations well below the phase transition and cause stepwise uncoupling of internal motions at specific sites, suggesting formation of less ordered, intermediate phases. Motions of the exocyclic C5' carbon, but not other sugar carbons, are frozen in ca. 50% of the molecules at concentrations as low as 6.5 mg/ml. Motions of backbone ring carbons (C3', C4') are frozen in a progressively larger fraction of molecules at concentrations above 46 mg/ml. Rapid C2' motions are unaffected below the critical concentration (193 mg/ml at 32°C), and still occur in the ordered phase. We conclude that very rapid internal motions of DNA monitored by NMR consist mostly of coupled, periodic bending deformations; and partially uncoupled local motions within the sugar ring, particularly at C2'. Supported by NIH grant GM-29778.

M-PM-J9 THE TORSIONAL ELASTICITY OF THE DNA DOUBLE HELIX DEPENDS UPON COMPOSITION AND SEQUENCE.

I. Hurley, C.P. Scholes, L.S. Lerman, Departments of Biological Science and Physics and Center for Biological Macromolecules, State University of NY at Albany.

Spin-labelled ethidium (SLE) was used as a probe of DNA torsional flexibility. The EPR spectrum of SLE depends markedly upon DNA base composition and sequence. Rigid limit determinations and comparison of X- and Q-band spectra show that the spectral dependence reflects differences in SLE motion. Studies of wet DNA fibers show that SLE motion is closely determined by motional differences in the DNA to which it binds. These differences reflect intrinsic properties of the double helix, not base specific variations in binding geometry or magnetic parameters. They are not attributable to bound proteins or polysaccharides, nor to single- or double-stranded length variations. The EPR measurements imply more than ten-fold differences between the torsional force constants or various DNA base pair duplexes, with AT-dense DNA being less flexible than GC-dense DNA. Sequence-dependent departures from simple compositional determination are also evident. The molecular basis of this effect and its implications for DNA-protein binding site recognition will be discussed. This work was supported by grant number 8111321 from the National Science Foundation.

M-PM-J10 SPECTROSCOPIC STUDIES OF THE LOW FREQUENCY MODES OF DNA

S. M. Lindsay and J. Powell
Department of Physics
Arizona State University
Tempe, AZ 85287, USA

The lowest lying zone center optic and acoustic modes of double helical calf thymus DNA have been studied using inelastic laser light scattering and a tandem interferometer.[1] The most striking feature in high resolution spectra is an intense and sharp line at $\sim$ 600 MHz. In fibers this mode is sensitive to the degree of fiber order, and appears to be localised. We do not observe such a feature in gels or solutions.

[1] S.M. Lindsay, M.W. Anderson and J.R. Sandercock, Rev. Sci. Instrum. 52(10), 1478-1486 (1981).

M-PM-J11 CONFORMATIONAL ENERGY STUDY FOR INTRAMOLECULAR BENDING IN PHENYLALANINE TRANSFER RNA. Chang-Shung Tung[a], J. Andrew McCammon[b], and Stephen C. Harvey[a], (a) Department of Biochemistry and Department of Physics, University of Alabama in Birmingham, Birmingham, AL 35924, and (b) Department of Chemistry, University of Houston, Houston, TX 77004.

We have used a computer based model for $tRNA^{Phe}$ to study the large scale intramolecular motions of the molecule. There are two principal improvements over our earlier study (S.C. Harvey and J.A. McCammon, Nature 294, 286 (1981)). First, our structural refinement algorithm combines steepest descent minimization with collective rotations of groups of atoms about virtual bonds. Second, we have found two suitable methods to determine the energy differences for different conformations which give very consistent results. These improvements allow the determination of a conformational energy map, $E(\alpha,\beta)$, where α and β are the angles for the two degrees of freedom corresponding to the rotations of the upper arm of the molecule relative to a coordinate system fixed to the lower arm. From this map we have found the lowest energy pathway for the molecule to bend from the most extended conformation (the two arms of the molecule nearly parallel) to the most compact conformation (acceptor end near the anticodon loop). (Supported by grants from the National Science Foundation).

M-PM-J12 DNA STRUCTURAL DYNAMICS: TOPOLOGICAL AND ENERGETIC CONSIDERATIONS IN THE B$\rightleftharpoons$Z TRANSITION. Stephen C. Harvey, Department of Biochemistry, University of Alabama in Birmingham, Birmingham, AL 35294.

The G-C base pairs have the Watson-Crick geometry in both B- and Z-DNA, but the B$\rightleftharpoons$Z transition requires all of the base pairs to flip 180°. If we think of a base pair as topologically equivalent to a coin, then the stack of coins in a vertical piece of B-DNA is arranged with alternating "heads" and "tails" up. Although the same is true for Z-DNA, the sense of each individual coin is reversed, so the B$\rightleftharpoons$Z transition is equivalent to ....HTHT.... $\rightleftharpoons$ ....THTH.... Topologically, there are two ways to flip a base pair, either maintaining the Watson-Crick hydrogen bonds during the flip or breaking them and flipping each base separately. For both of these topological mechanisms, there are two locations where the flipping can take place, either sliding the pair to be flipped out of the stack of bases that comprise the double helix, or leaving it in the stack and increasing the distance between the pairs above and below it to provide room for the flip. There are thus at least four possible pathways for the B$\rightleftharpoons$Z transition, and in this report I examine the energetics of the alternative pathways. (Supported in part by grant PCM-81-18827 from the National Science Foundation).

M-PM-J13 MACROMOLECULAR CONTACTS ON THE PATH OF NASCENT RNA THROUGH THE PROCARYOTIC TRANSCRIPTION COMPLEX, Michelle H. Palmer and Claude F. Meares, Chemistry Department, University of California, Davis, CA 95616

We have synthesized a cleavable dinucleotide photoaffinity probe, 5'(4-azidophenylthio)phosphoryladenylyl(3'-5')uridine (denoted N_3RSpApU), and used it to initiate transcription with E. coli RNA polymerase at the A1 promoter of bacteriophage T7 D111 DNA. Transcription complexes were prepared containing a range of RNA lengths, with N_3RSpApU at the RNA 5' end, ^{32}P at other locations in the nascent RNA, and a terminator at the RNA 3' end. Four reactions, each containing a base-specific chain terminator (A,G,C,U), were used so that the sequence of each transcript could be confirmed. The 5' end of the RNA was then covalently attached to DNA or RNA polymerase subunits by UV irradiation. Radiolabeled reaction components were separated by electrophoresis, after which the RNA oligonucleotides were cleaved off each component and analyzed for size and sequence. Results show that in the transcription complex, the DNA template is covalently labeled by the leading end of RNA oligonucleotides with lengths between 3 and 12 residues. The alpha subunit of RNA polymerase is not labeled by oligonucleotides which are less than 20 residues long. The beta and beta-prime subunits are not resolved by electrophoresis when they bear oligonucleotides; together they are labeled by RNA's from 3 to roughly 80 residues long. The sigma subunit is heavily labeled by the trinucleotide. Further experiments using other templates should reveal the effect of RNA secondary structure on its path through the transcription complex.

M-PM-J14 A LOW FREQUENCY LOCALIZED BASE DESTACKING MODE IN POLY(dG)·POLY(dC).

E.W. Prohofsky and B.F. Putnam, Dept. of Phys., Purdue U., W. Lafayette, IN 47907

As a result of a theoretical local mode analysis we predicted the existance of a low frequency resonant mode at a terminus of a DNA helix. Subsequently a resonant mode at ≈ 600 MHz has been observed by Lindsay and Powell. Further calculation by us on this mode indicate that it can be characterized as one in which the end base pair oscillates out from its usual stacked position. The calculated frequency is ≈ 600 MHz in agreement with the observed line. The calculated motion has a large amplitude in the rotation of the end base pair with respect to its neighbor base pair coupled with a large amplitude stretch of the end base pair hydrogen bonds. A large amplitude in this mode would turn outward the individual bases exposing the hydrogen bonding regions. Although the first calculation dealt with a helix terminus it is not necessary for the bonds along the backbone to be severed. The local mode is induced by altering the nonbonded interactions along the helix. The nature of the necessary perturbing forces are such that a large amplitude base displacement is likely to be able to propagate along the helix. Since the mode results from a change in the collective nonbonded forces the local mode could be created by a number of mechanisms along the helix as well as at the terminus. Nonbonded interactions between the helix and an adjacent molecule could induce this local mode. We are currently extending the calculations to explore the effect of large amplitudes and anharmonic force constants. This work supported by USPHS grant GM24443 and NSF grant DMR78-20602.